MANCHESTER 1824

The University of Manchester

DISSOLVED GAS ANALYSIS (DGA) OF TRANSFORMER INSULATING LIQUIDS UNDER LABORATORY SIMULATED THERMAL FAULTS

A thesis submitted to The University of Manchester for the degree of PhD

in the Faculty of Science and Engineering

2017

Xiongfei Wang

School of Electrical and Electronic Engineering

CONTENTS

LIST OF FIGURES

LIST OF TABLES

ABSTRACT

Dissolved Gas Analysis (DGA) is regarded as one of the most effective methods to diagnose transformer incipient electrical and thermal faults. Recently, alternative insulating liquids have been developed as potential replacement of mineral oil for transformers. Due to the lack of field experiences, the fault gas generation characteristics of alternative insulating liquids need to be investigated under laboratory testing scenarios which represent transformer faults. There are three methods in laboratory to simulate transformer thermal faults which are immersed heating method, tube heating method and bottle heating method. For the immersed heating method, it is easy to control the input power but difficult to measure and adjust the heating element temperature. The tube heating method can simulate thermal faults and cover the whole fault temperature range but it requires a complicated experimental setup. The bottle heating method can only simulate thermal faults below the flash point or fire point of the oil for safety consideration. Immersed heating method and tube heating method were investigated in this PhD research.

This PhD thesis summarised the gas generation characteristics under laboratory thermal faults of three types of transformer insulating liquids. For the experiments using immersed heating method, the pool boiling phenomenon was observed and reported for the first time in the investigated insulating liquids. The pool boiling curves of the three liquids were measured and reported. The Nukiyama temperature (the upper stable temperature limit of immersed heating element in nucleate boiling regime) of the investigated mineral oil was about 330 ℃, beyond which the heating element temperature was unstable and its measurement was unreliable. The Nukiyama temperatures of the investigated alternative liquids were about 390 ℃ which were higher than that of the mineral oil due to their higher boiling points. Based on this finding, the immersed heating method was proved difficult to cover the whole range of thermal fault temperature. As a result, the DGA experimental results with immersed heating method reported in previous publications might need to be reinterpreted.

As an alternative, a tube heating based DGA experimental system was developed in this PhD research work. The dissolved and free gas contents of three investigated liquids in the experimental system were measured, presented and compared under thermal faults from 250 ℃ to 750 ℃. Fault gas pattern varied among different oil types and different fault levels. Different key gas indicators of the tested liquids were found and reported. The gas generation results could provide diagnostic information on gas generation characteristics of the tested insulating liquids.

To calculate the gas in total value, the Ostwald coefficients were needed. Although the Ostwald coefficients for mineral oil and synthetic ester liquid could be obtained from literatures, those of gas to liquid (GTL) oil should still be determined in this PhD research. In addition, online DGA monitor and conventional laboratory DGA method have been used simultaneously to observe and quantify their difference.

DECLARATION

I declare that no portion of the work referred to in the thesis has been submitted in support of an application for another degree or qualification of this or any other university or other institute of learning.

COPYRIGHT STATEMENT

ACKNOWLEDGEMENT

I would like to express my sincere gratitude to my supervisor Prof. Zhongdong Wang and co-supervisor Dr. Qiang Liu, since any tiny step of my improvements in the last four years was tied closely with their great effort and kind encouragement. I thank them for their supervision, guidance and support to my PhD research, and their trust in my ability.

I would also like to express my gratitude to M&I Materials, National Grid, Scottish Power, Shell Global Solutions, TJ|H2b Analytical Services, UK Power Networks and WEIDMANN Electrical Technology for their financial and technical contributions to the transformer research consortium at The University of Manchester.

Great thanks are also given to Pascal Mavrommatis and Claude Beauchemin of TJ|H2b Analytical Services for their inspirational advices on the experimental system design. I would also like to thank John Hinshaw from Qualitrol for provide the training and support on the TM8 online DGA monitor and Ryan Patterson from GE Grid Solution on the Transfix online DGA monitor.

To all my colleagues in the transformer research group and others in the corridor of Ferranti building and the School of Electrical and Electronic Engineering, I appreciate your company and thank you for offering me an enjoyable working environment.

Last but not least, I wish to give my most sincere thanks to my parents for their continuous backup and understanding on my four years PhD study.

Chapter 1 Introduction

1.1 Background

1.1.1 General

Transformer is one of the most expensive and important component in electrical power system. It transfers energy through power networks with different voltage levels. Although transformer is reliable, electrical and thermal stress might still occur during operation. Some of these stresses might accumulate and produce transformer incipient faults. If not correctly diagnosed and well controlled, some incipient faults might further develop into transformer catastrophic failure, which will cause vast damage of transformer and nearby devices in substations. Therefore, condition monitoring and fault diagnosis of transformer is of great importance.

Fault is defined as unplanned occurrence or defect in an item which might result in one or more failures of the item itself or of other associated equipment [1]. In this PhD thesis, thermal fault in transformers is studied. The thermal fault is defined as excessive temperature rise in the insulation. The thermal fault in transformer can be caused by limited to overloading, insufficient cooling, excessive current circulating in adjacent metal parts or through the insulation and overheating of internal connection lead [1]. In transformers, typical thermal fault examples include local overheating of the core due to concentrations of flux, increasing hot spot temperatures; varying from small hot spots in core, shorting links in core, overheating of copper due to eddy currents and bad contacts/joints up to core and tank circulating currents [2].

The classification of thermal faults is based on visual inspection on the equipments after the fault has occurred in service. The thermal fault between 120 ℃ and 150 ℃ is general insulated conductor overheating [3] and is classified into T1 fault range [1]. The thermal fault above 700 ℃ is observed by metal fusion in transformers [4]. Therefore, the temperature of thermal faults in transformer might range from 120 ℃ to 800 ℃ or even

higher which needs to be covered in laboratory simulated thermal fault in this PhD research work.

Historically, attempts to study dissolved gas combination from failure transformer started early last century [2]. This method was developed into free gas analysis from Buchholz relay. Sooner it was realised that the dissolved gases slowly evolved and dissolved in oil should be effective in diagnosing transformer incipient fault. Until late last century, a comprehensive method has been built on DGA including oil sampling process, gas extraction process and data interpretation. Due to the development of semi-permeable material and improvement of gas detection technology, in this decade, various types of online DGA monitors have been developed [5].

Dissolved Gas Analysis (DGA) has been regarded as one of the most effective methods to diagnose transformer incipient faults [6]. Transformer insulation system is composed with liquid and solid insulating materials, such as insulating oil and paper. Insulation materials are generally consisted of carbon (C), oxygen (O) and hydrogen (H) chemical elements [7]. Under fault energy, insulation molecules will tend to decompose into small radicals. Those fractions might recombine into small hydrocarbon or carbon oxide molecules, i.e. gas molecules. Traditional DGA method considers all dissolved fault gases. Modern DGA method has been established based on 9 gas types: CO2, CO, H2, CH4, C2H6, C2H4, C2H2, O2 and N2. Three gases are key indicators related to thermal faults which are CH4, C2H4 and C2H2. Two gases are key indicators related to electrical faults which are H2 and C2H2. The H2 is related to partial discharge fault and C2H2 is related to discharge fault. Carbon oxides are key indicators related to faults with cellulose paper involved. Atmospheric gases (CO2, O2 and N2) are key indicators for transformer leakage.

Traditionally, DGA is carried out on transformer oil samples in professional analytic laboratory. The disadvantage of the conventional laboratory based DGA method is that it takes time for oil sampling and transportation. Therefore, online DGA monitors have been developed. The conventional laboratory based DGA measurement is an online monitoring technique if the analysed oil samples are taken from transformer in operation based on sample taken. The primary difference between online DGA monitor and

conventional laboratory DGA measurement is that the online DGA monitor analyses the oil directly on the operational transformer while the laboratory DGA measurement analyses the oil in laboratory to which the oil samples need to be delivered. Online DGA monitors have been widely installed all over the world. They are designed based on different technologies and manufactured by different companies, with different accuracy and detection limits. Performances of online DGA monitors are difficult to assess because of lacking in-service transformer failure experience. Therefore, it is essential to build up a test platform to simulate transformer insulation system under representative faults in order to investigate the performance of online DGA monitors.

In addition, potential replacements of mineral oil have been proposed since last century, such as natural ester oil, which is less flammable than mineral oil and environmentally friendly. So far, various types of transformer insulating oils have been developed. Some of those new oils have no field experience. Therefore, it is essential to have a platform to investigate gas generation characteristic of these new oils under simulated fault in laboratory.

1.1.2 Liquids under Investigation

Currently, the DGA knowledge system for mineral oil immersed transformers has been well established. The system contains DGA test methods and diagnosis methods which are built up on large amount of field experiments. In the previous decades, with the development and wide promotion of alternative insulating liquids, laboratory based DGA research works are completed, especially for natural ester liquids. The utilisation of synthetic ester liquid on large power transformers has been appealed. In addition, the novel gas to liquid (GTL) based transformer oil has been developed. However, there are limited field experiences for these two oils. Therefore, it is necessary to study the gas generation characteristics of these two oils under laboratory simulated transformer faults.

Mineral Oil

From early 1900s, nearly all load transformers in electrical power system use mineral oil, since it is relatively cheap to meet requirement of insulating fluid for transformer [7]. Mineral insulating oil is refinery product of petroleum crude oil during distillation procedure by selecting the boiling range of the mineral oil fraction [7].

Generally speaking, mineral insulating oil is composed of paraffinic, naphthenic and aromatic hydrocarbons. Combination of those components is determined by the crude oil stock. Paraffinic based mineral oil is used in early stage. However, the high pour point of paraffinic mineral oil is high. This is the effect of n-paraffinic hydrocarbon. In 1925, it was replaced by naphthenic based mineral oil [7]. Common hydrocarbon molecule structures in mineral oil are shown in Figure 1-1.

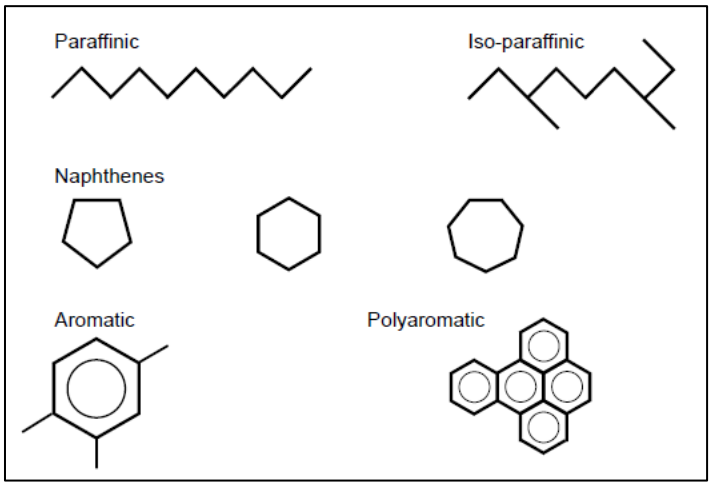

Figure 1-1 Common hydrocarbon structures in mineral oil [8]

Paraffinic structures can be straight or branch chains. The straight paraffinic chain, also named as n-paraffinic or linear paraffinic, is usually contained in paraffinic crude feedstock. The occurring of linear paraffinic component will affect low pour point so such oil need to be de-waxed and adding pour depressant in order to mitigate the limitation caused by pour point [7].

Naphthenic hydrocarbons, also named as cycloalkanes, are another major component of saturated hydrocarbon molecules in mineral oil. Its general chemical formula is C_nH_{2n}.

Naphthenic molecules structures can be hydrocarbon rings with five, six or seven carbons due to their higher thermal stability [9].

Aromatics are the unsaturated hydrocarbons in mineral oil. They have single-cycle or multi-cycle structures. Aromatic content has significant effect on dielectric strength. AC electric strength increases with high aromatic content, while impulse strength will be lowered with high aromatic content. It is a combined structure with paraffinic, naphthenic and aromatic content. Paraffinic takes about 30%, and for paraffinic based crude oil, it will take much more with rich n-paraffinic. Therefore mineral oil from paraffinic based crude oil need to be de-waxed to remove n-paraffinic content. In commercial mineral oil, the most components are naphthenic molecules with five, six or seven rings. The rest of saturated carbons are iso-paraffinic. Aromatic will be controlled to minimum level [10].

A typical oil molecule example is shown in Figure 1-2.

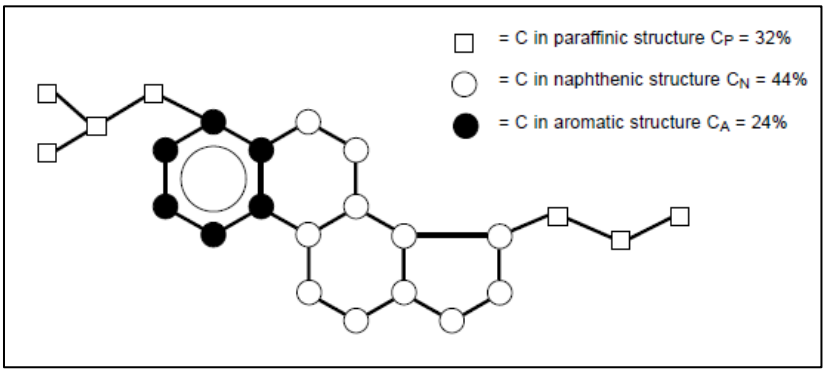

Figure 1-2 An example of oil molecule [8]

In this thesis, Nytro Gemini X is used as benchmark of conventional mineral oil.

Synthetic Ester Liquid

In late last century, synthetic ester liquid as one of ester-based transformer oils is considered as replacement of mineral oil for several reasons. Firstly, synthetic ester oils are environmentally friendly transformer insulating liquids. They are biodegradable oil, non-toxic and not harmful to aquatic life, recoverable and dispersible at sea using standard methods. Subsequently, synthetic ester oil can provide higher fire safety because of its high fire point (> 300 ℃). Synthetic ester oil also provides self-extinguishing property. Potentially lower fire protection costs are required for utilities. Finally, high

moisture solubility of synthetic ester oil will absorb more moisture than mineral oil, and almost prevent any free water in transformers. It will also absorb large amount of moisture from cellulose. This can somehow extend asset life and slow aging [11].

In this work, MIDEL 7131 is used as synthetic ester liquid provided by M&I Material. Esters are chemical compounds derived from inorganic acid or organic acid where at least one hydroxyl (-OH) group is replaced by an alkoxy (-O-alkyl) group. Chemically the synthetic ester is made by esterification of pentaerythritol, which is an organic compound with the formula C5H12O4. Its molecule has a carbon atom quaternary centre bonded to other four carbons with a tetrahedral structure of ester groups. In the esterification process, each hydroxyl group at the tetrahedral corner will be replaced by a carboxylate ester group. A Midel-7131 synthetic ester molecule is shown in Figure 1-3 in which the R groups are unsaturated hydrocarbons of either straight or branched chains of C5-10. The average molecular weight of MIDEL 7131 is 620.

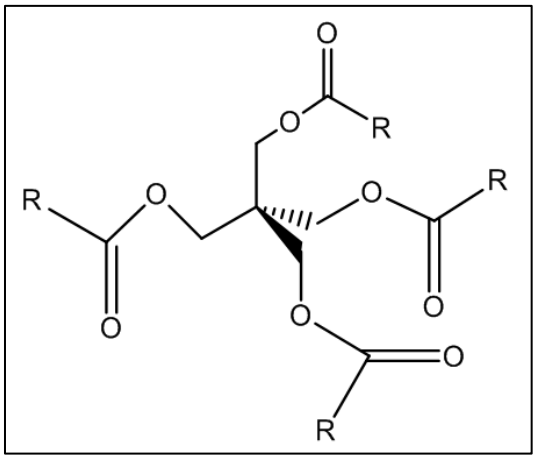

Figure 1-3 Molecule structure of Midel-7131 synthetic ester oil

Gas to Liquid (GTL) Insulating Oil

Gas-to-liquid (GTL) refers to refinery process which converts natural gas or other hydrocarbon gases into long-chain hydrocarbons. First commercial GTL plant was operated in Bintulu, Malaysia, and the largest GTL plant, Pearl GTL, was started in Qatar by Royal Dutch Shell. In GTL process, pure natural gas (methane) is firstly generated by removing water, condensates, sulphur and natural gas liquids. Subsequently, methane and oxygen are converted into synthesis gas or syngas (mixture of hydrogen and carbon

monoxide) in gasification unit at 1400 – 1600 ℃. Then, liquid waxy hydrocarbons are generated in Fischer-Tropsch process. Finally, liquid waxy hydrocarbons are hydrocracked and distilled into a wide range of GTL products. GTL naphtha is chemical feedstock for plastic manufacture. GTL Kerosene can be used as jet fuel mixture or indoor heating fuel. GTL paraffin is used for cost-effective detergents. GTL gasoil is diesel-type fuel. GTL Base oils are used to make high-quality lubricants [12].

As one of the GTL products, Diala S4 ZX-I transformer oil was launched and promoted by Shell. Because of the specific manufacture process, the new oil contains more than 90% of iso-paraffinic hydrocarbons. There are only less than 10% naphthenic molecules, and far less than 1% aromatic hydrocarbons [12]. Antioxidant (DBPC) is added to prevent oxidation. This new transformer oil has kinematic viscosity more than 75% below IEC 60296 limit. It also has better specific heat capacity and thermal conductivity characteristic compared with traditional mineral oil. Additionally, it has significantly less sludge and dielectric dissipation factor than IEC 60296 limits. Due to the extremely low aromatic content, it has higher breakdown voltage than traditional mineral oil. The structure of the iso-paraffinic hydrocarbon molecule of Diala S4 ZX-I is shown in Figure 1-4.

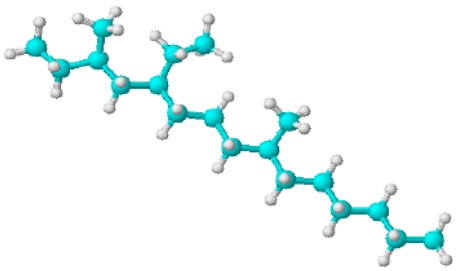

Figure 1-4 Molecular structure of iso-paraffinic contains in the Diala S4 ZX-I [12]

Physical and Chemical Properties of Investigated Liquids

After understanding the fundamental of the three investigated liquids, some typical values of basic properties of the investigated oils are listed in the Table 1-1, mainly based on the Product Data Sheet. These physical and chemical properties listed are related to the DGA studies of the liquids. For example, these physical properties might be relevant to the temperature distribution of thermal fault and the heat dissipation of heating element

which might affect gas generation. The chemical properties might also affect gas generation. For example, it has been indicated in a previous study that the aging products would affect gas generation [13].

Table 1-1 Basic properties of investigated liquids: Gemini X, Diala S4 ZX-I and MIDEL 7131

Property	Unit	Gemini X	Diala S4 ZX-I	MIDEL 7131
Density@20℃	kg/dm^3	0.87	0.805	0.97
Viscosity@40℃	mm^2/s	9.0	9.6	34
Specific heat@20℃	J/kg K	1860	2176	1880
Thermal conductivity@20℃	W/mK	0.126	0.143	0.144
Pour point	℃	-51	-42	-60
Flash point	℃	152	191	275
Boiling point	℃	>250		
Fire point	℃			322
Acidity	mg KOH/g	< 0.1	0.02	<0.03
Aromatic content	%	3	0	
Water content	%	<20	6	50
Antioxidant	Wt%	0.38	0.3	

1.2 Research Objectives

The aim of this PhD thesis is to investigate the fault gas generation characteristics of mineral oil and alternative insulating liquids under laboratory simulated thermal faults. Two types of thermal fault simulation methods are applied to generate representative transformer thermal faults. The dissolved gases are analysed by both online DGA monitors and conventional laboratory measurements. The following topics are covered in this thesis:

(i). Establishment of laboratory based thermal fault DGA experimental system

Thermal fault is one of the most important incipient fault types. Dissolved Gas Analysis (DGA) is sensitive to thermal fault as the gases are generated at very early stage of the fault and could be detected at low concentration levels. In recent decades, DGA experiments based on laboratory simulated thermal faults are performed driven by the

development of alternative transformer insulating liquids. Conventionally, there are three methods in laboratory to simulate thermal faults which are immersed heating method, tube heating method and bottle heating method. In this PhD research work, it is necessary to build up DGA thermal fault experimental system for fault gas generation study

(ii). Fault gas generation characteristics of investigated liquids under laboratory simulated thermal faults

To diagnose the thermal fault with alternative transformer insulating liquids filled transformers, the fault gas generation characteristics need to be investigated. The diagnostic information of the tested liquids can be obtained from the fault gas generation amounts and fault gas combination patterns. In this PhD research work, the fault gas generation of alternative insulating liquids need to be tested with the established thermal fault DGA experimental system. As a prerequisite, some key parameters are necessary for the alternative insulating liquids, such as the partition coefficients between oil and gas phase which needs to be measured.

(iii). Comparison between online DGA techniques and laboratory DGA measurements

Conventionally, the oil samples are analysed in professional laboratory. Recently, online DGA monitors are widely installed on transformers to analyse transformer oil. Some online DGA monitors are equipped gas detectors which use different detection techniques from the laboratory gas chromatography (GC) analyser in conventional DGA process. The extraction system of the online DGA monitors might also vary from the conventional extraction system in laboratory DGA process although they might be designed based on similar principles. Dealing with alternative insulating liquids, the partition between oil and gas phases is quite important as the online DGA monitors and laboratory DGA system might be calibrated based on different methods. Therefore, there might be significant discrepancy between laboratory DGA measurement and online DGA monitor measurement. In this PhD research work, the conventional laboratory DGA measurement method and online DGA monitor method need to be compared. In this thesis, the laboratory DGA measurement refers to the DGA analyse of oil samples which is carried

out in analytical laboratory. The online DGA measurement refers to the DGA analyse of the oil by online DGA monitors which includes TM8 measurement and Transfix measurement.

1.3 Outline of Thesis

A summary of the chapters in this thesis is presented as followed.

Chapter 1 Introduction

This chapter introduces the background and research objectives of this PhD study. It also gives the outline of this thesis.

Chapter 2 Literature review

This chapter reviews literatures related to this PhD study. The transformer faults and the fault gas evolution mechanism are introduced. The DGA procedures including oil sampling methods and data interpretation techniques are also introduced. In addition, recent laboratory based DGA thermal fault experiments are summarised.

Chapter 3 Key technical information in thesis

This chapter provides some key technical information related to this PhD study. In this research work, two extraction methods are used in DGA measurements. As the alternative insulating liquids are investigated, the partition between gas and oil phase in DGA extraction system is determined by the Ostwald coefficients. There are two types of gas detection methods in laboratory measurements and online DGA measurements which are also introduced in this chapter.

Chapter 4 Immersed heating experiments

In this chapter, the basic properties of the three types investigated liquids in this research work are introduced. In addition, the experimental system with immersed heating methodology is introduced including the setup description, test procedures and the gas in total concentration calculation. In addition, the experimental results are presented with

the immersed heating methodology. The pool boiling phenomenon was found during experiments with all three investigated liquids and the pool boiling curves are plotted. According to the pool boiling regimes, fault gas generation from three types of liquids are tested. The practical implication of the pool boiling phenomenon found in the immersed heating methodology is discussed. The comparison between the laboratory measurements and online DGA measurements are also presented.

Chapter 5 Tube heating methodology

This chapter introduces the established tube heating methodology based DGA experimental system. It starts with the overall system which is composed of the oil circulation system, oil heating system and gas expansion system. The detailed design and components of each part of the system are described. In addition, several preliminary trials are performed after the system has been established whose aim is to understand the operational characteristics of the system. Based on the preliminary trials, the experimental procedures are designed and provided in this chapter.

Chapter 6 Tube heating experimental results

In this chapter, the gas generation results of the three investigated liquids from the established tube heating experimental system are demonstrated. Initially, the measurement procedures are introduced. The experimental observations including the temperature profile during heating and heating pipe inner surfaces after faults are presented. The gas in total calculation of the tube heating DGA test system is introduced including the correction calculation of the alternative insulating liquids. The DGA measurement results of three tested oils are from three types of measurement methods which are given and compared with each other. According to the DGA measurements, the fault gas generation patterns under the tube heating system simulated thermal faults are presented.

Chapter 7 Conclusion and future work

This chapter summarises the major conclusions of the thesis. Some suggestions for the future work is provided which are required for further understanding of the fault gas

generation characteristics under laboratory simulated thermal faults and the applications of the gas generation patterns.

Chapter 2 Literature Review

2.1 Introduction

In this chapter, literatures related to the Dissolved Gas Analysis (DGA) and laboratory DGA experimental methods will be reviewed. DGA method is effective in diagnose the incipient electrical and thermal fault in transformers. The definitions of electrical and thermal faults will be introduced initially followed with a thermal fault case in real transformer as an example. The fault gases are generated from decomposition of oil molecules or cellulose material. Thermodynamic models have been proposed to estimate the fault gas generation characteristics of mineral oil. In addition, non-fault related gas sources and stray gassing will be introduced.

The oil from the transformers could be sampled with syringes, bottles or ampoules. In this PhD study, the oil is sampled with syringe only. Therefore, only sampling with syringe will be introduced as oil sampling method in this chapter. There are multiple data interpretation techniques to be reviewed which are used to diagnose transformer fault type according to the dissolved gas measurements.

Recently, laboratory based DGA experimental studies on alternative insulating liquids have been carried out due to the industry need for operating alternative liquid filled transformers. In laboratory, there are generally three types of thermal fault simulation methods: immersed heating method, tube heating method and bottle heating method. Typical experimental setups using these three methods will be introduced in this chapter.

2.2 DGA Related Transformer Fault Types

During operation, transformer will be subject to various severe conditions, such as electrical stress, thermal stress, chemical stress and mechanical stress. Some of those stresses will develop transformer incipient fault. Dissolved Gas Analysis (DGA) is sensitive to electrical and thermal incipient faults, under which circumstances molecules

of liquid and solid insulation materials will decompose and hydrocarbon gases or carbon oxides will generate. Fault levels and sizes related to DGA method have been defined by IEC and IEEE standards.

2.2.1 Thermal Faults

Thermal fault can be generated by general conductor overheating due to overloading. Additionally, concentrated flux or shorting links in core might cause local overheating. Deteriorated contacts or joints across laminations or copper conductor might also cause overheating hotspot [1, 14]. So far, it was found that the dissolved fault gases start to evolve from 120 ℃ which is defined as the stray gassing [1, 15]. Therefore, the thermal fault temperature in DGA studies should be considered from around 120 ℃.

Thermal fault was initially divided into four levels in IEC standard, i.e. thermal fault of low temperature (120 ℃ – 150 ℃), thermal fault of low temperature range (150 ℃ – 300 ℃), thermal fault of medium temperature range (300 ℃ – 700 ℃) and thermal fault of high temperature (> 700 ℃). Later the classification was unified with IEEE standard by combination of two fault types hotspot temperature of which are lower than 300 ℃. Currently, transformer thermal fault is divided into T1 (120 – 300 ℃), T2 (300 – 700 ℃) and T3 (> 700 ℃) [1, 14].

The classification of thermal faults is based on visual inspection on the equipments after the fault has occurred in service. The T1 fault is identified if paper has turned brownish. The T2 fault is identified if the paper has carbonised. The T3 fault is identified if oil carbonisation, metal coloration or fusion [4]. The thermal fault below 150 ℃ is general insulated conductor overheating [3] and is classified into T1 fault range [1]. Therefore, the temperature range of thermal faults in transformer might range from around 100 ℃ to above 800 ℃ which needs to be covered in laboratory simulated thermal fault.

2.2.2 Electrical Faults

In transformer, there are two types of electrical fault: partial discharge (PD) and discharge. Typical partial discharge occurs in gas-filled bubbles due to poor impregnation, paper moisture or oil saturation. Discharges include sparks between loose conductors and surface discharge on paper or pressboard. In some cases, local short circuits will cause high current density arcing, which is able to melt down metal part and cause destructive damage in equipment. Former discharge fault is defined as discharges of low energy, and latter is defined as discharges of high energy [1, 14].

Electrical fault is divided into three types in IEEE and IEC standards: Partial discharges (PD), discharge of low energy and discharges of high energy [1, 14].

Partial discharge refers to a discharge which only partially bridges the insulation between conductors [1]. Partial discharge of low energy density in transformer normally refers to discharge in gas filled cavities resulting from incomplete impregnation, super saturation, cavitation or high humidity. Partial discharge of high energy might lead to tracking or perforation of solid insulation which damages the solid insulation and might develop breakdown failure of the insulation [2]. Therefore, partial discharge of high energy density is concerned for the transformer operation and is identified as a fault that can be reliably identified by visual inspection [4].

2.2.3 Thermal Fault Case Example

In this section, a winding thermal fault case example is presented in Figure 2-1.

Figure 2-1 winding fault in a 400/132kV 240MVA transformer [16]

This case involves a 400/132kV 240 MVA transformer with increasing ethylene (up to 320 ppm). The CO2/CO ratio seems to indicate the thermal fault involving no much solid insulation. Off-line electrical tests found high resistance in one phase of common winding. Detailed forensic examination of the windings during the scrapping revealed the solid evidence of a developed local winding thermal fault, as shown in Figure 2-1. Fortunately the transformer was removed from service before a winding failure occurs. This case shows a typical winding thermal fault in transformer, which is successfully diagnosed by dissolved gas analysis method [16].

Some typical thermal fault types are listed associated with the inspected fault temperatures in Table 2-1 [4].

Table 2-1 Typical thermal faults associated with the fault temperature [4]

Fault temperature range	**Typical Faults in Transformers**
T1 (< 300 ℃)	Overheating of conductor
T2 (300 – 700 ℃)	Low temperature overheating of clamping beams of yokes by stray flux; Hot spot in paper; carbonised windings during heat run tests; circulating currents in LV windings
T3 (> 700 ℃)	Steel lamination eroded; Hot spot in lamination or on bushing; Burnt lamination during heat run test; Overheating of tap changer contacts; circulating current in clamping bolt; Ground wire burnt and ruptured by circulating current

Thermal faults in transformer might be generated by several faults types. Short turn fault is one of the most common fault types which is developed as a result of breakdown of the solid insulation and causes winding temperature rising up. The lack of cooling due to poor design might cause either general or localised high temperature overheating. Breakdown of insulation between the core and main tank might generate localised overheating due to circulating current [16]. Localised overheating in core might also be caused by the concentrations of flux [2]. Hot spot temperatures of thermal fault varies from small hot spots or shorting links in core, overheating of copper due to eddy currents and bad contacts or joints up to core and tank circulating currents [3].

2.3 Evolution of Fault Gases

Seven gases are regarded as representative gases in modern DGA method as they contain most incipient fault information. They are listed in Table 2-2 below. Dissolved oxygen and nitrogen are also analysed as complementary gases [1].

Table 2-2 Fault gases in DGA investigation

Hydrogen	Methane	Ethane	Ethylene	Acetylene	Carbon Monoxide	Carbon Dioxide
H2	CH4	C2H6	C2H4	C2H2	CO	CO2

2.3.1 Fault Related Gases

Diagnosis of fault type of failed transformer from generated gases started 50 years ago. It is developed into a detailed assessment of the fault type in terms of the gases collected from the Buchholz relay. It was soon realised that the gases can be generated from oil sufficient to trigger a Buchholz relay, slowly developing faults would produce fault gases which would be dissolved in oil. It should be possible to diagnose incipient fault faults and monitor transformer by analysing dissolved gases in oil [2].

In theory, the two principal sources of gas generation in an operating transformer: decomposition of liquid insulation and decomposition of solid insulation. Liquid insulation refers to transformer oil, and solid insulation refers to cellulose insulation, such as paper, pressboard and wood blocks.

2.3.2 Decomposition of Oil Molecules

Mineral transformer oil is taken as example to explain gas generation since it is still widely used as transformer insulating material. According to previous paragraph, mineral oils are composed of a blend of different hydrocarbon molecules containing carbon-hydrogen (C-H) and carbon-carbon (C-C) bonds. Under thermal or electrical fault energy, scission of some of the C-H and C-C bonds may occur. Small unstable hydrogen or hydrocarbon fragments are formed. These free radicals can combine with each other to form gas molecules, such as hydrogen, methane, ethane, etc. Further decomposition and

rearrangement processes lead to the formation of unsaturated molecules, such as ethylene and acetylene [17]. C3 and C4 hydrocarbon gases and solid particles of carbon and hydrocarbon polymers (X-wax) are other possible products. The formed gases will dissolve in oil, or accumulate as free gases if they are generated rapidly and in large quantities [1].

C-H bonds are the weakest bonds, whose scission might occur under low energy fault, such as partial discharges of the cold plasma type (corona discharges), and main recombination products are hydrogen. More energy or higher temperatures are needed for the scission of the C-C bonds and their recombination into gases with single, double or triple bonds. For example, ethylene is favored over ethane and methane at higher temperature. Acetylene requires temperature at least 800 ℃. In addition, small quantities of carbon oxides (CO and CO2) might be generated due to oil oxidation, which can accumulate over long periods of time into more substantial amounts [14]. Bond dissociation enthalpy values of different chemical bonds related to gas generation are listed in Table 2-3.

Table 2-3 Bond dissociation enthalpy [18]

Molecular bond	C-H	C-C	C=C	C≡C
Dissociation enthalpy (KJ/mol)	338	607	720	960

These decomposition processes discussed in previous paragraphs are related to the presences of individual hydrocarbon molecules, energy distribution, temperature in the neighborhood of the fault and contact time. Therefore, the specific degradations of transformer oil hydrocarbons and the fault conditions cannot be predicted reliably from chemical kinetic considerations [17]. To assess fault condition, an alternative approach is to assume that all hydrocarbons in the oil are decomposed into the same products and each product is in equilibrium with all others. Thermodynamic models can be used to calculate gas combination in decomposition reactions using known equilibrium constants. This will be introduced in subsequent section.

2.3.3 Decomposition of Cellulose Molecules

Solid cellulose insulation, i.e. paper, pressboard and wood blocks, contain polymeric chains which include a large number of anhydroglucose rings, weak C-O bonds and glycosidic bonds. Some of these chemical bonds are thermally less stable than the hydrocarbon bonds in mineral oil, which might decompose at lower temperatures. At temperatures higher than 105 ℃, significant rates of cellulose polymer chain scission occur. Above 300 ℃, polymer chains might be completely decomposed and carbonised [1]. A cellulose polymer molecule is shown in Figure 2-2.

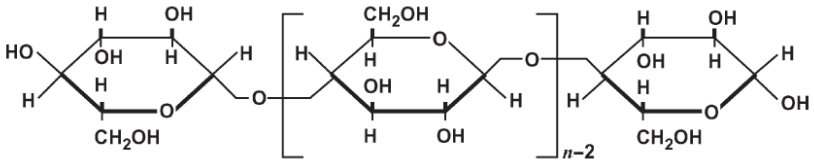

Figure 2-2 Cellulose polymer [19]

The thermal decomposition products of cellulose insulation are carbon oxides (CO and CO2), furanic compounds and water. Carbon oxides generation amount is much larger than those generated by oil oxidation at the same temperature in same period of time [20]. Minor amount of hydrocarbon gases, such as hydrogen and methane, might also be produced due to the impregnated oil [17]. Carbon oxides, as major products of thermal decomposition, increase with temperature, oxygen content of oil and moisture content of paper [20]. The rate at which they are produced depends exponentially on the temperature and on the volume of material at that temperature. Therefore, a large volume of heated insulation at moderate temperature might produce a same quantity of fault gases as a smaller volume of insulation at a higher temperature [17].

2.3.4 Thermodynamic Models for Fault Gas Generation

A theoretical thermodynamic model to assess gas formation from mineral oil was established by Halstead, which was published in 1973 [21]. The model suggested that decomposition gaseous hydrocarbons in mineral oil are in equilibrium with each other under equilibrium pressures at various temperatures. The portion of each gas product

varies with the temperature of decomposition region. This led to the assumption that the generation rate of any particular gas varied with decomposition temperature, and each gas would attain its maximum generation rate at a different temperature [2].

In Halstead's model, the decomposition products are same simple hydrocarbon molecules under different decomposition temperatures. The model system was taken as one in which all the oil molecules involved are totally decomposed to hydrogen, hydrocarbon gases and solid carbons. Each product is in equilibrium with all others. The overall pressure of the system was taken as 1 atm (10^5 N m^{-2}). The oil decomposition was assumed to occur through a series of chemical reactions, which are listed below. All these reactions are reciprocal reactions, and these reactions dominate combination of decomposition products. The equilibrium partial pressures of the various gas reaction products can be calculated using the equilibrium constants for the assumed reactions at temperature between 500 K (226 ℃) and 2000 K (1725 ℃) [21].

$$C(\text{solid}) + 2\,\text{H}_2 \rightleftarrows CH_4$$
$$2CH_4 \rightleftarrows C_2H_4 + 2H_2$$
$$C_2H_4 \rightleftarrows C_2H_2 + H_2$$
$$C_2H_4 + H_2 \rightleftarrows C_2H_6$$
$$C_2H_2 + 2H_2 \rightleftarrows C_2H_6$$

In Halstead's model, partial pressures of decomposition products in the equilibrium system are calculated. In a gaseous mixture equilibrium system, the partial pressure of a particular component is proportional to its amount of substances, i.e. gas in gas concentration. The reason is that in the gas mixture system, all components and overall gas mixture follow ideal gas law [21].

The results of Halstead's model are shown in Figure 2-3, in which the temperature unit is transformed to degree Celsius.

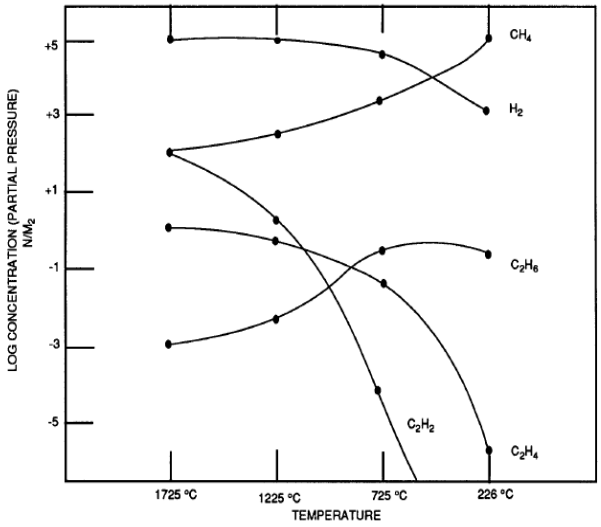

Figure 2-3 Equilibrium partial pressures as a function of temperature in Halstead's model [21]

Initially, in this model, generation of all decomposition products depend on temperature. At low temperature range hydrogen and saturated hydrocarbons (methane and ethane) dominate products combination; while at high temperature range large quantities of unsaturated hydrocarbons (ethylene and acetylene) will be generated. The quantity of hydrogen production is relatively high and less insensitive to temperature than other hydrocarbons. Portions of methane and ethane are relatively high at low temperatures, but will decrease with temperature increasing. Nevertheless, ethylene and acetylene are produced at low portions at low temperatures but increase with temperature increasing. Formation of acetylene becomes significant only at temperatures near 1000 ℃, thus it is regarded as key gas for severe fault condition.

The comparative rates of gas generation can be estimated by a gas generation chart, which is derived from the Halstead's model and demonstrated in Figure 2-4 (a). A new version of comparative gas generation chart was presented in which more detailed information was contained. The new version of comparative gas generation chart is shown in Figure 2-4 (b).

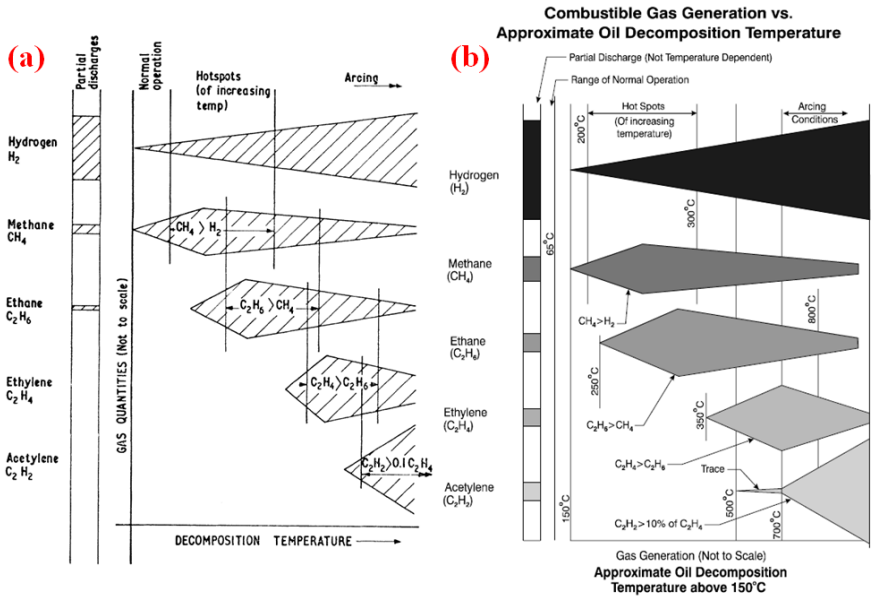

Figure 2-4 Comparative gas generation combination: (a) plotted in [2]; (b) plotted in [22]

These two charts are representative to show gas generation rates of fault gases changing with temperature. The gas generation rates in these charts are not to scale of real values. However, it is powerful to indicate that the gas combination is different at various temperatures. Different temperature levels will be dominated by particular fault gas generation.

A more realistic and comprehensive thermodynamic model was suggested in 1977 [9]. Similar to Halstead's model, this model was on basis of thermodynamic equilibrium, in which all decomposition products are in equilibrium with each other. There are two factors which make the latter model more realistic than Halstead's model. The first is that the decomposition process of different oil components are taken into consideration, for example, decomposition of paraffin, naphthene and aromatics. The second is that the thermal decomposition is categorised into two stages, i.e. primary decomposition and secondary decomposition, according to their different characteristics [9].

In primary decomposition, the decomposition products are in equilibrium with the parent hydrocarbons. When temperature of a hot spot in a transformer is low, or the contact time of oil in the hot spot is short, primary decomposition is dominant in the thermal decomposition. The decomposition products of primary decomposition contain hydrogen and hydrocarbons. Primary decomposition of a paraffinic hydrocarbon molecule is shown

in the following reactions. Products of primary decomposition of other oil components (naphthenic hydrocarbons and aromatics) can be assessed based on same method [9].

$$C_nH_{2n+2} \rightleftarrows H_2 + C_nH_{2n}$$
$$C_nH_{2n+2} \rightleftarrows CH_4 + C_{n-1}H_{2(n-1)}$$
$$\bullet\bullet\bullet$$
$$C_nH_{2n+2} \rightleftarrows C_{n-2}H_{2n-2} + C_2H_4$$

Decomposition products of C20H42 and C10H22 are shown in percentage in Figure 2-5. Both paraffinic hydrocarbons generate similar products under all temperatures. Percentages of saturated hydrocarbons (CH4, C2H6 and C3H8) are higher than those of unsaturated hydrocarbons (C2H4 and C3H6). All gas production quantities are increasing with temperature except for methane whose production is decreasing with temperature.

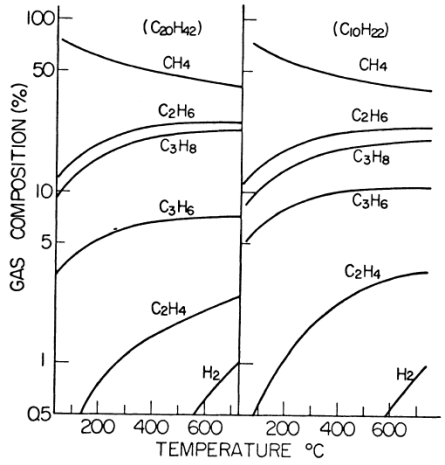

Figure 2-5 Primary decomposition products of C20H42 and C10H22 [9]

In some transformers, the gas composition generated in the primary decomposition of hydrocarbons does not fit with that dissolved in the insulating oil. The thermal decomposition of the oil in these transformers probably includes secondary decomposition. In secondary decomposition, products of primary decomposition will equilibrate with each other based on several chemical reactions. In reality, secondary decomposition always occurs with thermal decomposition of insulating oil. For example, Propane (C3H8) will be decomposed to methane and ethylene under particular temperature, but ethylene might be further decomposed to acetylene and hydrogen. The latter reaction is a secondary decomposition. In this thermodynamic model, all secondary

decomposition can be expressed as if they were primary decomposition. To take propane as an example, thermal decomposition including secondary decomposition can be expressed by the following reactions [9].

$$C_3H_8 \rightleftarrows CH_4 + C_2H_4$$
$$C_3H_8 \rightleftarrows C_3H_6 + H_2$$
$$C_2H_4 \rightleftarrows C_2H_2 + H_2$$
$$2CH_4 \rightleftarrows C_2H_4 + 2H_2$$

Different from primary decomposition, which connects parent hydrocarbons and products, secondary decomposition builds relationship among decomposition products. In other words, secondary decomposition takes thermal decomposition of light hydrocarbons into consideration in assessment of oil decomposition products. Figure 2-6 shows thermal decomposition of 1 mole of some light hydrocarbons. Above 300 ℃, decomposition products are hydrogen and hydrocarbons whose carbon number is less than 4 [9].

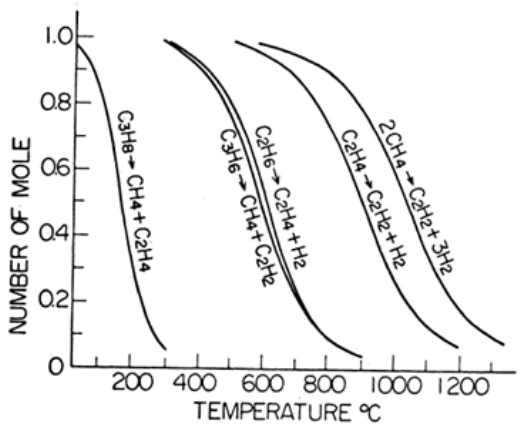

Figure 2-6 Thermal decomposition of some light hydrocarbons in the case of independent reaction [9]

As discussed before, thermal decomposition of oil hydrocarbon molecules can be assessed based on this thermodynamic model, which considered primary and secondary decomposition. Thermal decomposition products of 1 mole C20H42 molecules are shown in Figure 2-7. The C20H42 is a representative oil molecule because the average number of carbons in mineral insulating oil molecules is about 20.

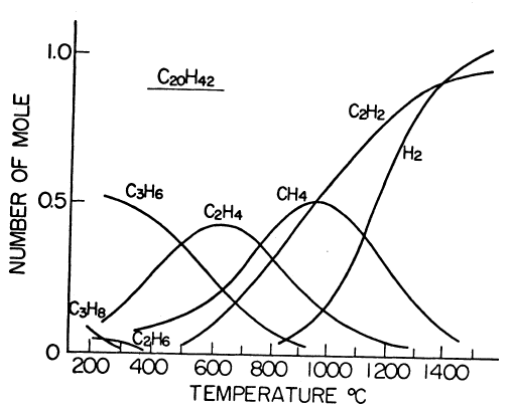

Figure 2-7 Thermal decomposition products of C20H42 under various temperatures [9]

Results of this new thermodynamic model indicate that decomposition products have different initiating temperatures and peak generation temperatures, which has been found in Halstead's model. However, in the new model, generation of ethylene is higher than that of methane at medium temperature range between 300 ℃ and 600 ℃. In addition, ethylene has a peak generation temperature lower than that of methane. These phenomena are different from DGA field experiences, possibly because incorrect parameters used in calculation or some other reasons. In general, this model gives a theoretical basis to the interpretation of fault gas generation from mineral oil.

Secondary decomposition has been found in a recent publication in which fault gas generation in mineral oil under overheating was investigated in laboratory environment. In this work, oil decomposition under low temperature range (100 ℃ – 300 ℃) with 50 ℃ interval between each two fault levels. When comparing average generation rates of ethane and ethylene under different temperatures, it can be found that the increasing ratio of average ethylene generation rate is larger than that of ethane when temperature increased from 250 ℃ to 300 ℃; while the increasing ratio of average ethane generation rate is larger than that of ethylene from 200 ℃ to 250 ℃. This result indicates that more ethane is transformed into ethylene by the secondary decomposition at higher temperature. It is also found that activation energies of methane, ethylene and ethane are larger at higher temperatures than those at lower temperatures. Accordingly it seems that the secondary decomposition of mineral oil is more likely to occur at higher temperatures [9].

2.3.5 Non-fault Related Gases

Gases may be generated in some cases not as a result of faults in the equipment but through rusting or other chemical reactions involving steel, uncoated surfaces or protective paints. Hydrogen may be produced by reaction of steel with water, as long as oxygen is available from the oil nearby. Large quantities of hydrogen have thus been reported in some transformers that had never been energised. Hydrogen may also be formed by reaction of free water with special coatings on metal surfaces, or by catalytic reaction of some types of stainless steel with oil, in particular oil containing dissolved oxygen at elevated temperatures. Hydrogen may also be formed in new stainless steel, absorbed during its manufacturing process, or produced by welding, and released slowly into the oil. Gases may also be produced by exposure of oil to sunlight or may be formed during repair of the equipment. Internal transformer paints, such as alkyd resins and modified polyurethanes containing fatty acids in their formulation, may also form gases. These occurrences, however, are very unusual, and can be detected by performing DGA analyses on new equipment which has never been energised, and by material compatibility tests [1].

Some large power transformers in the field have exhibited a phenomenon that moderate levels of hydrogen are produced when the unit is under over-excitation operation. Investigations on these units, brought back to the factory for extensive testing, showed no corona (PD) problem which is usually associated with hydrogen generation [23]. The hydrogen generation is due to oil decomposition between moderately heated core steel lamination where the hotspot temperature exceeds 130 ℃. Model tests showed that the generation rate is high at first but levels off possibly due to passivation of the core steel surface [23]. It is reasonable that the core lamination is involved in the catalytic decomposition of the oil to produce hydrogen.

2.3.6 Stray Gassing

Unexpected gas generations at low temperatures have been reported since 1990s [24]. Several unusual cases of gassing in service transformers were reported in 2006, in which

generation of hydrogen or hydrocarbon gases might be developed without faults [25]. Hydrogen production might be due to strongly hydro-treated oils as well as transformer materials [25]. Unusual ethylene production was even found in oil of in-service transformer at low temperature [26]. Dissolved gas analysis (DGA) has been used to diagnose transformer faults. Such unusual but common non-fault related gas has been regarded as a drawback to using DGA [27].

The thermal decomposition of oil under low temperature range was defined as "stray gassing". One definition for thermal stray gassing is the formation of gases from insulating mineral oils heated at relatively low temperature (90 ℃ to 200 ℃) [15]. Another is the production of gases at low temperature (< 120 ℃) without thermal or electrical faults, sometimes even without operational stress [28]. It is also noted that inhibited oils typically produce less stray gassing than uninhibited ones [28]. In other presentations and reports it has been suggested more severe refining technology could be responsible for stray gassing [24].

Test procedures of oil stray gassing are suggested in a CIGRE report in 2004 [15]. Stray gassing was performed at 120 ℃ and 200 ℃. Oil samples will be degassed under vacuum, saturated with air or nitrogen by bubbling through the oil. At 120 ℃, oil samples were placed in three 30-mL glass syringes and in an oven. After 16 hours, the first syringe was analysed by DGA to determine the initial stray gassing of the oil. After 164 hours, the second one is analysed to determine if a gassing plateau has been reached [27]. The third one was degassed, re-saturated with air or nitrogen and then put back into the oven for another 16 hours to determine if stray gassing is recurrent after having been heat-treated. At 200 ℃, procedures were same as those at 120 ℃ except that three glass vessels instead of syringes were used [28].

In the 120 ℃ tests, the main gas produced in general was hydrogen, followed by methane. Gas formation was commonly higher in the initial 16 hours of tests. During the following 164 hours, the rate of gas formation was reduced. The gas generation plateau therefore appeared to be related not only to the reduction in oxygen content of the tested oil but also to the type of oil [15]. Similar plateau phenomenon was also found in other publications [23, 25]. Gas generation in the final 16 hours tests appeared to be recurrent

[15]. In the tests, oil samples from a same brand manufactured before and after the year 2000 have been tested together. Stray gassing behavior had changed dramatically between those two samples, possibly as a result of different crude oils and refining techniques used [15].

In the 200 ℃ tests, the main gases produced were methane and ethane, then hydrogen and ethylene. Normally ethylene is considered as products of oil decomposition under medium or high temperature ranges [1, 21]. However, in stray gassing investigations, ethylene was also found to be produced [15, 24, 26]. The reaction mechanism at 120 ℃ and 200 ℃ seems to be quite different. Gassing also reached a plateau but didn't appear to be recurrent [15].

Depending on the type of oil, stray gassing in service may be mistaken as partial discharge faults. However, it can be distinguished by examine the methane/hydrogen ratio of gases formed in service [15].

The mechanisms of stray gas formation are not known for sure. It is considered to be related to oxidation or weaker chemical structures left in the oil after refining [15]. The generation of hydrocarbon gas was observed to be related to the water content of paper/oil [27]. Another investigation found that uninhibited oil, or oil with only natural inhibitors, consumed more oxygen and generated more stray gasses than inhibited oil. It was also found that severely hydro-treated naphthenic based oil generated less stray gases [24]. Stray gassing is also considered to be related to oil oxidation [29].

2.4 Sampling of Oil by Syringe

Sampling oil from transformer is the first step of DGA method. Oil from transformers could be sampled by bottles, syringes and ampoules. Sampling with syringe and bottles are techniques widely used to take oil samples from transformers. The syringe sampling method is recommended by IEC standard and represents best industry practice. In this thesis, the syringe sampling method is used as the bottle sampling method is concerned inaccurate for DGA measurement [30]. Oil samples are usually taken at the bottom of the tank or from the drain valve. For special purposes, it can also be sampled at the top of the

tank, from the radiators or the gas relay. The filled syringe will be sent to the analytical laboratory [30].

Methods and procedures of sampling oil from oil-filled equipment are documented in IEC standard [30, 31]. Suggested apparatus are syringe, ampoule or bottle. In this thesis, only sampling procedures with gas-tight syringe is introduced, which is shown in Figure 2-8 because it is the most popular method. Firstly, a gas-tight syringe with enough capacity will be connected to sampling valve of the transformer. Normally volume of syringe ranges from 20 mL to 250 mL is required for DGA oil sampling. Then the syringe will be flushed by oil sampled in first round as shown in Figure 2-8 (b) – (c). After purging the flush oil out, formal oil sample will be taken and sealed by the stopcock. Finally, the oil sample will be sent to laboratory for further analysing. Air bubbles in syringe should be purged out as much as possible since it will affect DGA accuracy. Some other influences on oil sample transportation and storage should be avoided, such as light and storage temperature.

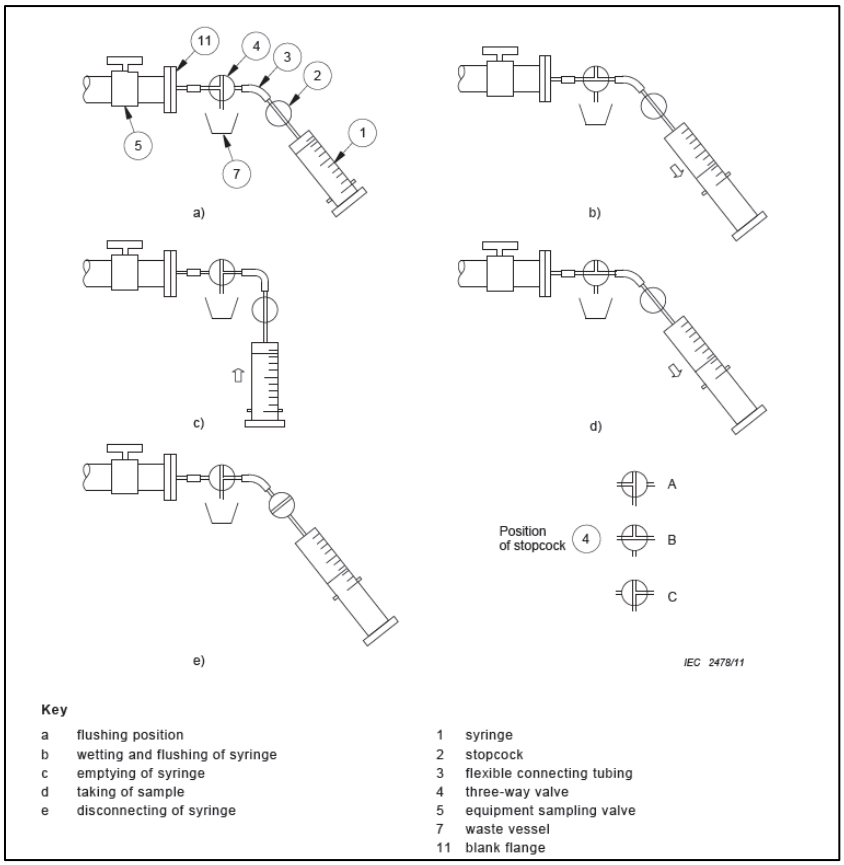

Figure 2-8 Oil sampling procedures by syringe [30]

2.5 DGA Data Interpretation Methods

Once dissolved gases are extracted and analysed, combination of dissolved gas concentration (DGA fingerprint) is obtained. Main gases formed from transformer electrical and thermal faults are H2, CH4, C2H6, C2H4, C2H2, CO and CO2. Interpretation of DGA fingerprint is necessary to make effective diagnosis of transformer condition. Various data interpretation methods have been proposed and developed. According to gas formation mechanism, types and combination of some fault gases can indicate fault type and level. Therefore, DGA data interpretation method can be divided into two types: percentage and ratio. Percentage based interpretation methods take all or part of fault gases into consideration, but pay more attention on specific gas types. However, ratio based interpretation methods rely on ratio and relationship between certain gases, in order to understand fault type. Popular DGA data interpretation methods include Key Gas Method, Doernenburg Ratio Method, Rogers Ratio Method, IEC Ratio Method and Duval Triangle Method. Novel artificial intelligence based data interpretation techniques, such as Fuzzy logic [32] and neural network [33, 34] have been developed recently.

Key Gas Method

Key Gas Method is a percentage based method, which diagnose fault type from dominant gas. In theory, fault gases generation originates from chemical bonds breaking in molecules of insulating material. Previous discussion about dependence of decomposition gases on temperature proves that determination of fault type from gases can be approached by dominant gas type. Figure 2-9 shows charts of Key Gas Method, which contains overheating of oil, overheating of cellulose, partial discharge in oil and arcing in oil. These four common fault types are distinguished by percentage combination of total dissolved combustible gases (TDCG).

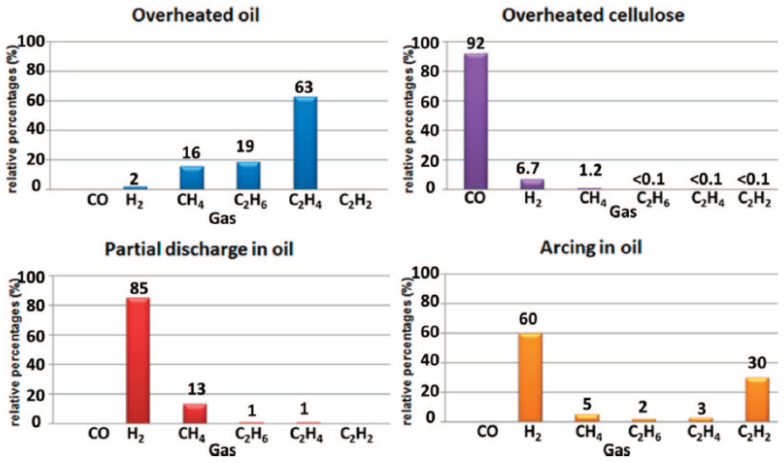

Figure 2-9 Charts of Key Gas Method [17] (replotted by [34])

According to thermodynamic theory, gas generation is a stochastically process, which relies on intensity of dissipation energy. Moreover, situation is more complicated in real life. Different transformer has different insulation configuration, such as oil-paper ratio, winding structure, conductor design and so on. Therefore, even various fault types in the Key Gas Method such as "Overheated oil" or "Arcing in oil" in different transformers can hardly generate same fault gas patterns as given in Figure 2-9. Assessment based on IEC database of faulty transformers shows that Key Gas Method has only 42% accuracy [34]. However, the Key Gas Method is a straightforward method which provides general fault gas combination patterns of four major transformer fault types [35].

Rogers Ratio Method

Apart from percentage based interpretation techniques, various ratio based method are also well accepted [2]. Doernenburg Ratio Method, Rogers Ratio Method and IEC Ratio Method are very famous among those methods. According to the aforementioned thermodynamic model of mineral oil, theoretically, either ratio between two hydrocarbon gases can be regarded as an indicator. Different ratio combination and threshold values are applied in each ratio method. Rogers Ratio Method is introduced in detail, since it is one of the most common used DGA interpretation methods, especially in UK, which is proposed by Rogers. Doernenburg Ratio Method is required by the concentration of combustible dissolved gases exceed an L1 concentrations. The L1 concentrations are defined as special gas concentrations values used to ascertain whether there really is a

problem with the unit and then whether there is sufficient generation of each gas for the ratio analysis to be applicable [14]. The L1 concentrations are listed in Table 2-4 [14].

Table 2-4 L1 Concentrations for Doernenburg Ratio Method [14]

Key Gas	H2	CH4	CO	C2H2	C2H4	C2H6
L1 Concentrations (ppm)	100	120	350	1	50	65

These concentration limits are same as Condition 1 defined concentration values. Condition 1 is considered as boundary of normal operation [14]. If total combustible gases content are higher than Condition 1, or increasing rate is higher than certain value, further analysis is required. Another suggested threshold concentration values are 90% typical concentration values. However, fault gas generation depends on transformer design, loading profile and even local condition, such as weather and temperature. Moreover, different DGA method will bring different typical values for same network [36]. Therefore, trend analysis is suggested as preference for transformer condition monitoring rather than typical values.

Originally, four gas ratios are used in Rogers Ratio Method, namely C2H6/CH4, C2H2/C2H4, CH4/H2 and C2H4/C2H6, leading to 12 suggested results [2]. However, C2H6/CH4 ratio was proved of little interpretation value. This ratio was ignored in revised Rogers Ratio Method. Original 12 proposed diagnoses were simplified by 6 results, including normal operation. Accuracy of this method is lower than Duval Triangle, which is 58.9% for correct fault type interpretation [2]. Table 2-5 shows the revised Rogers Ratio Method criteria.

Table 2-5 Revised Rogers Ratio Method for DGA Interpretation [2]

Case	C2H2/C2H4	CH4/H2	C2H4/C2H6	Fault Diagnosis
0	< 0.1	> 0.1 to < 1	< 1	Normal
1	< 0.1	< 0.1	< 1	Lower energy density PD
2	0.1 to 3	0.1 to 1	> 3	Arcing
3	< 0.1	> 0.1 to < 1	1 to 3	Lower temperature thermal fault
4	< 0.1	> 1	1 to 3	Thermal fault < 700 ℃
5	< 0.1	> 1	> 3	Thermal fault > 700 ℃

IEC Ratio Method uses three same ratios as in Rogers Ratio Method, but different values are proposed for diagnosis. Additionally, another gas ratio, C2H2/H2, was suggested to

monitor condition of on-load tap changers. Moreover, graphical representation for IEC Ratio Method has been developed based on 2-D and 3-D charts. Similar as Duval Triangle, graphical representation is direct and clear to show boundaries of fault types. Table 2-6 shows IEC Ratio Method values and diagnoses.

Table 2-6 IEC Ratio Method for DGA interpretation [1]

Case	Fault Diagnosis	C2H2/C2H4	CH4/H2	C2H4/C2H6
PD	Partial discharges	NS	< 0.1	< 0.2
D1	Discharges of low energy	> 1	0.1 – 0.5	> 1
D2	Discharges of high energy	0.6 –2.9	0.1 – 1	> 2
T1	Thermal faults T < 300 ℃	NS	> 1 but NS	< 1
T2	Thermal faults 300 ℃ < T < 700 ℃	< 0.1	> 1	1 – 4
T3	Thermal faults T > 700 ℃	< 0.2	> 1	> 4
NS = not significant whatever the value.				

The 3-D graphical representation of IEC Ratio Method is shown in Figure 2-10 . As ratio based interpretation method, IEC Ratio Method has lower accuracy than Duval Triangle [37]. However, since ratio based method has its diagnosis range, which can be found as "blanket" area in Figure 2-10, some fault cases may have no prediction in ratio methods. Therefore, IEC Ratio Method and Rogers Ratio Method have high accuracy of prediction, rather than diagnosis [33, 38].

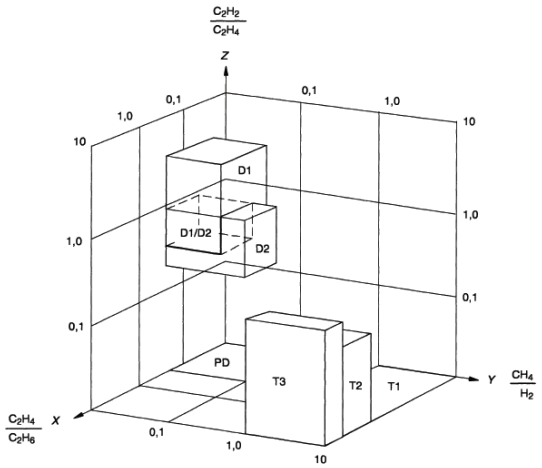

Figure 2-10 Graphical representation of IEC Ratio Method in 3-D chart [1]

Duval Triangle

A general rule in DGA gas formation is that the unsaturation degree of fault gases is related with fault energy density. For example, Triple bond gas, acetylene (C2H2), is considered to be generated at most severe fault, such as arcing. Double bond gas, ethylene (C2H4), can be generated under thermal faults. Single bond gas, methane (CH4) can be detected even under operational temperature. In Duval Triangle method, only these three hydrocarbon gases are considered. Relative percentage of each component was obtained through transformer inspection and laboratory simulations.

First version of Duval Triangle was introduced and revised in 1980s [39]. Figure 2-11 shows a latest version of classic Duval Triangle. Fault zones are: PD = partial discharge; D1 = discharges of lower energy; D2 = discharges of high energy; T1 = thermal faults of temperature T < 300 ℃; T2 = thermal faults of temperature 300 ℃ < T < 700 ℃; T3 = thermal faults of temperature T > 700 ℃; DT = mixtures of electrical and thermal faults.

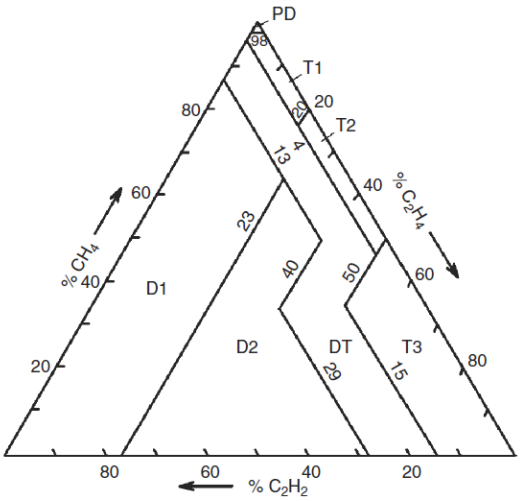

Figure 2-11 Classic Duval Triangle for mineral oil immersed transformers [40]

This method is well accepted, partially because fault diagnosis is directly reflected using graphical presentation. In addition, since this method was developed from IEC database and some laboratory simulations, it provides higher accuracy than other methods [33].

Operation of load tap changers (LTC) involves more frequent arcing than main tank of power transformer [41]. A new triangle, Duval Triangle 2, was developed for oil type LTC diagnose based on classic Duval Triangle [40]. Similar as classic Duval Triangle,

boundaries in Duval Triangle 2 rely on published inspected cases of transformer faults based on IEC database. Other fault cases also show accordance of this diagnosis method [42]. Figure 2-12 shows Duval Triangle 2. Different electrical fault diagnosis areas are shown in this method: N = normal operation; X1 = abnormal arcing D1 or thermal fault in progress; D1 = abnormal arcing D1; X3 = fault T2 or T3 in progress with light coking or increased resistance of contacts, or severe arcing D2.

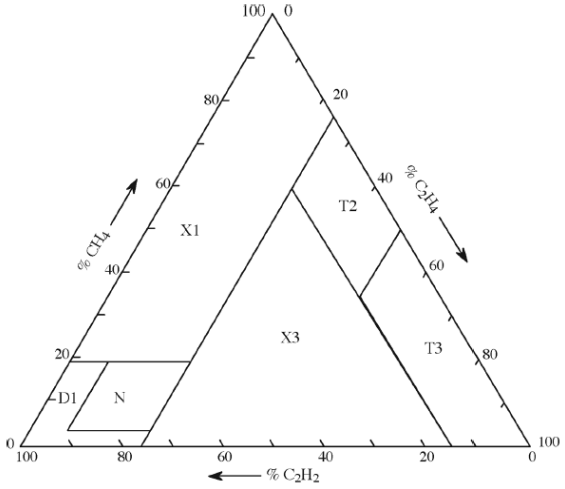

Figure 2-12 Duval Triangle 2 for oil type LTC interpretation [40]

Although mineral oil is still widely used as transformer insulating liquid, alternative liquids are increasingly used because they are environmentally friendly and less flammable. New versions of Duval Triangle for non-mineral oils are developed, such as silicone oil, natural ester (FR3 and BioTemp) and synthetic ester (MIDEL). Since these alternative fluids are currently not widely used in transformers, lack of fault experiences exist for developing the method. Duval Triangles for these non-mineral oils were proposed based on several laboratory simulations [43, 44]. Duval Triangle for synthetic ester oil (MIDEL) is shown in Figure 2-13 as an example, in which the boundaries of some fault types were adjusted. However, same fault gases for diagnosis are used as in classic Duval Triangle.

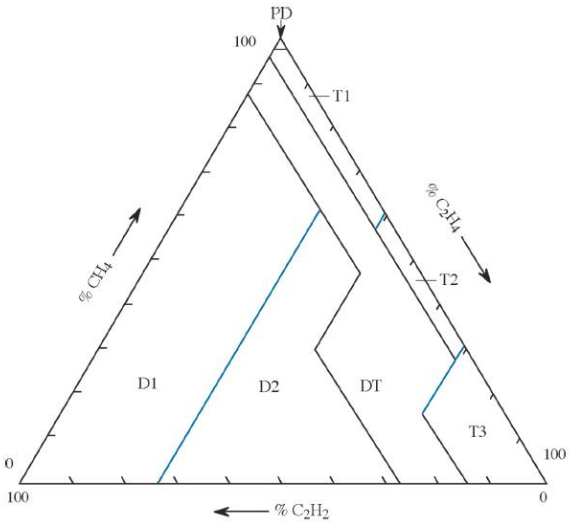

Figure 2-13 Duval Triangle for fault interpretation in MIDEL [40]

In addition, there are Duval Triangles for low temperature faults [40]. In transformer condition monitoring, low temperature faults are difficult to distinguish from normal operation. Moreover, stray gases are generated as dissolved gases. Thermal stray gassing is defined as the formation of gases from insulating oils at relatively low temperatures from 90 ℃ to 200 ℃. Stray gassing is regarded as unexpected phenomenon, and has been report by several publications. Therefore, Low temperature faults Duval Triangles are now the only published DGA interpretation which include stray gassing phenomenon. The developing methodology of new Duval Triangle versions, especially those for alternative insulating fluids, is valuable. Laboratory simulation is effective in assessing fault gas generation in alternative fluids, which there are seldom in-service experience.

A new complementary tool for DGA interpretation, Duval Pentagon, was published recently [45]. In this method, all hydrocarbon gases and hydrogen are included. Apart from fault types considered in classic Duval Triangle, stray gas effect is also taken into consideration. Similar as Duval Triangle, boundaries of this new Pentagon are estimated by on-field transformer experience. Since this is a new published method, efficiency and accuracy are not proved by other research works. However, this method is so far a brilliant combination of Key Gas Method and Duval Triangle series, whose interpretation depends on both all hydrocarbon gases and fingerprint (percentage) of all faulty gases. Duval Pentagon is compatible with oil fault only, because no carbon oxides are included.

2.6 Review of Previous DGA Laboratory Studies

Thermal faults are generally simulated by three methods: immersed heating, tube heating and oven heating. Immersed heating is the most popular method, in which the heating element will generate thermal fault in tested oil sample. Usually metal wire will be used as heating element in order to reach high temperature. The limitation of this method is melting of heating element. Tube heating method heats oil with tubing in furnace. In this method, temperature can be gradually controlled. However, heating energy is difficult to estimate in this method. Moreover, only small portion of test oil is heated. Oven heating method is popular in evaluating fault gas generation under low temperature thermal stress. In this method, test oil will be heated in oven with headspace vials or bottles. Because of low flash point of mineral oil, this method is commonly used for thermal fault below 150 ℃, such as investigating stray gassing.

2.6.1 Fault Simulation Method I – Immersed Heating Method

A typical immersed heating setup is shown in Figure 2-14. A sealed test vessel was built with clamps and conductors on the lid. Heating element was immersed in test oil. Generated gas was collected by a reversed funnel leading to a measuring burette and gas chromatography. Heating wire was made of Constantan which is a copper-nickel alloy. It usually consists of 55% copper and 45% nickel. It allowed a local heating up to 1000 ℃. In addition, an equalising vessel was fit to relieve heating expansion pressure. There are three major limitations in this setup. The first one is that it could only analyse the free gas generation rather than dissolved gas. The second one is that the dissolved gas might leak from the equalising vessel. The third one is that the heating element temperature could not be measured or controlled.

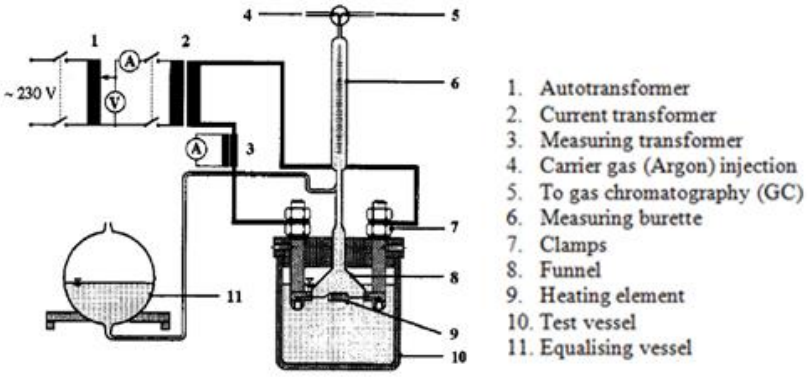

Figure 2-14 Test setup for localised thermal DGA experiment [46]

In this work, ester liquid and mineral oil were both tested. Undissolved gases after 1000 ℃ thermal fault are shown in Figure 2-15.

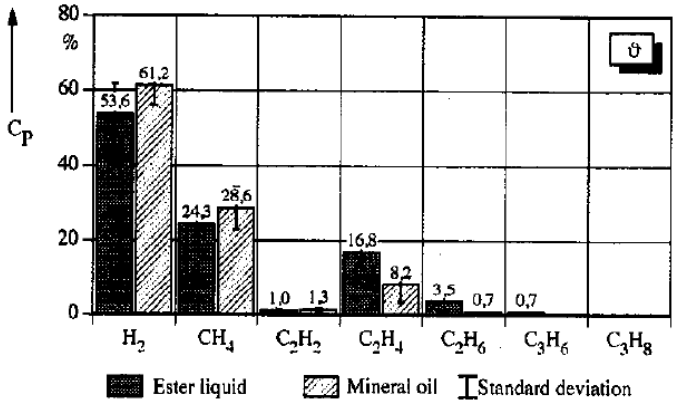

Figure 2-15 Concentration of undissolved gases after 1000 ℃ thermal fault in natural ester oil and mineral oil [46]

Hydrogen and hydrocarbon gases were generated in both fluids in similar gas pattern. Hydrogen generation was higher than 50% in both fluids as major indication gas in dissolved gas analysis (DGA) method. Methane (CH4) and Ethylene (C2H4) were key gases in both liquids. Since the results reflected undissolved gases, gas pattern should be different due to different solubility. For example, hydrogen and methane are light gases. Therefore, hydrogen and methane reported in Figure 2-15 might be higher than gas pattern of dissolved fault gases.

Another group localised thermal fault experiments was approached in University of Stuttgart [47-49]. A localised thermal fault test vessel as shown in Figure 2-16 was built.

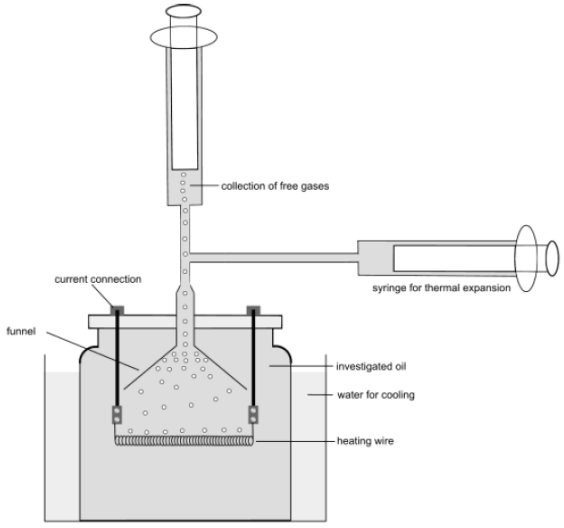

Figure 2-16 Experimental setup for localised thermal fault [48]

Heating wire was 0.6 mm diameter and length varied from 10 to 50 cm depending on heat output. In experiment with mineral oil, maximum temperature of heating element was 400 ℃. However, in natural ester liquid, maximum temperature reached 600 ℃, probably because higher viscosity of natural ester prevent heating energy dissipation. In this work, a gas tight syringe was used to collect test sample, and another syringe was used for thermal expansion. The whole vessel was coated in water for cooling [48]. This experimental setup could collect oil and gas for DGA measurement. However, the limitation of this setup is that the oil is sampled at the top of the vessel which might distort the DGA results if there is free gas get involved in the syringe. In addition, the temperature of the heating element is not measured.

A larger volume glass cylinder was used to evaluate gas generation of hotspot in transformer. As shown in Figure 2-17, a 15 litres vessel with heating wire in the middle of cylinder was designed for this test. Because oil volume was large compared with heating energy, expansion vessel was not fitted. Heating temperature was set at 300 ℃, 500 ℃ and 700 ℃. Duration of heating lasted from several hours to several days depending on fault level. The limitation of this setup is that the heating element temperature is not measured. Besides, the free gas generation under fault is ignored.

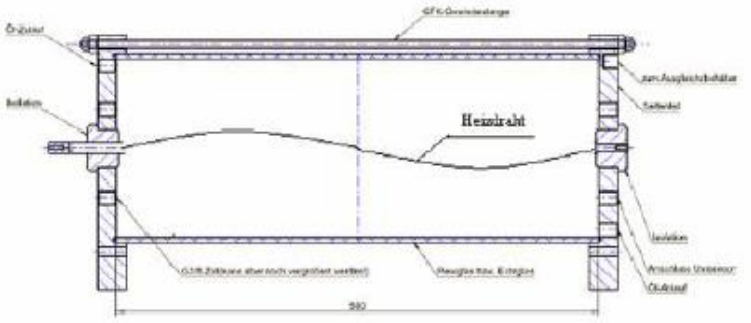

Figure 2-17 Large volume hotspot thermal experimental setup [47]

Figure 2-18 shows fault gases generation rate under localised thermal faults at 300 ℃, 400 ℃, 500 ℃ and 600 ℃ in natural ester oil.

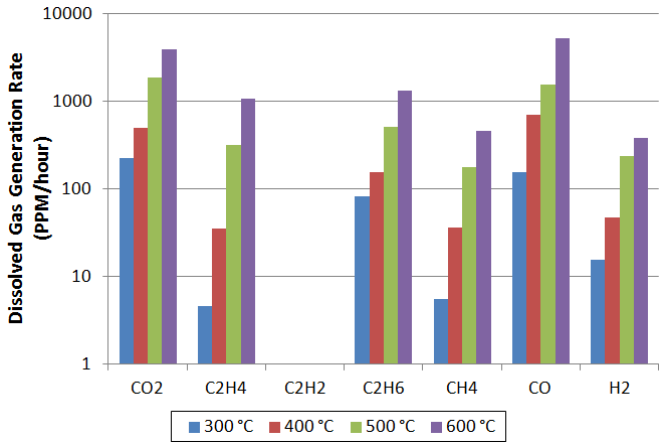

Figure 2-18 Dissolved gas generation rate in natural ester oil under thermal faults [48]

Almost all fault gases generation rates are increasing logarithmic linear. Ethane (C2H6) is dominant in hydrocarbon gases under all temperatures. In addition, similar as in mineral oil, methane (CH4) is generated more than ethylene (C2H4) under 300 ℃ and 400 ℃, but reversely under 500 ℃ and 600 ℃. These performances might be caused by hydrocarbon chains in ester molecules. Different from that in mineral oil, carbon oxides are generated even more than hydrocarbons.

Gas generation profile in mineral oil is plotted in Figure 2-19. Methane (CH4) is key hydrocarbon gas under 300 ℃, but under 400 ℃ ethylene (C2H4) is key hydrocarbon gas. Carbon oxides might be produced by oxidation of heating element.

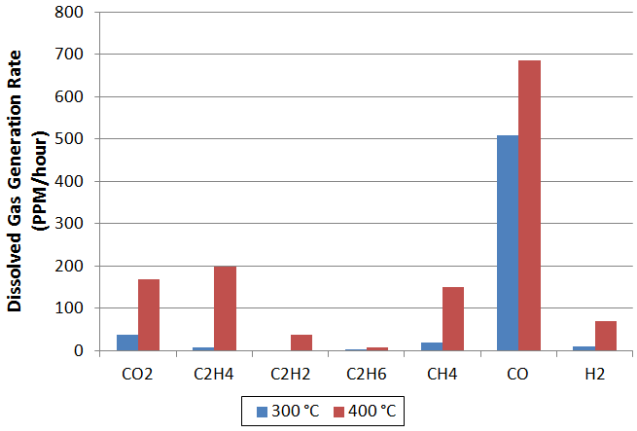

Figure 2-19 Dissolved gas generation rate in mineral oil under thermal faults [48]

Gas generation patterns in the large tank hotspot thermal test are shown from Figure 2-20.

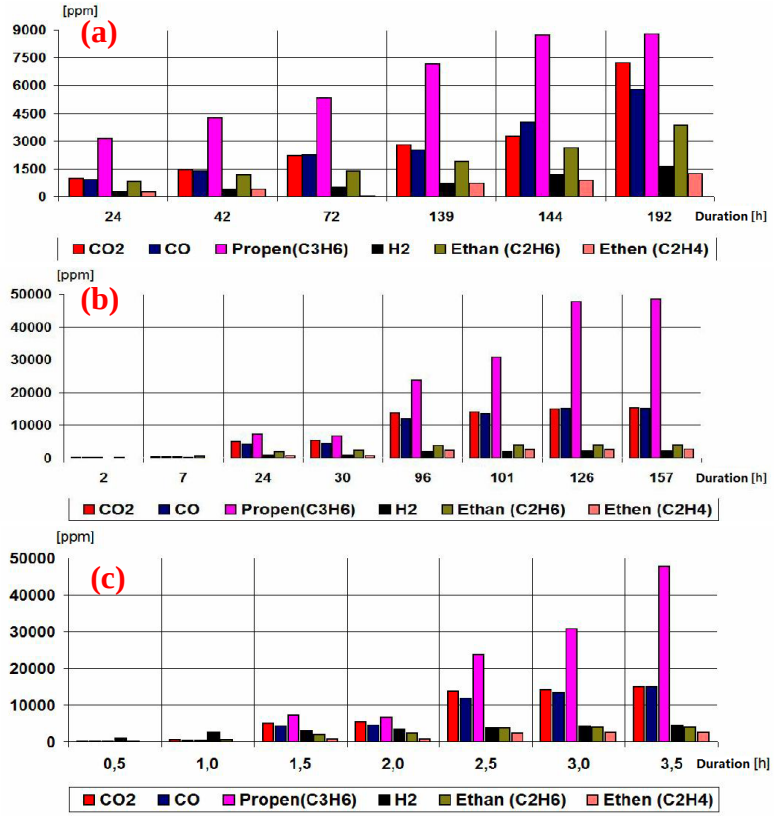

Figure 2-20 Dissolved gas generation in natural ester oil: (a) at 300 ℃ thermal fault; (b) at 500 ℃ thermal fault; (c) at 700 ℃ thermal fault [49]

Gas generation is linear related to fault duration. Under 300 ℃, ethane (C2H6) and carbon oxides are key gases, and small amount of ethylene (C2H4) is generated. Under 500 ℃ thermal faults, gas generation rates for all gases are higher than in 300 ℃. Ethane (C2H6) and ethylene (C2H4) are generated as thermal indicators. However, carbon

oxides are generated much higher than hydrocarbons. At 700℃ thermal fault, gas generation rate is 50 times higher than in 500℃. Key gases are similar as before. In addition, in this work, propene (C3H6) was detected as fault gas. It is proved that propene is also increased with heating duration.

Another localised thermal fault experiment was done in University of Manchester [18]. Online DGA monitor was used in this work for gas detection. Test setup is shown in Figure 2-21.

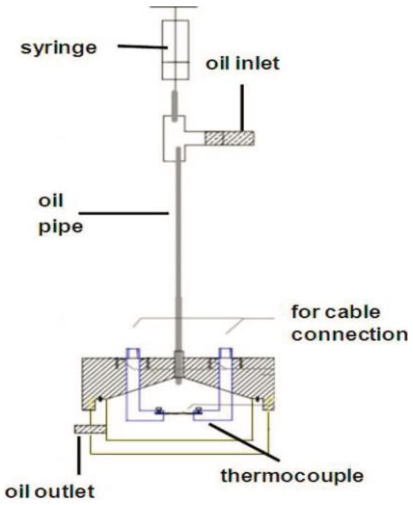

Figure 2-21 Localised thermal fault simulation experimental setup [18]

A sealed circulatory platform was established with test cell and online DGA device of two litres volume. A syringe was installed at top of test setup. Free gas bubbles were purged by this syringe during oil filling process. During thermal expansion, syringe worked as expansion vessel to relieve expansion pressure. The online DGA monitor circulated oil from bottom oil outlet valve and return test cell from top oil inlet valve, which helped fault gas distribution during experiment. A copper wire was used as heating element. Same as previous experimental setup, in mineral oil, only 400℃ can be approached. More electrical energy injection will lead to heating element melting. In natural ester oil, up to 600 ℃ temperature thermal fault can be obtained. In this setup, the oil is mixed by circulation. The limitation in this setup is that the temperature of the heating element is not accurately measured due to the heating element design.

In this work, natural ester oil and mineral oil were both tested. Fault gas generation rates at various fault temperatures are shown in Figure 2-22. Temperature was controlled at

300 ℃, 400 ℃, 500 ℃ and 600 ℃. All gases generation rates, except for acetylene (C2H2), were in logarithmic relation with fault temperature. Same as the work in University of Stuttgart, ethane (C2H6) is key gas. Methane and ethylene are also key gases. At 600 ℃, small amount of acetylene (C2H2) was found generated, possibly due to the local high temperature hotspot. In addition, compared with hydrocarbon gases, carbon oxides were generated at higher rate.

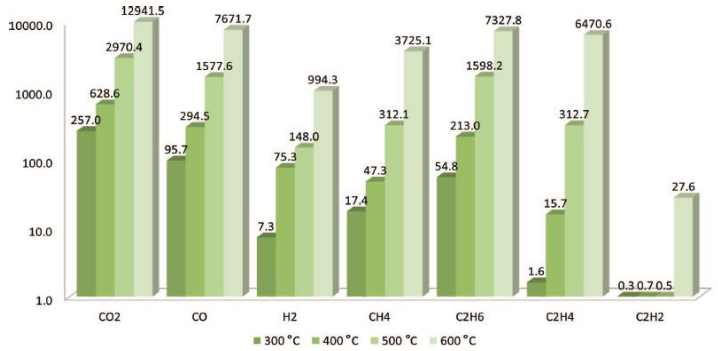

Figure 2-22 Dissolved fault gas generation rate (ppm/hour) in natural ester oil [18]

Fault gas generation patterns under thermal faults in mineral oil are shown in Figure 2-23.

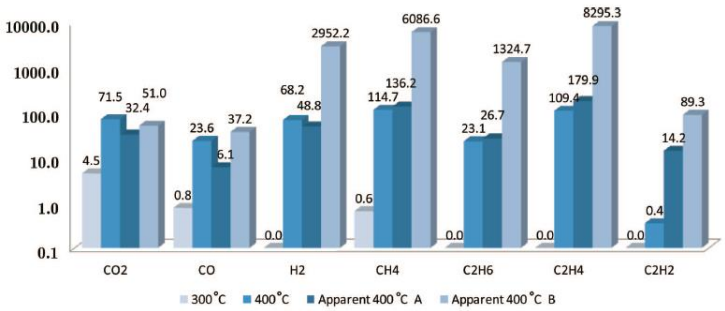

Figure 2-23 Dissolved fault gas generation rate (ppm/min) in mineral oil [18]

In this work, 300 ℃ and 400 ℃ thermal fault levels were approached. In the other two fault levels, although temperature readings from thermometer were 400 ℃, hotspot temperatures were much higher due to the melting of heating element. Estimated maximum temperature was 1100 ℃, which is the melting point of copper. Gas generation rate largely increased from 300 ℃ to 400 ℃. At 300 ℃, only methane (CH4) was produced as T1 fault key gas. Ethylene (C2H4) was dominant in gas generation at 400 ℃, followed by methane and small amount of ethane (C2H6). In "Apparent 400 ℃" fault level, ethylene was still dominant gas indicator, but obvious acetylene (C2H2) generation was detected, which reflected the extremely high temperature. Hydrogen (H2) generation

started from 400 ℃, which implies that hydrogen is not effective at 300 ℃ thermal fault. Moreover, carbon oxides were found in all fault levels at similar generation rate, probably due to oxidation of heating wire.

2.6.2 Fault Simulation Method II – Tube Heating Method

TJH2B has built up a tube heating method based setup for thermal gas investigation [50]. Figure 2-24 shows experimental test setup of this work. A main tank with defined volume gas space and oil space connected with an expansion chamber. The expansion chamber was maintained at atmosphere pressure. Small tube was installed in a heating oven, and circulated with a pump. Pressure in gas space was monitored by a pressure gauge in order to calculate gas generation. Temperature was controlled by oven thermometer. The limitation of this setup is the temperature of the heated oil is not measured and only controlled by the furnace.

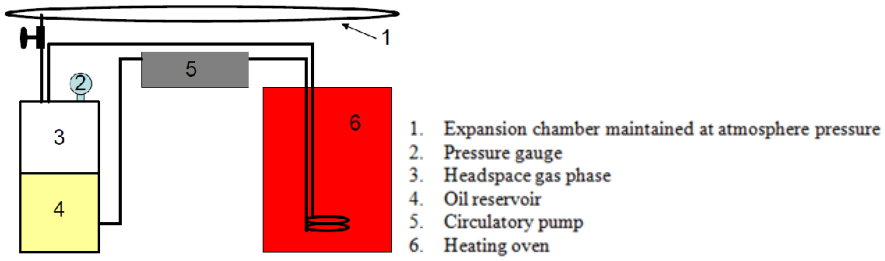

Figure 2-24 Tube heating method based experimental setup [50]

Dissolved gas generation pattern is shown in Figure 2-25 as percentage relative to total dissolved combustible gas (TDCG).

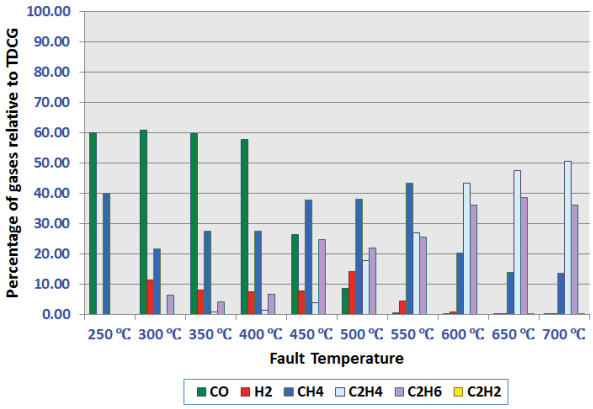

Figure 2-25 Dissolved gas generation in TJH2B tube heating test platform [50]

In this representation method, gas pattern and key gas are clear to study. Advantage of tube heating method can be seen in this result, which is continuously changing temperature from 250 ℃ to 700 ℃ with 50 ℃ interval. In DGA fingerprint, methane (CH4) was dominant gas up to 550 ℃. At temperature above 550 ℃, ethylene (C2H4) was produced more than methane. Therefore, methane is regarded as key gas for T1 thermal fault, and ethylene for T3 thermal fault. Ethane (C2H6) was found higher than 20% between 450 ℃ and 700 ℃. In addition, hydrogen (H2) generation percentage decreased above 550 ℃. Possibly hydrogen is indicator for all types of faults, but not a diagnostic gas for thermal fault levels.

Another example of tube heating method is shown in Figure 2-26. This DGA test platform was established in Chongqing University (CQU) [51]. The limitation of this setup is that the oil is being heated above the container which might lead the oil flow back to the container. In addition, the temperature of the heated oil is not measured.

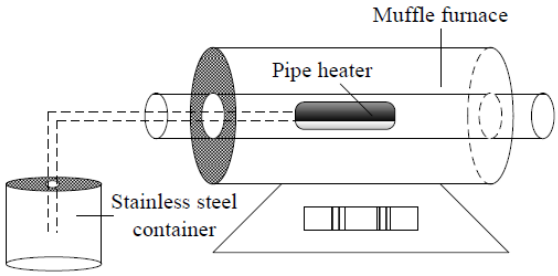

Figure 2-26 Sketch of CQU tube heating thermal fault simulation system [51]

A five litres main tank was filled with test oil. A special L-shape stainless steel tube was connected on the top of main container. The other side with 30 ml oil was located in a muffle furnace as thermal simulation. Temperature of thermal heating was ranging from 300 ℃ to 800 ℃ with a 100 ℃ interval. Duration of fault simulation varied from 2.9 minutes to 15 minutes depending on fault level.

In this work, mineral oil and natural ester oil (FR3) were both tested. Figure 2-27 shows results of all experiments as percentage of hydrocarbon gases.

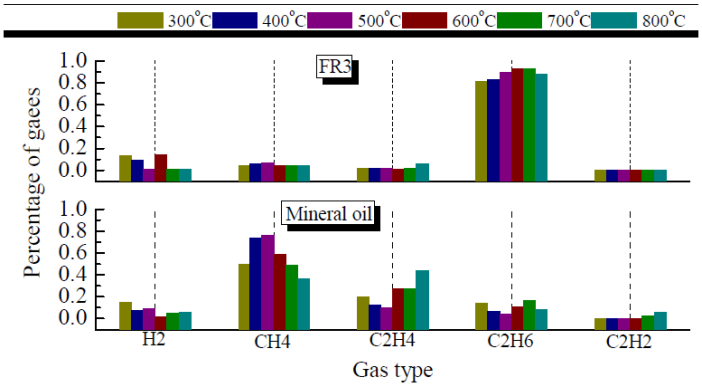

Figure 2-27 Relative percentages of dissolved hydrocarbon gases [51]

In natural ester oil, ethane (C2H6) was found dominant for all temperature levels. Small percentage of methane (CH4) was found generated between 300 ℃ and 500 ℃. Ethylene (C2H4) was produced between 500 ℃ and 800 ℃. In all fault temperatures, hydrogen (H2) was generated, which proves that hydrogen can be regarded as fault indicator for all fault levels. However, in mineral oil, methane and ethylene were key gases. Methane was dominant in gas generation but decrease in percentage from 500 ℃. On the other hand, small percentage of ethylene was produced from 300 ℃, but increased from 500 ℃. Therefore, methane and ethylene are proved as thermal fault indicators. Moreover, hydrogen is also fault indicator. And trace amount of acetylene (C2H2) generation began from 700 ℃.

2.6.3 Fault Simulation Method III – Bottle Heating Method

A typical overall heating method based test setup is shown in Figure 2-28.

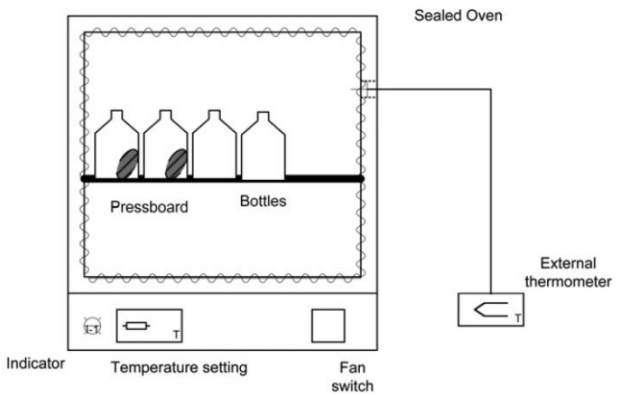

Figure 2-28 Bottle heating method DGA overheating test setup [52]

This experiment was performed in University of New South Wales [52]. In this work, dried, normal and wet mineral oil and natural ester oil were tested in this work. Special designed bottles for use at vacuum or extreme pressure conditions were used to heat oil sample in oven. Temperature was maintained between 130 ℃ and 140 ℃ for 96, 150 and 204 hours. Temperature setting was limited by flash point of mineral oil. Another experiment up to 200 ℃ was done in only natural ester oil because this temperature is still safety for natural ester liquid. Pressboard samples were placed in some of those bottles, in order to study influence of pressboard in gas generation under overall heating thermal fault. A small gas space was necessary for oil thermal expansion. Argon gas was filled in the headspace of the bottle, and bottles were gas tight sealed. Fault gas generation patterns in two types of oil with and without pressboard are shown in Figure 2-29 and Figure 2-30.

L1 limit in DGA diagnostic method is defined as boundary between normal operation and fault occurrence in a transformer in a DGA diagnostic method. It is a set of gas concentrations which is also known as limit of normal operation. If any gas concentration for a transformer is above L1 limit of a specific diagnostic method, it is considered effective. Otherwise, the diagnosis of the method is considered unreliable [22]. In Figure 2-29 and Figure 2-30, the L1 limit of Duval Triangle method is plotted.

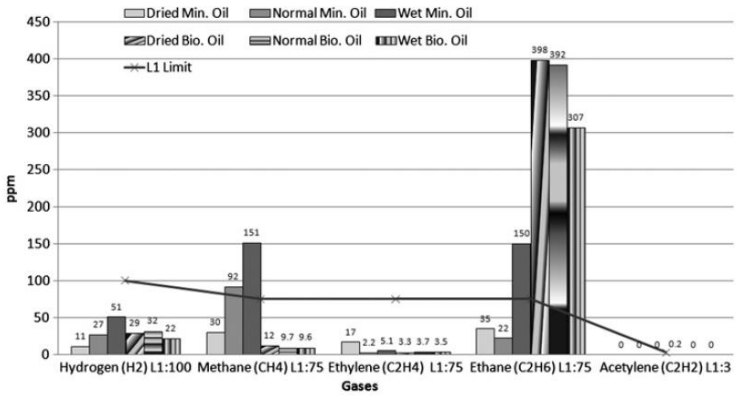

Figure 2-29 Dissolved gas generation in mineral oil and natural ester oil under thermal fault without pressboard [52]

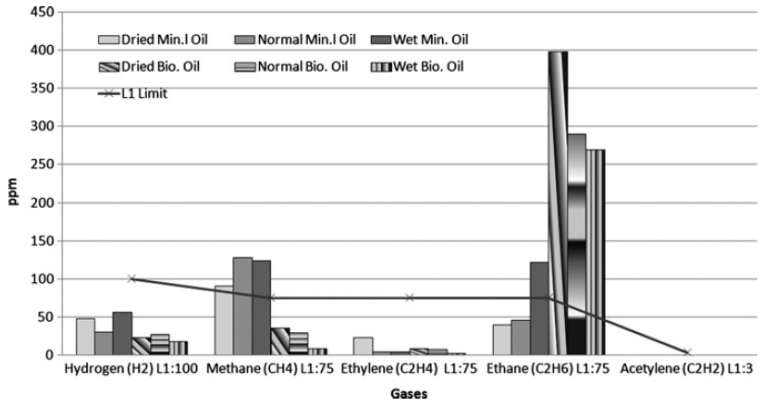

Figure 2-30 Dissolved gas generation in mineral oil and natural ester oil under thermal fault with pressboard [52]

Fault temperature is below between 130 ℃ and 140 ℃. According to definition of Cigre report, stray gas is defined as gas generation under overheating at temperature below 200 ℃. This work investigated stray gas generation instead of localised thermal fault above 300 ℃. Therefore, key gases generated in mineral oil were hydrogen, methane and ethane, which are stray gases found by several publications. In mineral oil, gas generation is influenced by moisture content. In some cases, fault gas concentration is lower than L1 concentration limit, which further proves that L1 concentration limit is not effective.

Compared with mineral oil, natural ester generated lower amount of methane, but much higher amount of ethane. Different from in mineral, moisture has reverse effect on key gases generation. Gas patterns in oil sample with pressboard are general similar to those without pressboard. Moreover, ethylene was generated in all cases at trace levels, and the amount of this gas is not affected by moisture content or pressboard.

The limitation of this heating method is that it could not simulate thermal fault above the oil flash point due to safety consideration. In addition, leakage might be caused during experiments due to the overpressure in the bottle caused by thermal expansion.

2.6.4 Comparison among Different Thermal Fault Simulation Methods

In general, there are three methods to simulate thermal faults in DGA experiments in laboratory environment. The advantages, disadvantages and key features of these three methods are listed in Table 2-7.

Table 2-7 Comparison among various methods of thermal fault simulation in laboratory DGA experiments

Reference	Method	Advantages	Disadvantages	Features
[18, 47-49]	**Immersed heating**	Easy to operate; Economical	Cannot cover whole fault temperature range; heating element easy to burnout	Localised thermal fault; inhomogeneous heating; atmospheric pressure
[50, 51]	**Tube heating**	Cover whole fault temperature range; easy to control	Complex system configuration; complicated operation procedures	Small portion oil overall heated; atmospheric pressure
[52]	**Bottle heating**	Easy to operate; Economical	Could not cover whole fault temperature range; Overpressure and possible leakage during heating	Overall heating; overpressure with possible leakage

The immersed heating method is easy to operate and economical to establish. However, it could not generate thermal fault which could cover the whole fault temperature range. And the heating might become inhomogeneous and burn the heating element with high input power. During heating, the thermal fault is localised under which the oil around the heating element is decomposed. The whole system is normally under atmospheric pressure and normal temperature which is far below the fault temperature.

The tube heating method usually requires a more complicated system which needs a furnace with adequate power and complex oil circulation system where a portion of oil is heated in the furnace. It could cover the whole thermal fault temperature range. During heating, only a small portion of oil is heated in the furnace chamber. Similar to the immersed heating method, the whole system is normally under atmospheric pressure and normal temperature during experiments.

The bottle heating method is widely accepted in oil aging tests rather than DGA experiments. In this method, the whole oil and headspace in the bottle are heated up to the fault temperature. There is virtually no temperature gradient in the oil. The inner pressure is much higher than the atmospheric pressure. Therefore, the leakage during heating in this method is much more severe than the other two methods. In addition, the bottle heating method could not cover high temperature thermal faults for safety consideration. In recent, this method is more accepted in DGA stray gassing study.

2.7 Summary

DGA is effective in diagnose transformer thermal and electrical faults. Under fault energy, the oil molecules are decomposed and recombine into small molecules, i.e. the fault gases. In transformers, the fault gases can be generated from oil decomposition and cellulose decomposition. Thermodynamic models are studied to show that the thermal fault gas combination pattern is related to the fault temperature. In addition, there are several gas generation sources which are non-fault related.

In DGA process, the oil should be sampled. The sampling method with syringe is introduced. The fault could be diagnosed with various types of data interpretation methods. The data interpretation methods are in general based on gas combination. Classic methods are reviewed, such as key gas method, Duval triangle method and Roger ratio method.

Fault gas generation characteristics of insulating liquids could be investigated under laboratory simulated thermal faults. In general there are three types of thermal fault simulation methods with their pros and cons. Previous laboratory based DGA studies are reviewed. The previous established DGA thermal fault simulation systems are based on three fault simulation methods: immersed heating method, tube heating method and bottle heating method. The immersed heating method is easy to control input power but the heating element temperature is difficult to be measured and controlled. The tube heating method could simulate thermal fault covering the whole temperature range of transformer thermal faults but it requires a complicated experimental system. As the bottle heating

method could only simulate thermal fault below the flash point or fire point of the oil, new setups based on immersed heating method and tube heating method are required in order to simulate fault covering the whole temperature range.

Chapter 3 Key Technical Preparation Information

3.1 Introduction

Currently, there is no technique to measure all the dissolved gases in oil directly, although there are single gas sensors which could directly measure gas concentration in oil such as solid state Pd/Ag hydrogen sensor [53, 54]. Therefore, the dissolved gases need to be extracted out from the oil before analysing in order to measure all the DGA investigated gases. In a DGA process, there are normally four steps. First, the oil is sampled and transported to the analytical facility. Second, the dissolved gases are extracted from the oil. Third, the concentrations of the extracted gases are measured. Fourth, the measurement results are interpreted in order to analyse the fault type related to the oil sample.

In this thesis, the dissolved gases are measured by both laboratory DGA measurement and online DGA monitors. For external laboratory measurements, the oil is sampled by syringe. For online DGA monitor, the oil is sampled by the pump of the online DGA monitor through oil circulation loop.

In the laboratory DGA measurements, the dissolved gases are extracted by both headspace extraction method and vacuum extraction method. In the online DGA monitors, headspace based extraction method is widely used to remove dissolved gas from the oil.

In the headspace extraction method, the gases between the headspace gas phase and oil phase are in equilibrium state under which the dissolved gas concentration in the oil can be calculated based on the gas concentration in the gas phase. The concentrations in the oil phase and in the gas phase are correlated with the Ostwald solubility coefficient under equilibrium condition. The Ostwald coefficients are necessary for DGA measurements with headspace extraction method. In this work, the Ostwald coefficients for Gemini X and MIDEL 7131 are listed. The Ostwald coefficients for Diala S4 ZX-I are measured by phase ratio variation method.

In this work, two online DGA monitors are used to analyse the dissolved gas in the oil. The dissolved gases are extracted in the extractor system with headspace extraction based methods. The gases are analysed by laboratory grade gas chromatography (GC) system in the TM8 online DGA monitor and photo-acoustic spectroscopy (PAS) method in the Transfix online DGA monitor. In addition, the oil from the test system is sampled for conventional laboratory based DGA measurements.

3.2 Dissolved Gas Extraction Methods

Removal of dissolved gases from oil for analysis may be accomplished by vacuum extraction method, stripping method or headspace method [30]. In stripping extraction method, the extraction of dissolved gases is carried out by the carrier gas itself bubbling through a small volume of the oil. Typically an oil volume between 0.25 mL and 5 mL is used. The stripper column contains a high surface area bead [30]. The gases are then flushed from the stripper column into a gas chromatograph for analysis. Testing of silicone liquids by this test method is not recommended for systems which are also used to test mineral oil, as excessive foaming should cause contamination of columns after the stripper [5]. The time required to extract larger volumes would give unacceptable gas chromatograms except when used with cold traps or for hydrogen analysis only [30]. Due to such limitation, this method is less popular than the other two methods.

Among these extraction methods, headspace extraction is relatively new but well-accepted. The first headspace extraction system for DGA was developed in 1982 using calibrated glass bottles for the extraction. It operated at room temperature and pressure, and allowed unattended operation on a large number of oil samples per day [55]. However, this method was applied to Gas Chromatography for DGA in 1989 in the USA. Extraction was done in the vials at 90 ℃ and 1.7 bar overpressure of argon. In 1990, similar equipment was used at lower extraction temperature to 50 ℃. The calibration method of extraction system was proposed with gas-in-oil sample as reference [55]. The latest developments of the headspace procedures have been described in detail in the next edition of IEC Publication 60567 [30].

As new developed gas extraction method, shake test was invented by Morgan Schaffer in 1993. It is a simplified headspace process, which is very popular for fast on-site analysis. Moreover, a single column GC online DGA monitor is developed by Morgan Schaffer. In 1993, mercury-free Toepler pump was invented by National Grid, and mercury-free partial degassing was developed in 1998 by Siemens. Extraction efficiency of mercury-free Toepler is almost 100%, and for the partial degassing method, efficiency ranges from 90% to 99%. Similar as headspace method, efficiency of shake test is much lower, because lower portion of gases can be extracted. Typical efficiency is between 1% and 30%, depending on phase ratio and gas type [5].

3.2.1 Vacuum Extraction by Partial Degassing Method

Vacuum extraction, according to the number of strokes, can be divided into multi-cycle vacuum extraction (Toepler) method and single-cycle vacuum extraction (partial degassing) method [30]. A typical vacuum extraction scheme is shown in Figure 3-1.

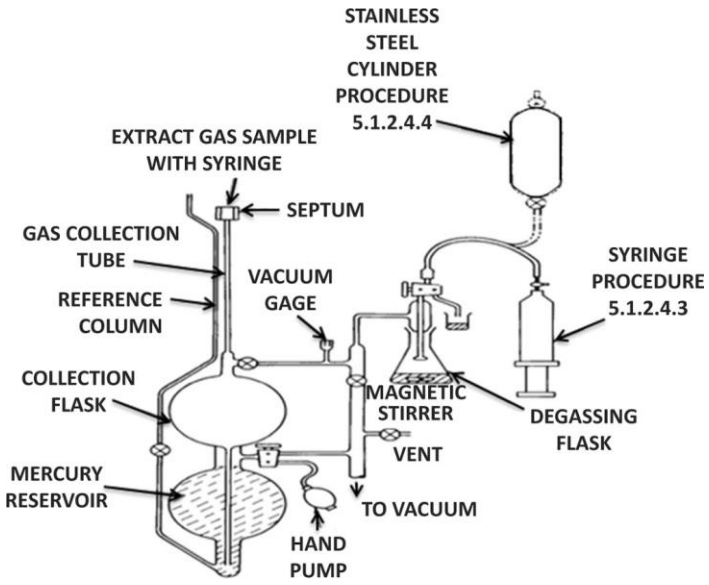

Figure 3-1 Extraction of dissolved gases from insulating oil using the vacuum extraction method [55]

Mercury-Free techniques were introduced to vacuum extraction about ten years ago [5]. They are variations on the standard vacuum techniques of Toepler and partial degassing, using a mechanical piston inside a cylindrical vessel instead of a mercury piston [5]. The extraction efficiency of the standard Toepler method and its Mercury-Free version is

almost 100% for all gases typically after eight strokes. Partial degassing method use only one extraction stroke so their efficiency varies from 90% to 99% depending on the volume of gas expansion chamber and solubility of the gas [5].

3.2.2 Headspace Extraction Method

In this method, a volume of oil is introduced in a glass vial in contact with a gas phase (headspace). A portion of the gases dissolved in the oil transfers to the headspace until reaching equilibrium conditions of temperature and pressure. The gas sample in headspace can be transferred to an injection loop or directly in the column of the Gas Chromatography (GC) depending on the practical apparatus. Calibration curves are used to establish the concentration of each gas in the headspace. Then the concentration of the gases in oil can be calculated by using Henry's law and the experimentally determined partition coefficients of the oil. Alternatively, dissolved gas concentrations can be directly calculated with the calibration curves determined with gas-in-oil standards. A schematic representation of this method is shown in Figure 3-2 [30].

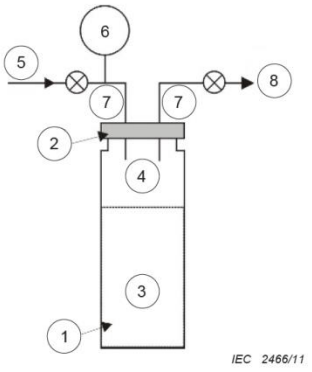

Key

1	vial	5	carrier gas
2	septum	6	pressurization gauge
3	oil sample	7	headspace sampler needles
4	gas phase	8	to GC injection loop and detectors

Figure 3-2 Schematic of headspace vial in GC application [30]

Measurement results are closely dependent on operation condition, such as total volume of the vial, volume of oil, sealing condition, temperature and pressure in the vial during measurement. If calibration curves will be used to determine the gas concentrations, exactly the same parameters should be kept for field samples, gas standards and oil

standards [30]. The system can be calibrated with gas-in-oil standards or gas standards. The advantage of gas-in-oil standards is that partition coefficients are not needed. The advantage of gas standards is that there is no requirement to prepare gas-in-oil standards. However, partition coefficients need to be determined accurately [30].

Once the oil/gas mixture in headspace vial reaches equilibrium, gas-in-gas concentration above oil surface will be measured. Based on determinate oil/gas phase volume, partition coefficients, equilibrium pressure and temperature, gas-in-oil concentration could be calculated as following equation (1) [55]:

$$C_L^0 = C_G \times \left(K + \frac{V_G}{V_L}\right) \quad (1)$$

Where, C_L^0 is the detected concentration in oil sample;
C_G is concentration of gas in headspace gas phase;
V_G is volume of headspace gas phase;
V_L is volume of oil sample;
K is Ostwald (solubility) coefficient of this gas type

Partition coefficients provided in publications are suitable for certain temperatures. For instance, IEEE C57.104 [14] and ASTM 3612 [55] list Ostwald coefficients of mineral oil at 25 ℃, while IEC 60599 [1] lists Ostwald coefficients at 20 ℃ and 50 ℃. Nevertheless, all Ostwald coefficient values suggested are measured under 1 atm (760 mmHg), which means the slightly changed pressure in headspace vial due in equilibrating might be neglected. In addition, currently a wide range of mineral oil types has been used worldwide. Mean values on some of the current types of transformer mineral insulating oils are capable of representing real values if the density of mineral oil falls into a specific range [1, 56]. In modern headspace method application, such as in online DGA monitors, extraction condition (temperature) is not well controlled. Correlation Ostwald coefficients with temperature is also considered.

When an oil sample is processed in headspace method at certain operational temperature and pressure conditions, detected concentration can be corrected to atmospheric pressure and temperature by the following equation (2) [1, 55]:

$$C_L^0 = C_L^{0*} \times \left(\frac{P}{P_S}\right) \times [\frac{T_S}{T}] \quad (2)$$

Where, C_L^{0*} is concentration under headspace operational condition;
C_L^0 is concentration under standard condition;
P, T are headspace operational pressure and temperature;
P_S, T_S are standard pressure and temperature

3.3 Partition between Gas and Oil Phases

The dissolved gases in the oil are volatile and are easily diffuse into the headspace gas phase above the oil surface. If a portion of oil is filled into a sealed vessel with a considerable amount of gas above the oil, the dissolved gases would diffuse into the gas phase until the gases in the two phases are in equilibrium condition. In this state, the gas concentrations in the liquid phase and in the gas phase are correlated by the partition coefficients which are known as the Ostwald solubility coefficients. The Ostwald coefficient of a particular gas dissolved in a certain type of oil is defined as the equation (3).

$$K = \frac{C_{gio}}{C_{gig}} \quad (3)$$

Where, C_{gio} is the concentration of the gas dissolved in the oil under equilibrium state;
C_{gig} is concentration of gas in the gas phase under equilibrium state;
K is Ostwald solubility coefficient.

The Ostwald coefficients depend on the affinity between gas and oil molecule. Therefore, the Ostwald coefficients of different gas types are different which might also be different for different oil types. In general, the Ostwald coefficients of light gases, i.e. hydrogen, are smaller than that of heavy gases, i.e. ethane, which means hydrogen is more likely to stay in gas phase than ethane in equilibrium state. Ostwald coefficients are related to equilibrium temperature. Theoretically, the gases are less likely to be dissolved in the oil under higher temperature than that under lower temperature which means the Ostwald coefficients are decreasing with equilibrium temperature increasing.

As there is no technique which could analyse all the DGA fault gas contents in oil, the dissolved gases need to be extracted from the oil and then be measured. The dissolved gases could be totally extracted by vacuum extraction method or partially extracted. In the latter extraction method, only part of the dissolved gases is extracted and measured in the headspace gas phase. The total gas amount needs to be calculated based on the gas concentration in the headspace and the partition coefficients which are the Ostwald coefficients in the headspace method. Therefore, the Ostwald coefficients are of importance in dissolved gas analysis of transformer oils.

The Ostwald coefficients of DGA investigated gases in mineral oils are measured. It is found that a typical set of Ostwald coefficients values could be used for mineral oils providing that the density of the oil is in a narrow range[56]. The Ostwald coefficients of a mineral oil with known density can be calculated from the Ostwald coefficients of the specific mineral whose density is 0.855 g/cm^3 at 15.5 ℃ according to the equation (4) [55]. It is also mentioned that the Ostwald coefficients are changed by the same factor. The absolute Ostwald solubility of each of the gases will change if different oil is used, the ratio of the solubility of one gas to another gas will remain constant [55].

$$K_{corrected} = K\frac{0.98 - density}{0.13} \tag{4}$$

Where, $K_{corrected}$ is the Ostwald coefficient of the mineral oil of interest;

K is Ostwald coefficient of the Ostwald coefficient of the specific mineral oil having a density of 0.855 g/cm^3 at 15.5 ℃;

$density$ is the density of the mineral oil.

3.3.1 Ostwald Coefficients of Mineral Oil

The Ostwald coefficients under different temperatures of mineral oil are measured and published in literatures and international standards. The Ostwald coefficients of mineral oil at 70 ℃ are listed in Table 3-1. The Ostwald coefficients of mineral oil at 25 ℃ are listed in Table 3-2.

Table 3-1 Ostwald coefficients of mineral oil at 70 ℃ from literatures [30, 55, 56]

	IEC60567	ASTM3612-02	Measured
density	0.864	Voltesso 35 (0.871)	Voltesso 35 (0.871)
CO2	1.02	1.02	0.936
CO	0.12	0.12	0.146
H2	0.074	0.074	0.093
CH4	0.44	0.44	0.446
C2H6	2.09	2.09	2.068
C2H4	1.47	1.47	1.456
C2H2	0.93	0.93	1.076
O2	0.17	0.17	0.206
N2	0.11	0.11	0.121

Table 3-2 Ostwald coefficients of mineral oil at 25 ℃ from literatures [14, 30, 55, 57]

	IEC60567	ASTM3612-02	IEEE C57.104	Cigre443
density	-	0.855	0.88	-
CO2	1.09	1.17	0.9	1.1
CO	0.132	0.133	0.102	0.125
H2	0.056	0.0558	0.0429	0.0504
CH4	0.429	0.438	0.337	0.423
C2H6	2.82	2.59	1.99	2.88
C2H4	1.84	1.76	1.35	1.81
C2H2	1.24	1.22	0.938	1.25
O2	0.172	0.179	0.138	0.172
N2	0.091	0.0968	0.0745	0.091

In general, the Ostwald coefficients can be measured by gas-in-oil standards, the vapor-phase equilibrium method and so on [30, 58]. It has been indicated that the Ostwald coefficients measured by different laboratories using various methods are not reliable and reproducible [30]. There are significant discrepancies between Ostwald coefficients from different literatures. For example, in Table 3-1 the hydrogen Ostwald coefficient of Voltesso 35 mineral oil at 70 ℃ from ASTM 3612-02 is 0.074 while it is measured as 0.093. There is a difference of more than 20%.

At 25 ℃ in Table 3-2, the maximum discrepancy of hydrogen Ostwald coefficient is about 30% which is between the Ostwald coefficients from ASTM 3612-02 and from IEEE standard. In laboratory DGA measurements, if the system is calibrated with gas-in-

oil standards, the Ostwald coefficients are not involved. However, for online DGA monitors or laboratory DGA measurements calibrated with gas standards, the errors might be caused by inaccurate Ostwald coefficients.

3.3.2 Ostwald Coefficients of Synthetic Ester Liquids

The Ostwald coefficients of synthetic ester liquids for different temperatures are listed in the Table 3-3.

Table 3-3 Ostwald coefficients of synthetic ester liquids under various temperatures [30, 56, 57]

	IEC60567 (synthetic esters @ 25 ℃)	Cigre443 (MIDEL 7131 @ 20 ℃)	Measured (Envirotemp 200 @ 70 ℃)
density	-	0.97	0.97
CO2	2.05	2.08	1.365
CO	0.127	0.13	0.143
H2	0.051	0.0479	0.103
CH4	0.381	0.378	0.355
C2H6	2.19	2.2	1.504
C2H4	1.87	1.85	1.31
C2H2	4.38	4.26	2.459
O2	0.152	0.152	0.193
N2	0.0872	0.091	0.137

The Ostwald coefficients at 25 ℃ of synthetic ester liquid are published in IEC standard 60567 the specific oil type of which is not mentioned. The Ostwald coefficients of MIDEL 7131 at 20 ℃ are published in Cigre brochure 443 and those of Envirotemp 200 are published based on laboratory measurements.

The results listed in Table 3-3 are not reliable. For example, the hydrogen Ostwald coefficient is increasing with the temperature increasing, which means the hydrogen would be dissolved more in oil under higher temperature. This phenomenon is not reasonable from chemistry principle. The reason might be due to the chemical structure of the oil sample used in the three measurements are not similar. In addition, the different methods of measurement might also generate errors in Ostwald coefficients.

3.3.3 Determination of GTL Oil Ostwald Coefficients

In the thesis, three types of oils are investigated: Gemini X, Diala S4 ZX-I and MIDEL 7131. The MIDEL 7131 is tested as synthetic ester liquid. Diala S4 ZX-I is tested as the gas-to-liquid based insulating liquid. Gemini X is tested as the benchmark of mineral oil. The Ostwald coefficients of three oils at room temperatures are required to correct the DGA measurements from the online DGA monitors. The coefficients at 70 ℃ are also required to correct the laboratory measurements using headspace extraction method.

The Ostwald coefficients of the Gemini X for 25 ℃ and 70 ℃ are using the published values from the IEC standard 60567 as the Gemini X is a typical mineral oil. The Ostwald coefficients of the MIDEL 7131 for 25 ℃ and 70 ℃ are using the published values from Table 3-3. However, as the Diala S4 ZX-I is newly developed oil, there is no published Ostwald coefficients. Therefore, the Ostwald coefficients of the Diala S4 ZX-I at room temperature, 50 ℃ and 70 ℃ are measured. This is the first time that the Ostwald coefficients of the Gas to Liquid transformer oil are measured and reported.

The phase ratio variation test method is used to determine the Ostwald coefficients of the Diala S4 ZX-I [55, 58]. In this method, a certain amount of oil samples are firstly degassed. Then the oil is sealed with a portion of gas mixture in a vessel which is continuously shaken under low temperature in order to dissolve as much gas in the oil as possible. Subsequently, the oil is distributed and sealed into a series of same headspace vials with different oil volume. By adjusting the oil volumes in each headspace vial, the phase ratio of each headspace vial is different from the others. Finally, all the headspace vials with oil are analysed in the gas chromatography (GC) with headspace extraction at either room temperature or 70 ℃. The peak area of each gas on the GC spectrum of every headspace vial is recorded. The peak area of each gas under the different phase ratios are plotted in a graph with the reciprocal of the peak area as the Y-axis and the phase ratio as the X-axis. From the regression analysis of these data, the slope and the intercept can be obtained. The partition coefficient, i.e. the Ostwald coefficient, can be calculated as the equation (5) [55].

$$K = \frac{intercept}{slope} \tag{5}$$

The detected Ostwald coefficients of Diala S4 ZX-I under 70 ℃ are listed in the Table 3-4. Two same tests are performed to obtain the results. In the linear regression analysis of the peak area against the phase ratio shows acceptable R-square values in all linear regression, which means the experimental results are reliable. The results from two tests show a good repeatability of the Ostwald coefficient measurements.

Table 3-4 Ostwald coefficients measurement results of Diala S4 ZX-I under 70 ℃

	Test 1@70 ℃	Test 2@70 ℃	Average
density	0.805		
CO2	1.01	0.97	**0.992**
CO	0.16	0.12	**0.142**
H2	0.20	0.18	**0.190**
CH4	0.42	0.41	**0.415**
C2H6	2.06	2.17	**2.115**
C2H4	1.39	1.44	**1.411**
C2H2	0.97	0.87	**0.923**
O2	0.26	0.15	**0.204**
N2	0.16	0.25	**0.203**

Comparing with the Ostwald coefficients of mineral oil in Table 3-1, the Diala S4 ZX-I Ostwald coefficients of all gases are close to those of the mineral oil except for the hydrogen. The hydrogen Ostwald coefficient of Diala S4 ZX-I is 0.19 which is two times higher than the mineral oil. The possible reason might be due to the gas leakage during experiments and the error caused in the GC analysis process.

The detected Ostwald coefficients of Diala S4 ZX-I GTL oil under 50 ℃ are listed in the Table 3-5. The results are also measured based on two repeated tests. The Ostwald coefficients under 50 ℃ are provided for the Diala S4 ZX-I users who proceed DGA measurements of oils with headspace extraction method under 50 ℃. The Ostwald coefficients of all gases under 50 ℃ are larger than those under 70 ℃ which verifies that the gas is easier to be dissolved in the oil under lower temperature.

Table 3-5 Ostwald coefficients measurement results of Diala S4 ZX-I under 50 ℃

	Test 1@50 ℃	Test 2@50 ℃	Average
density	0.805		
CO2	1.18	1.28	**1.234**
CO	0.39	0.40	**0.394**
H2	0.43	0.40	**0.415**
CH4	0.72	0.79	**0.755**
C2H6	2.98	3.04	**3.011**
C2H4	1.99	1.98	**1.989**
C2H2	1.40	1.48	**1.440**
O2	0.23	0.21	**0.218**
N2	0.26	0.27	**0.267**

The detected Ostwald coefficients of Diala S4 ZX-I GTL oil under 28 ℃ are listed in the Table 3-6. The results are also measured based on three repeated tests. The aim of the experiment is to measure the Ostwald coefficients of Diala S4 ZX-I under 20 ℃ room temperature. However, the method requires the operation of GC equipment where the lowest temperature could be only achieved with the heater being closed. In the present day of the tests, with the heater of the headspace extraction system closed the temperature is measured as 28 ℃.

Table 3-6 Ostwald coefficients measurement results of Diala S4 ZX-I under 28 ℃

	Test 1	Test 2	Test 3	Average	RSD%
density	0.805				
CO2	1.727	1.891	1.827	**1.815**	5%
CO	0.382	0.306	0.374	**0.354**	12%
H2	0.283	0.389	0.315	**0.329**	17%
CH4	0.812	0.768	0.797	**0.792**	3%
C2H6	4.177	4.252	4.104	**4.178**	2%
C2H4	2.698	2.756	2.636	**2.697**	2%
C2H2	1.695	1.792	1.708	**1.732**	3%
O2	0.422	0.401	0.433	**0.419**	4%
N2	0.309	0.298	0.247	**0.285**	12%

The Ostwald coefficients are averaged from three repeated test results. The relative standard deviations in percentage (RSD%) of all gases are all within 5% except for the carbon monoxide, hydrogen and nitrogen, which are all above 10%. The RSD% of

hydrogen is 17%. In general, the results from three tests show good repeatability. The larger RSD% of hydrogen and carbon monoxide might be because these two gases are easier to leak from the oil. Similar to the previous discussion, the Ostwald coefficient measurements of atmospheric gases, i.e. the oxygen and nitrogen, might not be reliable considering the probable air ingression.

The measured Ostwald coefficients are suitable for the headspace extraction in dissolved gas analysis of the Diala S4 ZX-I with GC facility. Normally, the GC system is calibrated with mineral oil. The laboratory measurement results of Diala S4 ZX-I are based on the mineral oil Ostwald coefficients. Therefore, the laboratory results need to be corrected with the Ostwald coefficients of the Diala S4 ZX-I according to the equation (6).

$$C_{git}^{GTL} = \frac{C_{git}^{min} \times (K_{GTL} + \beta)}{K_{min} + \beta} \tag{6}$$

Where, K_{min} is the Ostwald coefficient of the mineral oil at the temperature at the test temperature;

K_{GTL} is Ostwald coefficient of the gas to liquid transformer oil at the test temperature;

C_{git}^{min} is the gas in total concentration measurement results based on mineral oil Ostwald coefficients;

C_{git}^{GTL} is the gas in total concentration calculated results of the gas to liquid transformer oil;

β is the phase ratio of the oil in the headspace vial used in the DGA measurement.

In the phase ratio variation test method, there are several factors which could cause measurement errors. Normally, the accuracy of GC equipment in the DGA measurement is 20% [30]. Therefore, the reciprocal of the peak area might have measurement error up to 25%. The gas leakage and air ingression during tests might also cause errors which would reflect on the linear regression calculation. In addition, the oil in each headspace vial is injected by syringe which also measures the oil volume. The oil volume measurement could also generate errors. Compared with the 25% measurement error on the reciprocal of the peak area, the volume measurement error is negligible. It is found that a random error within 25% on the linear regression curve might cause significant error on Ostwald coefficient results. In addition, the pressure in the headspace vial of the

phase ratio variation method is normally larger than atmosphere pressure while in the other methods the equilibrium pressure is same as the atmosphere pressure, which would cause different Ostwald coefficient measurements.

3.4 Gas Detection Methods

Once dissolved gas is removed from oil sample, they will be injected into gas detection device. Gas Chromatography (GC) is mostly used in laboratory based DGA facilities. Common type of gas chromatography is used in separating and analysing compounds in vaporized gas mixture. It can be used to detect particular substance, separate different composition from a mixture and purify mixture from certain substances. The structure and working principle of GC system are shown in Figure 3-3.

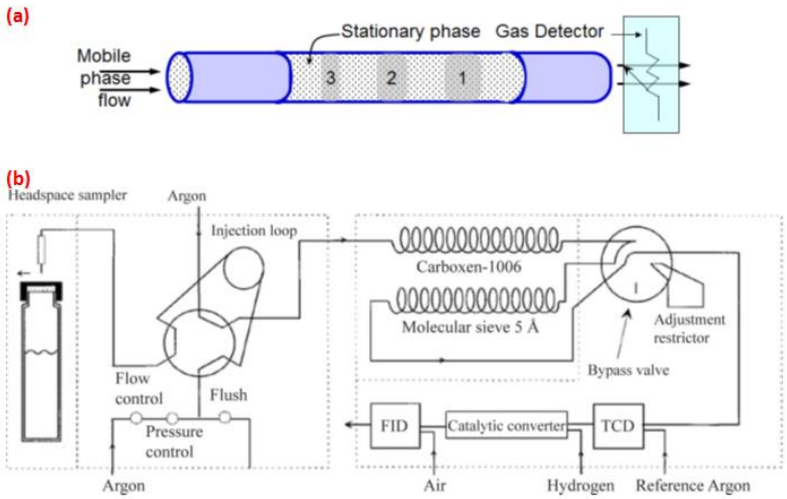

Figure 3-3 Gas Chromatography system: (a) Sample mixture separations in gas chromatography column; (b) Schematic diagram of gas chromatography system [34, 59]

Figure 3-3 (a) shows working principle of gas chromatography in separating gas mixture. Special designed inner surface of column is able to sustain substances, which is referred as stationary phase. Detected gas sample mixture is injected as mobile phase flow by carrier gas. With flowing through column, components of mixture will be differentiated based on their retain time with stationary phase, and purged out one by one. Through specific design and calibration, spectrum of each gas chromatography column can be

confirmed. Combination of spectrum and detector reading, concentration of each component in gas mixture can be assessed.

Scheme of typical laboratory GC system is shown in Figure 3-3 (b). Sample is injected and carried into GC column for separation. Separated gas will be then purged through detector, where components of gas mixture are detected. Flame ionization detector (FID) and thermal conductivity detector (TCD) are common gas detectors in DGA gas chromatography. They are sensitive to a wide range of components and cover wide range of detection value. Detection of TCD depends on thermal conductivity change of gas passing through filament with a current. FID detector is electrodes placed near a flame source, and pyrolyse detected gas sample. Since detected gas is not consumed in TCD, it can be set before a FID, in which gas sample will be burnt, to provide complementary detection.

Recently, a lot of efforts are devoted in improving DGA and online DGA technology, including gas extraction, gas detection and portable device [60]. Various gas detection methods based on different technologies are developed. One of the most popular technologies is Photo-Acoustic Spectroscopy (PAS) based on photo-acoustic effect, discovered by Alexander Bell in 1880. In this theory, sound waves will be formed by light emit through a material [61]. The photo-acoustic effect is quantified by measuring the amplitude of sound signals with detector, such as microphones. Photo-acoustic spectrum refers spectrum of emit light signals with different wavelengths. It can be obtained by record sound amplitude at each light wavelength. This spectrum can be used to identify absorbing components of sample in order to detect components in detected mixture sample [61].

Photo-acoustic spectroscopy was firstly applied in DGA method by GE Kelman [61]. Figure 3-4 shows schematic diagram of a generic photo-acoustic analyser. An infrared (IR) light source is used as light energy source. Light is concentrated by a parabolic mirror. Light frequency is controlled by a chopper wheel at constant rotating speed. From IR light, certain wavelength is selected by the filter wheel in order to detect certain substance. Sample to detect and light of selected wavelength are injected into analysis chamber.

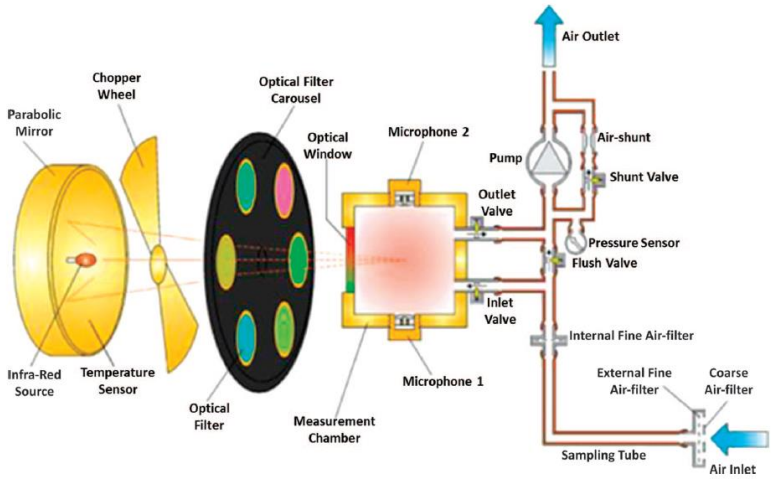

Figure 3-4 Diagram of a Photo-Acoustic analyser [62]

Sound signal cause by molecule vibration is detected and recorded by microphone. Usually even number of microphones will be set symmetrically to eliminate background noise disturbance. Figure 3-5 shows response location of several chemical bonds on wavelength spectrum.

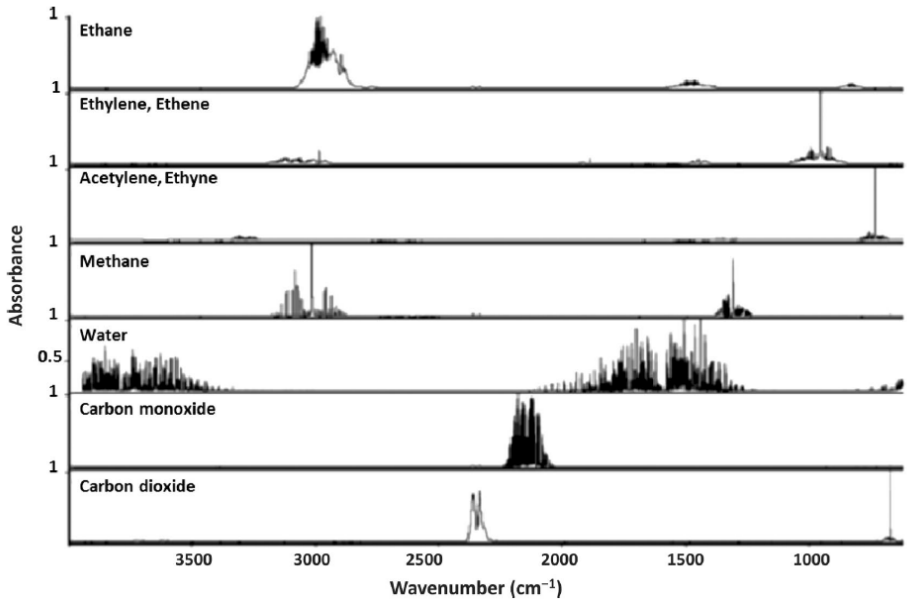

Figure 3-5 Characteristic absorption of fault gases in Photo-Acoustic Spectroscopy [62]

The detection sensitivity of the equipment varies from gas to gas, and its detection accuracy is influenced by the external environment, e.g., temperature and pressure, and by vibration [63]. In DGA fault gases, hydrogen has no photo-acoustic effect, thus in Photo-Acoustic Spectroscopy based online DGA devices another hydrogen sensor need

to be fit in addition. Accuracy and repeatability of photo-acoustic spectroscopy is assessed by comparing online DGA monitor with PAS detector and conventional GC facilities.

3.5 Online DGA Monitors

The development of online DGA monitoring technology was initiated by invention of semi-permeable technique, which can partially separate dissolved gases from oil (mostly hydrogen) by diffusion through the polymer layer (hollow tube or membrane) [5]. The early hydrogen detector was invented by Morgan-Schaffer in 1974 using a thermal conductivity detector. In 1977, the hydrogen monitor was designed using a fuel cell detector [64]. Several attempts at monitoring the other fault gases online or on-site have been tried later. In 1993, a multi-gas analyser was developed by Morgan-Schaffer based on Shake Test. The Shake Test provides the capability for on-site measurement of syringe samples of oil. Online transformer monitor, the TNU (Transformer Nursing Unit) was developed in 1997, which intended for the temporary online monitoring of suspect equipment [5]. So far, various types of online DGA monitors with different functions and technologies have been developed. They can be divided, according to functionality, single (one or two) gas DGA monitor and multi-gas DGA monitor. The former is intended for online monitoring and pre-fault warning; while the latter is able to monitor equipment condition and diagnose fault. In the following paragraphs, typical online DGA devices will be introduced.

SERVERON TM8 Online DGA Monitor

SERVERON TM8 is a classic multi-gas online DGA monitor developed by SERVERON. It is based on laboratory graded GC detector. Dissolved gases will be extracted by semi-permeable membrane. DGA measurement period can be set from hourly to every four hours. The software will provide data interpretation, including IEEE ratio, IEC ratio and Duval Triangle, as well as trend analysis and pre-warning [65]. Figure 3-6 shows the working principle of TM8 when it is monitoring a transformer.

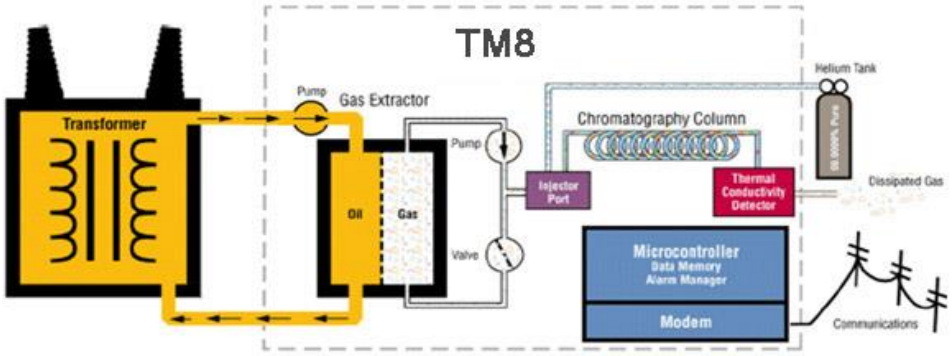

Figure 3-6 Working principle of TM8 monitoring transformer [66]

During TM8 in-service operation, roughly 600 mL oil will be continuously circulated into extractor. Distribution of dissolved gases in oil in extractor is similar to that in transformer if the oil sampled is effective, which is sampled from main tank or oil circulation path instead of bottom dead oil. Dissolved gas will migrate through semi-permeable membrane and injected into gas detector by carrier gas. In TM8 system, high purity Helium gas is used as carrier gas. Gases will be analysed by a dual-column GC and TCD detector. Gas detector can be calibrated by a gas-in-gas standard calibration cylinder [59].

GE Transfix Online DGA Monitor

The Transfix is a 9-gas online transformer DGA monitoring unit. It was developed by Kelman Corporation based on special Photo-Acoustic technology. Dissolved gases will be extracted by headspace method with carrier gas bubbling. Moisture level is also monitored in Transfix. Composition and working principle of Transfix is shown in Figure 3-7 as stand-by state of Transfix.

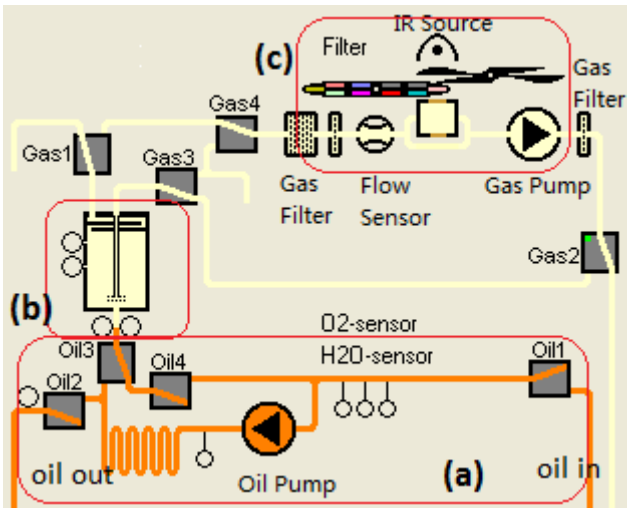

Figure 3-7 Structure and working principle of Transfix: (a) manifold; (b) headspace cell; (c) Photo-Acoustic Gas Analyser.

In general, Transfix is composed of manifold, headspace cell and PGA gas detector, which work as oil circulation system, gas extraction system and gas detection system, respectively. In stand-by condition, Transfix oil circulation system is isolated from outside by oil valve 1, 2 and 4. Meanwhile, gas system is connected to atmosphere through gas valve 1 and 2, in order to keep air evenly distributed in gas phase. When a detection cycle is started, oil will be pumped into headspace cell through oil valve 1 and 3. An optical sensor will trigger to stop pump once oil volume in headspace cell reaches 50 mL. Another optical sensor is installed near the top of headspace cell for security. Gas phase will be isolated from atmosphere with gas valve 1 and 2. After 50 mL oil is sampled into headspace cell, dissolved gas will be purged out by air bubbling with gas pump circulation. Extracted gas will be detected by Photo-Acoustic Gas Analyser. After concentrations of all target gas components have been determined, extracted gas will be purged out through gas valve 2, and oil sample will be returned back through oil valve 2, 3 and 4.

In Transfix gas detection system, air is used as carrier gas to send gas sample into detector, therefore trace amount of CO2 and O2 from atmosphere will migrate into transformer. Principle of PAS (Photo-Acoustic Spectroscopy) detector is introduced in Figure 3-4. All fault gases can be detected except for hydrogen which has no photo-acoustic effect. Transfix has equipped hydrogen sensor for hydrogen detection.

3.6 Summary

In this thesis, two types of dissolved gas extraction methods are utilised. The vacuum extraction method is performed by a Toepler pump. It is a single stroke extraction which is partial degassing. The headspace extraction method removes the dissolved gas from the oil in a sealed headspace vial. By measuring the gas concentration in the headspace gas phase, the total gas concentrations in the oil sample could be calculated according to known Ostwald coefficients of the tested oil and phase ratio. Headspace extraction method is also used in the two online DGA monitors which are slightly different from the conventional headspace method. The TM8 uses semi-permeable membrane to separate dissolved gases while the Transfix purges the dissolved gas by air bubbling through the oil.

The partition between gas and oil phase in the headspace vial under equilibrium state is determined by the Ostwald coefficients. In this thesis, three types of oil are under investigation. The Ostwald coefficients depend on the equilibrium temperature and oil types. The Ostwald coefficients of Gemini X mineral oil and MIDEL 7131 synthetic ester liquid under room temperatures (20 ℃ and 25 ℃) are listed from publications. The Ostwald coefficients of Diala S4 ZX-I gas to liquid transformer oil under room temperature (28 ℃), 50 ℃ and 70 ℃ are measured by phase ratio variation method which is the first time that the Ostwald coefficients are measured and reported for this new developed insulating liquid.

The dissolved gases are analysed by two methods throughout this research. Gas chromatography (GC) facility equipped with thermal conductivity detector (TCD) and Flame ionisation detector (FID) is utilised to detect the dissolved gas in the oil samples in the professional analytic laboratory. The same detection method is used in the TM8 online DGA monitor. The photo-acoustic spectroscopy (PAS) method is applied in the Transfix to detect the extracted gases.

Chapter 4 DGA Experiments with Immersed Heating Fault Simulation Method

4.1 Introduction

In this chapter, a DGA experimental system with immersed heating fault simulation method is introduced. There are two major objectives to build up this system. First, gas generation of various types of transformer insulating liquids under different levels of immersed thermal faults could be investigated. Second, this system is capable of operating multiple online DGA monitors in parallel through which the performance of online DGA monitors could be assessed in terms of comparing with conventional laboratory results.

In this thesis, three types of transformer insulating liquids are studied in the immersed heating DGA system. Firstly, Nytro Gemini X is tested as benchmark of mineral oil. Subsequently, Diala S4 ZX-I is tested as a novel gas to liquid (GTL) based insulating liquid. Finally, MIDEL 7131 is tested as synthetic ester liquid. These insulating liquids are introduced in detail in the second section of this chapter.

The immersed heating DGA system is consisted of test cell, heating element, online DGA monitors and expansion syringes. The heating element is embedded in the test cell. The heating element temperature is controlled by adjusting the input power. The tested oil is circulated from the bottom of the test cell and returned back from the top by the circulating pump of the online DGA monitors. There are two expansion syringes to relieve expansion pressure during heating and provide oil conservation during online DGA measuring. This DGA system is introduced in detail in the third section of this chapter.

The DGA experimental system aims to study the fault gas generation under localised thermal faults generating by the immersed heating element. Specific test procedures should be strictly followed during experiments. In general, there are four major steps. First, the system is assembled without leakage and filled with oil. Second, the dissolved

gas contents are measured as background gas level. Third, heating element operates as localised thermal fault generated. Fourth, the dissolved gas contents after fault are measured. The procedures are introduced in detail in the fourth section of this chapter.

4.2 Test Setup

4.2.1 Overall System

Established platform for DGA thermal fault experiments with immersed heating fault simulation method is shown in Figure 4-1.

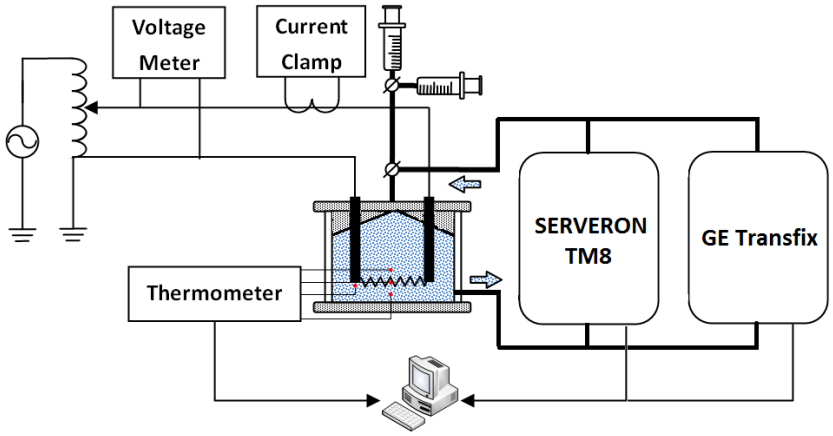

Figure 4-1 Experimental setup of two online DGA devices parallel operation

A 2.1 litres gas-tight test cell was manufactured by workshop. Vessel body was made of Perspex, and lid was made of nylon. Two copper bars were fitted on lid for heating element installation. O-rings were used to seal between lid and vessel. One oil circulation valve was installed on top of test cell, and the other on bottom side, which ensures the whole bulk oil to be circulated. The valve was sealed by standard PTFE tapes. Lid top was designed as a reverse funnel of 120 ° top angle for air bleeding. Energy of heating element is supplied by an AC socket. Input energy is controlled by an auto-transformer and measured by voltmeter and current transformer.

Two online DGA monitors are connected to test cell. Both devices pump oil from bottom valve and return oil back through top valve. Since TM8 is embedded with stronger pump than Transfix, to prevent oil reverse flow, check valves are installed on both devices

before connecting to test cell. A 50 mL gas-tight syringe is installed on top of oil circulation system to relieve thermal expansion pressure during experiment. The other 100 mL syringe is fitted to provide conservative oil volume for Transfix oil sampling. The total oil volume in the system is 2.95 litres including the oil in test cell and the oil in two online DGA monitors.

The sealing condition of the test system is assessed before experiments. Before oil is filled into the system, a portion of air is injected into the sealed system raising the pressure in the system to 100 mbar positive. Then the pressure in the system is continuously monitored in 24 hours in order to evaluate the sealing condition in the required duration. It is found that the test system could maintain more than 80 mbar positive pressure in 24 hours which indicates the test system is properly sealed within the required experimental duration.

4.2.2 SERVERON Online DGA Monitor

Transformer oil will be continuously circulated into a 575 mL gas extractor inside the TM8 DGA monitor, where dissolved gas will diffuse into gas phase through semi-permeable membrane. Circulating pump speed can be set from 240 mL to 420 mL depending on viscosity of oil. Laboratory grade Gas Chromatography (GC) columns and thermal conductivity detector (TCD) detection system are equipped in TM8. To detect all fault gases, GC system in TM8 is a dual-column system for different molecular size range of fault gases. Calibration with gas-in-gas standard is available for TM8 during service.

To have representative oil sample, circulatory online DGA monitor need to sample oil from top of transformer main tank and return oil back through bottom. Oil circulates through extractor where dissolved gas will be extracted into gas phase. Extracted gas sample will be purged into GC system by carrier gas. TM8 uses helium as carrier gas. For remote control and condition monitoring, TM8 is embedded with communication and relay components. For example, TM8 has its own low limit level setting and alarm setting, which might be complementary for smart grid. Detection range and accuracy of TM8 are shown in Table 4-1.

Table 4-1 Accuracies and detection ranges of TM8 online DGA monitor

Gas	CO2	CO	H2	CH4	C2H4	C2H6	C2H2	O2	N2
Accuracy	±5% or ± LDL	±5% or ± LDL	±5% or ± LDL	±5% or ± LDL	±5% or ± LDL	±5% or ± LDL	±5% or ± LDL	±10% or +30/-0 ppm	±10% or ± LDL
Range (ppm)	5-30,000	5-10,000	3-3,000	5-7,000	3-5,000	5-5,000	1-3,000	30-25,000	5,000-100,000

LDL: low detection limit

Accuracy of all fault gases are ±5% or low detection limit. Detection range of fault gases ranges from 3000 ppm of H2 to 10000 ppm of CO. Low detection limit of fault gases ranges from 1 ppm of C2H2 to 5 ppm of several gases. Usually in transformer, concentration of C2H2 is much lower than CH4 and C2H6, because it is related to most dangerous fault cases, such as arcing or extremely high temperature thermal fault. The low detection limit setting for different fault gases is reasonable.

4.2.3 GE Transfix Online DGA Monitor

Compared with traditional laboratory DGA methods and TM8, Transfix is a novel online DGA device. Firstly, instead of using noble gas as carrier gas, Transfix directly use air as carrier gas. Subsequently, apart from factory calibration, during online operation, calibration is not required, while TM8 has equipped with calibration gas cylinder to calibrate GC system every day. Finally, Transfix uses a Photo-Acoustic Gas Analyser as gas detector. The advantage of Transfix is that there is no requirement for consumable elements, such as carrier gas and calibration gas. However, the reliability and uncertainty of performances of the Photo-Acoustic Gas Analyser are still unclear.

Different from Serveron TM8 which circulates oil continuously; Transfix will sample oil into a headspace vial and extract dissolved gases. During detection, 50 mL oil will be pumped into headspace vial. Degassed oil sample will be returned back. Therefore, a conservative syringe is necessary for 50 mL sample volume in setup shown as Figure 4-1.

Accuracy and detection range of Transfix is shown in Table 4-2.

Table 4-2 Accuracies and detection ranges of Transfix

Gas	CO2	CO	H2	CH4	C2H4	C2H6	C2H2	O2	N2
Accuracy	±5% or ± LDL	±5% or ± LDL	± 5% or ± LDL	±5% or ± LDL	±5% or ± LDL	±5% or ± LDL	±5% or ± LDL	±10% or ± LDL	±15% or ± LDL
Range (ppm)	20-50,000	2-50,000	5-5,000	2-50,000	2-50,000	2-50,000	0.5-50,000	100-50,000	10,000-100,000

LDL: low detection limit

Similar to TM8, Transfix has ±5% or low detection limit accuracy for all fault gases. Detection ranges of all fault gases are higher than those of TM8 except for H2. The reason might be that H2 is measured by an external hydrogen sensor since the Photo-Acoustic Gas Analyser could not measure hydrogen concentration.

4.2.4 Material and Geometry of Heating Element

The Kanthal A-1 furnace coil is used as the material of immersed heating element. The composition of the Kanthal A-1 is shown in Table 4-3.

Table 4-3 Chemical composition and properties of the Kanthal A-1 alloy

	Chromium (Cr)	Aluminum (Al)	Iron (Fe)	Other Component (C, Si, Mn)
Nominal Composition (%)	-	5.8	Bal.	-
Min Composition (%)	20.5	-	Bal.	-
Max Composition (%)	23.5	-	Bal.	1.18
Resistivity ($X10^{-8}$ Ω m)	13	2.7	9.7	-
Melting Point (℃)	1857	660	1200-1600	-

The major component of the alloy is iron which takes up more than 70%. The melting point of the Kanthal A-1 is 1400℃ which is in the range of the iron melting point. The resistivity of the Kanthal A-1 at 20℃ is $145 \cdot 10^{-8}$ Ω m. The primary reason is that the oxidation product of aluminum component in the Kanthal A-1 material could efficiently raise the resistant of the alloy. The resistivity and melting point of Kanthal A-1 are much higher than conventional heating wire material such as copper or iron. Therefore, the Kanthal A-1 heating element could be used under relatively high voltage and low current

compared with copper wire heating element which requires low voltage and high current power supply in order to reach enough input power. In addition, the higher melting point of the Kanthal A-1 heating element could withstand higher thermal fault levels since one of the major limitation of the immersed heating element in DGA experiments is the melting of heating element.

The heating element in the experimental setup is in a coil shape 0.5 cm in diameter made by 0.6 mm wire as shown in Figure 4-2 (a). The length of the heating element is 7 cm. A piece of ceramic thermocouple insulator is inserted in the coil. The ceramic insulator is shown in Figure 4-2 (b). A thermocouple is inserted in the ceramic insulator which measures the temperature of the heating element.

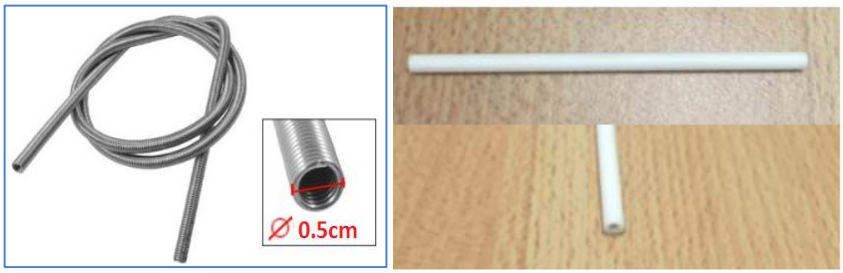

Figure 4-2 Heating element components: (a) Kanthal A-1 coil; (b) ceramic insulator.

4.3 Test Procedures

The experimental procedures are shown in Figure 4-3.

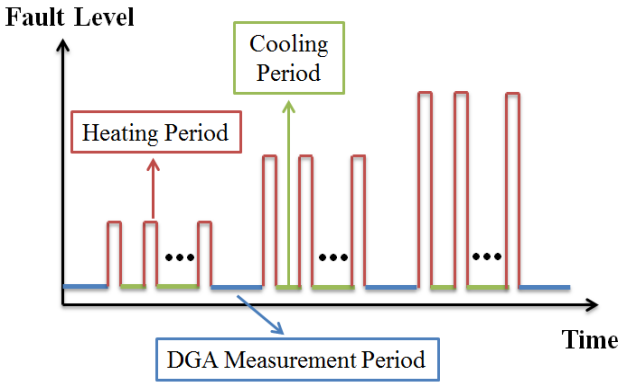

Figure 4-3 Test procedures of the DGA experiment with immersed heating element

Before heating, dissolved gas contents are measured by the two on-line DGA monitors as the background gas level. Subsequently, the thermal fault is generated by injecting

controlled input power into the heating element in the heating period. In the cooling period, the oil expanded into the syringe reaches its capacity limit so that the heating needs to be ceased. The oil is mixed and cooled by circulation until the expanded oil flow back from the syringe when the heating is restarted. This is repeated until the total heating time reaches the designated fault duration. Finally, the gas contents are measured again with the TM8 as gas level after thermal fault. The whole procedures are repeated with another thermal fault level controlled by input power. In a T3 thermal fault, free gas is significantly generated. It needs to be noticed that the free gas volume is measured by the syringe after thermal fault in order to calculate the total gas amount.

Another test indicated that the fault gases in the system would reach equilibrium state three to five hours after the thermal fault. This was found in the phenomenon that the detected gas concentration was usually increased in the initial two hours after thermal fault and then reached a plateau after the third to fifth hour of measurement. Therefore, the gas level after fault is calculated from the average of detection values during the plateau period.

The test procedures are shown in Figure 4-4 in terms of the online DGA measurements of methane (CH4) as an example, since methane is the key gas for all thermal fault levels.

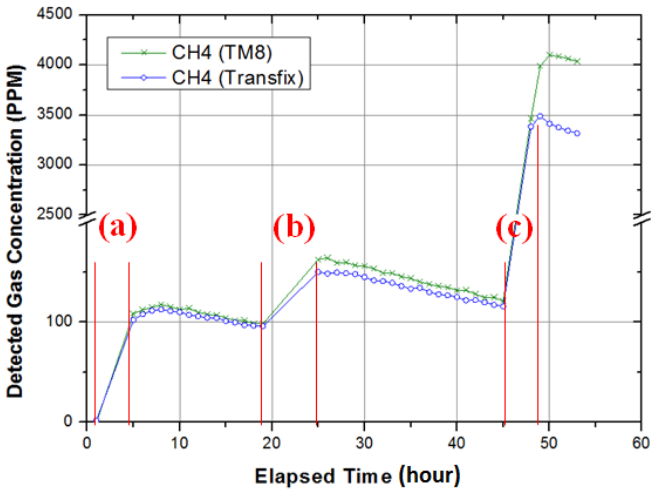

Figure 4-4 Online DGA measurements in a set of thermal fault experiments: (a) T1 fault generating period; (b) T2 fault generating period; (c) T3 fault generating period.

Initially, there is virtually no methane in the oil. After a T1 thermal fault, the methane concentration level increases from about 100 ppm and level off from the fourth

measurements. The highest methane concentration is regarded as the after fault gas level. The gas concentration is decreasing because the measurement of Transfix would cause gas loss. Subsequently, another thermal fault is generated and followed by the online DGA measurements. The difference between the after fault gas level and the background gas level is the gas generation in the thermal fault.

Once the online DGA measurements are completed, the oil from the test system can be sampled manually with syringes for laboratory measurements. In this stage, the oil in the whole system is circulated for several hours. Therefore, the fault gases are evenly distributed in the oil. The oil sample is representative and comparable to the oil analysed by the online DGA monitors.

4.4 Gas-in-total (GIT) Calculation

In the sealed oil circulatory system, gas-in-total (GIT) concentration of a certain type of gas can be calculated according to the detected gas-in-gas (GIG) concentration in headspace and the gas/liquid phase volume ratio when the system reaches equilibrium state. Calculation method is shown in equation (7) [30, 55].

$$GIT = GIG \times [K(T) + \beta] \times P_1/P_0 \times T_0/T_1 \quad (7)$$

Where, *GIT* and *GIG* are the gas-in-total and gas-in-gas concentrations in parts-per-million (ppm), respectively;
K(T) is the Ostwald solubility coefficient at the extractor;
β is the volume (phase) ratio between gas phase and liquid phase;
T_1, P_1 are temperature and pressure at the extractor in Kelvin and psi, respectively;
T_0, P_0 are temperature and pressure under standard condition, i.e. 298 K and 14.7 psi, respectively.

Either the relative gas amount (ppm) or the absolute gas amounts (μL) are closely related to temperature and pressure. The dissolved gases measured by the on-line DGA monitor are extracted at operational extractor temperature and pressure and need to be converted to unified condition [30]. Hence, the unit of DGA is temperature and pressure dependent. There are commonly three temperature conditions of unit for DGA results, all of which

are at standard atmosphere pressure: 0 ℃ (STP), 20 ℃ (IEC) and 25 ℃ [60]. In this paper, the condition of unit is 25 ℃ set by the on-line DGA monitor.

4.5 Relationship between Heating Element Temperature and Input Power

At steady state, the heating element temperature is related to the input power. The relationship between heating element temperature and input power in Gemini X mineral oil is shown in Figure 4-5.

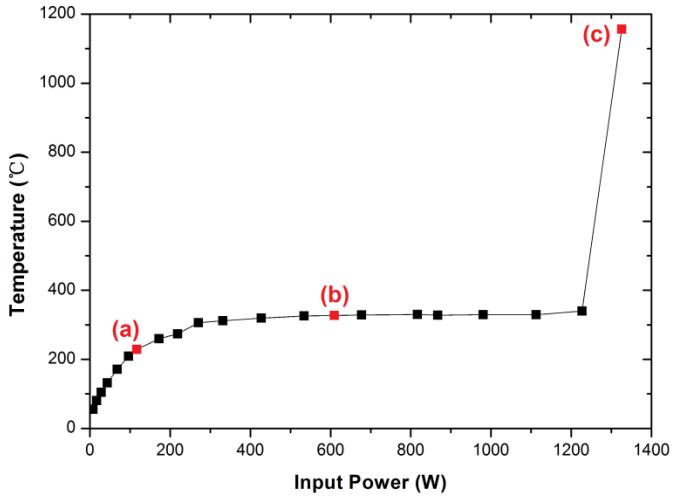

Figure 4-5 Relationship between heating element temperature and input power of Gemini X mineral oil

The heating element temperature increases with input power below 200 W. However, it becomes stable or "saturated" above 200 W which remains in between 320 ℃ and 330 ℃. In this constant region, the temperature could not be increased with a large input power increment. If the input power keeps rising, e.g. input power approaching 1000 W, the temperature along the heating element would suddenly become inhomogeneous and hotspot temperature might reach higher than 1000 ℃.

The experimental phenomenon is shown in three photos in Figure 4-6. They are correlated to three points on the heating element temperature curve marked as red points in Figure 4-5.

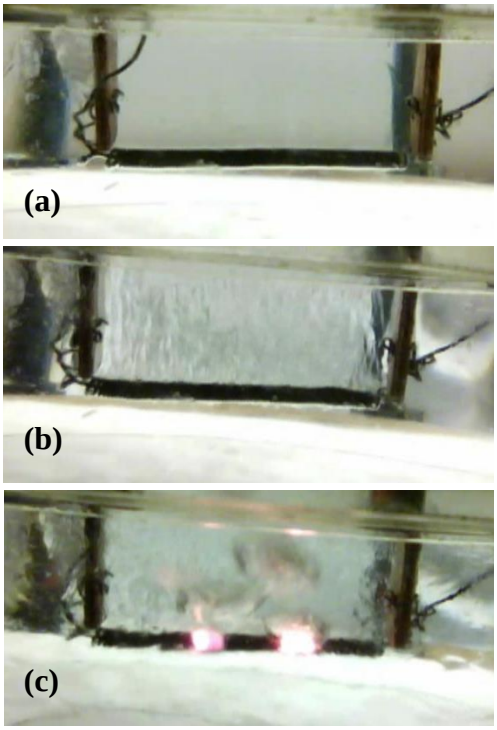

Figure 4-6 Experimental phenomenon of thermal fault simulated with immersed heating element in Gemini X mineral oil: (a) gentle convection; (b) strong convection and vaporization; (c) inhomogeneous heating.

When the input power is below 200 W, the heating element temperature is lower than 300 ℃. During heating, there is only gentle convection near the heating element as shown in Figure 4-6 (a). With input power increasing into the "saturated" region, surrounding oil starts vaporising and generates strong oil convection as shown in Figure 4-6 (b). At input power approaching 1000 W, the heating becomes inhomogeneous. Some section on the heating element emits visible light due to the radiation heat transfer where the pale yellowish color indicates the temperature is higher than 1000 ℃ as shown in Figure 4-6 (c). In this case, large amount of free gas bubbles are generated.

4.6 Pool Boiling Curve of Mineral Oil

In this study, Gemini X is tested as benchmark of conventional mineral oil. Boiling curve of Gemini X is tested and shown in Figure 4-7. It is the first time that the boiling curve of mineral insulating oil is measured and reported. It is plotted in the same format as the boiling curve (ABCC'E) of water in [67]. The pool boiling theory of water is introduced in Appendix II.

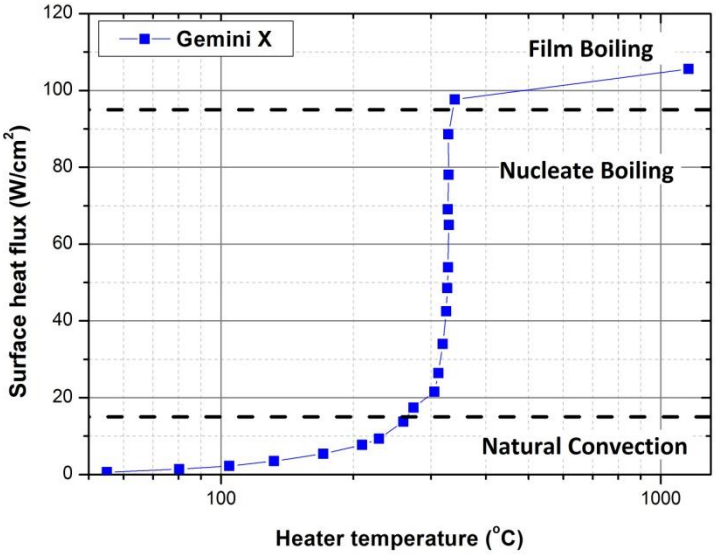

Figure 4-7 Pool boiling curve of Gemini X

When the input power is below 200 W, the boiling curve is in natural convection region where the heater temperature is below the oil boiling temperature. Once the input power is higher than 200 W, nucleate boiling is initialised with vapor bubbles generated. In the nucleate boiling region, the heater temperatures remains in between 320 ℃ and 330 ℃ with input power largely rising up. After the input power approaches 1000 W, the heating becomes inhomogeneous as shown in Figure 4-6 (c). This is in the film boiling region. Since the temperature is measured by thermocouple inserted in the center of the heating element, it reflects the average temperature rather than surface hotspot temperature. Hence, the measured temperature in the film boiling region could not reflect the highest temperature. It is proved that the pool boiling phenomenon exists in immersed heating process in oil. In Gemini X mineral oil, the temperature in the nucleate boiling region is between 320 ℃ and 330 ℃. Then the temperature would suddenly jump to a temperature above 1000 ℃ where the heating is inhomogeneous and the heating element is likely to burnout.

In the nucleate boiling region, the heating element temperature is constant with a large amount of input power increment. The extra energy is dissipated by the vaporisation as well as more severe convection than in natural convection region. This is proved by the gas generation results shown in Figure 4-8.

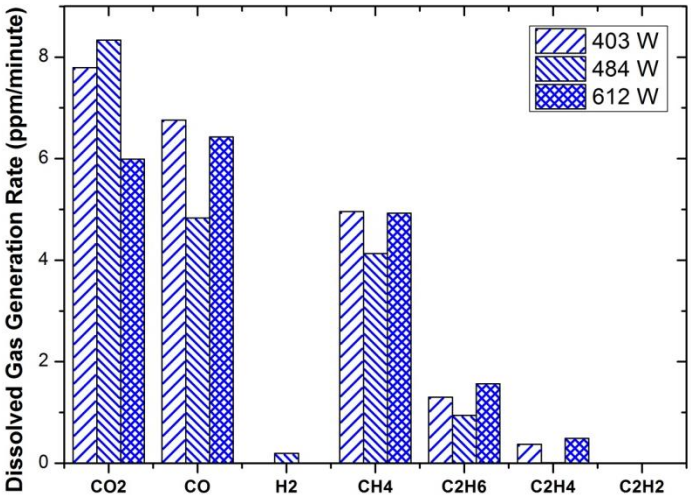

Figure 4-8 Gas generations from Gemini X in nucleate boiling region under various input power

In this study, the heating element is heated to nucleate boiling with three different input powers from 403 W to 612 W where the input power increased up to 50%. However, the gas generation results are similar and comparable. This proves that the increment of input energy might not increase the temperature of the heating element in the nucleate boiling region. The energy is dissipated through physical process such as vaporisation and convection.

4.7 Pool Boiling Curves of Alternative Liquids

The boiling curves of Diala S4 ZX-I and MIDEL 7131 are tested as alternative transformer oils. The Diala S4 ZX-I is manufactured from Gas to Liquid process. In the GTL process, the natural gas is firstly reacted with oxygen to produce synthesis gas. Subsequently, the synthesis gas is converted into liquid waxy hydrocarbons in a Fischer-Tropsch process. Finally, the liquid waxy hydrocarbons are hydrocracked and distilled into various GTL products including GTL based transformer mineral oil [12]. Due to the special manufacture process, the GTL mineral oil, Diala S4 ZX-I, contains primarily iso-paraffinic oil molecules with virtually no impurities such as aromatics. However, in this stage the Ostwald coefficients of conventional mineral oil are used for Diala S4 ZX-I since their molecule structures are similar. Therefore, the thermal and electrical properties of GTL oil would be different from conventional mineral oil [12]. The MIDEL 7131 is

tested as typical synthetic ester oil.

Boiling curves of Diala S4 ZX-I and MIDEL 7131 are shown in Figure 4-9. The boiling curve of Gemini X is plotted as a reference. It is worth noting that this is the first time of pool boiling phenomenon being found in insulating liquids which is one of the main contributions of this thesis. It is also the first time that the pool boiling curves of Gemini X mineral oil and two alternative insulating liquids are measured and presented.

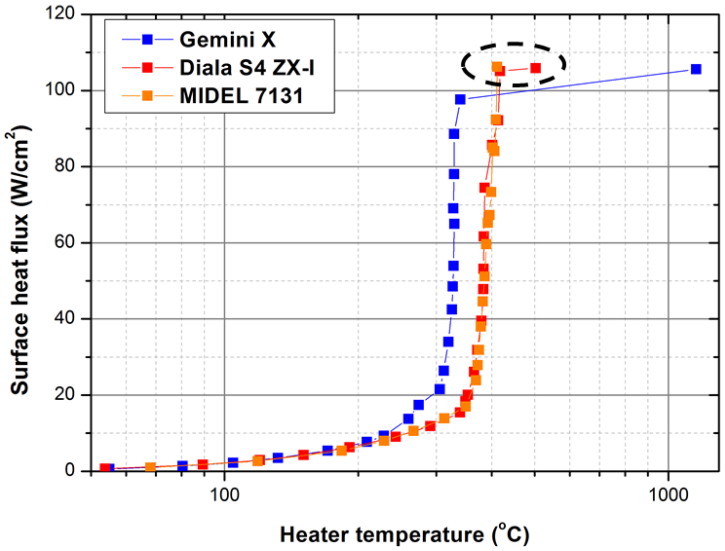

Figure 4-9 Pool boiling curve of Gemini X and alternative transformer oils

In the natural convection region, the boiling curves of the three oils almost overlap with each other. In the nucleate boiling region, the heater temperatures in alternative liquids are between 380 ℃ and 390 ℃ in both two oils in a wide range of input power. . In the film boiling region, the heating is inhomogeneous. The measured temperature might not reflect the surface temperature due to the same reason as in the mineral oil. When the Gemini X is heated to film boiling region, the measured temperature is higher than 1000 ℃ which might be quite close to the real temperature because the thermocouple location is coincidentally in the red hot zone as shown in Figure 4-6 (c). In the Diala S4 ZX-I and MIDEL 7131, the highest measured temperatures are 500 ℃ and 420 ℃ as highlighted in Figure 4-9, respectively. The reason might be that the red hot zone is not at the thermocouple location. The film boiling region in these two cases can be verified visually by the red hot zone on the heating element.

In the nucleate boiling region, the "saturated" temperatures of heating element in Diala S4 ZX-I and MIDEL 7131 are similar but they are quite different from that of Gemini X. This might be due to the different boiling points. Gemini X is a type of naphthenic mineral oil. Since the conventional mineral oil is a mixture of multiple types of hydrocarbon compounds, the boiling point is not a constant value. For Gemini X, the initial boiling point and boiling range is above 250 ℃ [8]. The Diala S4 ZX-I and MIDEL 7131 have constant and similar boiling points because they contain much less impurities than conventional mineral oil and can be considered as pure substances. Their boiling points are higher than Gemini X.

The highest temperature in the nucleate boiling region is known as Nukiyama temperature. The Nukiyama temperatures of a range of n-alkanes from pentane to hexadecane were investigated. They were found to be about 40 ℃ higher than the boiling point [68]. Therefore, the temperature of heating element in the nucleate boiling region could be higher in the fluid with higher boiling point. The boiling points of Diala S4 ZX-I and MIDEL 7131 are higher than Gemini X. Therefore, there is an about 60 ℃ difference between the Nukiyama temperature of Gemini X and the two tested alternative liquids. The difference depends on the difference between boiling points.

4.8 DGA Results in Natural Convection and Nucleate Boiling Regions

Total fault gas generation of three tested oils under natural convection region are listed in the Table 4-4. They are averaged from the results of three repeated tests. The dissolved gas contents are measured by the TM8 online DGA monitor and corrected with the Ostwald coefficients of the specific oil. The total experimental fault duration is 40 minutes.

Table 4-4 Total fault gas generation (ppm) from three tested oils under natural convection region

Oil \ DGA		CO2 (ppm)	CO (ppm)	H2 (ppm)	CH4 (ppm)	C2H6 (ppm)	C2H4 (ppm)	C2H2 (ppm)
Gemini X	μ	72.3	71.6	0.1	58.4	7.5	1.4	0.8
	σ	15.9	13.1	0.3	11.5	3.0	2.4	1.3
Diala S4 ZX-I	μ	68.4	27.5	0.0	54.6	14.2	4.2	0.0
	σ	20.7	5.0	0.0	9.7	7.7	5.7	0.0
MIDEL 7131	μ	102.1	39.5	2.1	12.0	14.7	7.6	0.2
	σ	21.6	5.8	1.1	2.1	4.5	4.8	0.6

μ: average of the gas generation results from repeated tests;
σ: standard deviation of the the gas generation results from repeated tests.

The gas generation amounts of CO2, CO, CH4 and C2H6 in all three oils are above the detection limit of the TM8 online DGA monitor. Trace amount of C2H4 generation is detected during experiments in all three oils which might be generated due to the localised hotspot where the temperature is much higher than the average temperature of the heating element. The standard deviations (σ) of all gases are calculated based on three repeated tests which show good repeatability of the tests. The gas generation amount ranges up to about 100 ppm.

The total gas generation rates of the three tested liquids in natural convection region are shown in Figure 4-10 averaged from three repeated tests.

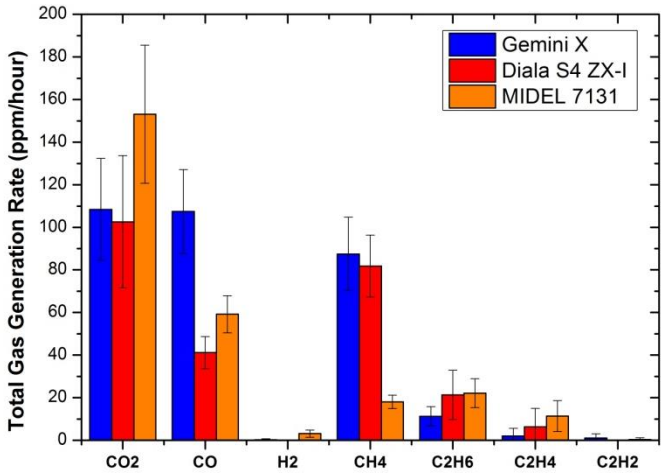

Figure 4-10 Total gas generation rates from three tested oils under natural convection region

The input power is 200 W. It can be seen that the total gas generation rates in the three liquids are comparable in natural convection region under the same fault energy. Methane (CH4) is mostly generated from Gemini X and Diala S4 ZX-I as major hydrocarbon gas.

MIDEL 7131 generates less hydrocarbon gases than the other two liquids with ethane (C2H6) as major hydrocarbon gas.

Total fault gas generation of three tested oils under nucleate boiling region are listed in the Table 4-5. They are averaged from the results of three repeated tests. The dissolved gas contents are measured by the TM8 online DGA monitor and corrected with the Ostwald coefficients of the specific oil. The total experimental fault duration is 12 minutes. The gas generation amounts of CO2, CO, CH4, C2H6 and C2H4 in all three oils are above the detection limit of the TM8 online DGA monitor. Trace amount of C2H2 generation is detected during experiments in all three oils which might be generated due to the localised hotspot where the temperature is much higher than the average temperature of the heating element. The standard deviations (σ) of all gases are calculated based on three repeated tests which show good repeatability of the tests. The gas generation amount ranges up to about 260 ppm.

Table 4-5 Total fault gas generation (ppm) from three tested oils under nucleate boiling region

Oil \ DGA		CO2 (ppm)	CO (ppm)	H2 (ppm)	CH4 (ppm)	C2H6 (ppm)	C2H4 (ppm)	C2H2 (ppm)
Gemini X	μ	89.7	84.6	1.9	61.7	14.3	3.0	0.5
	σ	25.6	12.9	3.3	6.5	3.4	2.2	1.1
Diala S4 ZX-I	μ	110.0	49.7	8.5	193.5	254.2	54.3	0.2
	σ	10.7	9.6	9.5	11.9	41.5	27.3	0.5
MIDEL 7131	μ	267.1	200.6	9.6	90.1	161.6	93.9	0.9
	σ	36.2	16.5	1.8	9.1	17.9	12.4	1.8

μ: average of the gas generation results from repeated tests;
σ: standard deviation of the the gas generation results from repeated tests.

The total gas generation rates of the three tested liquids in natural convection region are shown in Figure 4-11 averaged from three repeated tests.

In this case, the total gas generation rates from Diala S4 ZX-I and MIDEL 7131 are much higher than Gemini X with the similar input power. Diala S4 ZX-I and MIDEL 7131 generate more gases than Gemini X. The major hydrocarbon gas for the two alternative liquids is ethane while methane for Gemini X. In addition, MIDEL 7131 generates more carbon oxides. The reason is that the heating element temperature in the nucleate boiling region is higher in liquids with higher boiling point. On the other words, the fault gas

generation could be different under the transformer thermal faults with similar fault energy if the oil is changed.

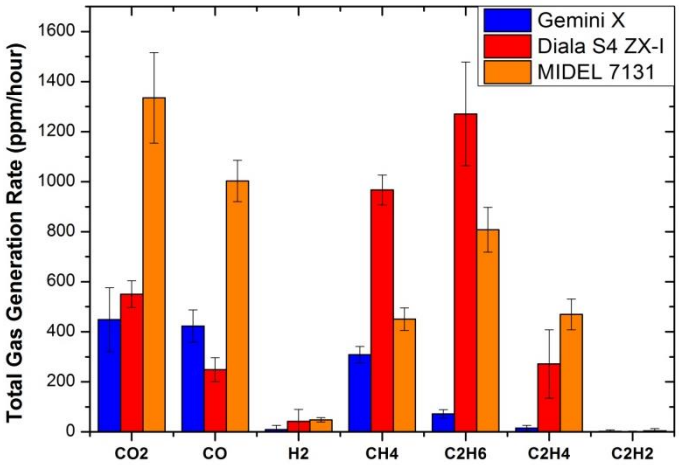

Figure 4-11 Total gas generation rates from three tested oils under nucleate boiling region

4.9 DGA Results in Film Boiling Region

Total fault gas generation of three tested oils under film boiling region are listed in the Table 4-6.

Table 4-6 Total fault gas generation (ppm) from three tested oils under film boiling region

Oil \ DGA		CO2 (ppm)	CO (ppm)	H2 (ppm)	CH4 (ppm)	C2H6 (ppm)	C2H4 (ppm)	C2H2 (ppm)
Gemini X	μ	414	215	7296	8487	1464	11330	401
	σ	186	116	1748	3837	638	5180	167
Diala S4 ZX-I	μ	366	359	8057	10558	2453	21080	593
	σ	251	384	3506	4008	1256	7338	146
MIDEL 7131	μ	3281	4151	2947	3907	997	8460	491
	σ	1011	1051	1211	843	242	2132	403

μ: average of the gas generation results from repeated tests;
σ: standard deviation of the the gas generation results from repeated tests.

They are also averaged from the results of three repeated tests. The dissolved gas contents are measured by the TM8 online DGA monitor and corrected with the Ostwald coefficients of the specific oil. The total experimental fault duration is determined by the duration of red hot on the heating element which is quite random. In general, the fault duration ranges from a couple of seconds to about one minute. The gas generation amounts of all fault gases in all three oils are above the detection limit of the TM8 online

DGA monitor. The standard deviation (σ) of all gases are calculated based on three repeated tests which are in general higher than under the previous two boiling region. The reason might be that the fault size of the heating element in film boiling region depends on the area of the red hot. In each test, the red hot area occurs randomly on the heating element.

In the film boiling region, the input power is higher than 1000 W. When the immersed heating element is in the film boiling region, large amount of free gas bubbles are generated. It is estimated in the experiment that the free gas generation rate is about 1 – 3 mL/sec. However, in the natural convection region and nucleate boiling region, there is virtually no free gas bubble generated.

The total gas generation rates are shown in Figure 4-12 averaged from three repeated tests.

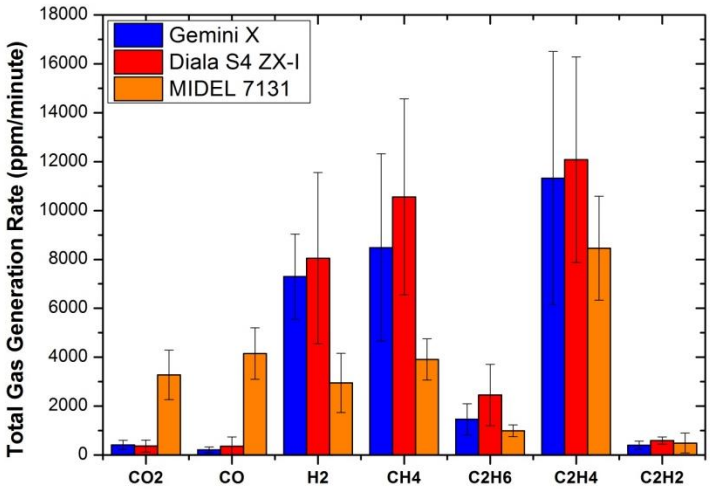

Figure 4-12 Total gas generation rates from three tested oils under film boiling region

In this situation, the temperature distribution along the heating element is quite inhomogeneous where the hotspot could be higher than 1000 ℃ with red hot phenomenon. The fault area is difficult to estimate since it is difficult to measure the red hot area. Therefore, the standard deviations of these results are larger than the results in natural convection and nucleate boiling regions.

According to the pool boiling theory, the burnout temperature is not relevant to the liquid properties in film boiling region. Therefore, the gas generations from Gemini X and from

Diala S4 ZX-I are similar and comparable in which hydrogen and hydrocarbon gases such as ethylene and methane are largely generated. In the MIDEL 7131, the hydrocarbon gas generation is significantly less than the other two oils. The carbon oxides generations in MIDEL 7131 are significant while in the other two oils are negligible. This might verify that the carbon oxides might be generated from oil decomposition process of MIDEL 7131 because there are considerable amount of oxygen atoms in the synthetic ester oil. Acetylene as the key indicator of T3 thermal fault is generated in all three oils.

4.10 Practical Implication

The temperature of immersed heating element is limited by the pool boiling phenomenon. In conventional mineral oil, the boiling point is normally in the range of 250 ℃ – 300 ℃. The Nukiyama temperature is between 290 ℃ and 340 ℃. Once beyond this temperature, the heating element would jump into the film boiling region where hotspot temperature is higher than 1000 ℃. The whole range of the transformer thermal fault is difficult to approach with the immersed heating method. Therefore, any reported thermal faults of immersed heating element above the possible Nukiyama temperature of mineral oil in previous studies [18, 48] need to be re-interpreted.

The phenomenon that the heating wire is easily burnout and large amount of free gases are evolved at 400 ℃ in the DGA thermal experiment [18] could be explained as the heating element is already in film boiling region and the measured temperature is not accurate. In the other DGA thermal experiment, the fault gas generation seems to be a T3 fault according to Duval triangle method at 400 ℃ where the percentage of methane, ethylene and acetylene is 38.7%, 51.4% and 9.9%, respectively [48]. This could also be due to the actual heating element surface temperature is much higher than the measured 400 ℃. The actual fault temperature might be above 800 ℃ due to the significant amount of acetylene generation [1]. In alternative transformer insulating liquids, such as natural ester, the stable approachable heating element temperatures are higher than in mineral oil [18, 48]. It could also be explained by the pool boiling theory that the boiling point of natural ester liquid is much higher than conventional mineral oil.

Based on the pool boiling theory, the heating element would be in nucleate boiling in a wide range of input power. According to the previous discussion, the low boiling point of insulating liquid could somehow limit the temperature of immersed heating element below the film boiling region. The immersed heating element in liquid with higher boiling point could achieve higher temperature in nucleate boiling region which could bring more severe damage to the other insulation materials in transformers. Hence, it is quite necessary to measure the boiling curves of transformer insulating liquids in order to know the Nukiyama temperature.

In addition, the boiling point is relevant to the surrounding pressure. The Antoine equation is a semi-empirical correlation which describes the relationship between vapor pressure and boiling temperature. For example, the boiling point of hexadecane under atmosphere pressure is 286 ℃ while 320 ℃ under 2 bar absolute pressure. Therefore, if an immersed thermal fault in nucleate boiling region occurs at the bottom of the transformer, the temperature could be higher than that at the top due to the surrounding oil pressure.

4.11 Comparison between Online DGA and Laboratory Measurements

The oil in the test system is analysed by the two online DGA monitors synchronously. During experiments, the oil is sampled by gas-tight syringe and transported to professional analytical laboratory. In the laboratory, conventional laboratory based DGA measurements are performed on the oil samples. The aim is to compare the DGA measurements of the online DGA monitors with the conventional laboratory DGA measurements in order to assess the measuring performance of the online DGA monitors.

In Cigre brochure 409, the Round Robin Tests (RRT) on comparison between laboratory DGA measurements and online DGA monitor measurements are performed with the routine gas concentrations and low gas concentrations [60]. The routine gas concentration is defined as the oil sample with concentration of dissolved gas 5 times higher than the detection limit of the online DGA monitor. The low gas concentration is defined as the dissolved gas concentration is in between 2 and 5 times of the online DGA monitor detection limit [60].

In the experiments, the oil samples are taken after both T1 and T3 faults in order to compare online DGA monitors and laboratory measurements under two different gas concentrations. To confirm the detection effectiveness of the laboratory measurements, two syringes of samples are taken each time. The samples are taken after several hours of online DGA monitor measurements when the oil in the test system is fully mixed. In addition, the oil is sampled right after a DGA detection of online DGA monitors to mitigate the error. The last online DGA measurements before sampling are used to compare with laboratory measurements.

The comparison results between online DGA monitors and laboratory measurements of oil sample after a T1 fault in Gemini X mineral oil are shown in Table 4-7. Two oil samples are taken by two syringes. The oil samples are extracted by headspace extraction method and analysed by laboratory GC facility.

Table 4-7 Comparison between laboratory measurements and online DGA measurements (ppm) of Gemini X mineral oil under fault gas level after T1 fault

T1	Syringe 1 (ppm)	Syringe 2 (ppm)	Average (ppm)	TM8 (ppm)	D of TM8	Transfix (ppm)	D of Transfix
CO2	353	327	340	318	**-6%**	390	**15%**
CO	68	67	67.5	65	**-4%**	45	**-33%**
H2	0	0	0	0		4	
CH4	68	70	69	57	**-17%**	55	**-20%**
C2H6	9	10	9.5	14	**47%**	16	**68%**
C2H4	17	14	15.5	18	**16%**	12	**-23%**
C2H2	2	2	2	3	**50%**	1	**-50%**

The measurements of Syringe 1 and Syringe 2 are similar which shows the repeatability of the laboratory measurements. The averages of the two syringes are regarded as the benchmark of laboratory DGA measurements. The columns of TM8 and Transfix give the last DGA measurements before oil sampling of TM8 and Transfix, respectively. The difference between online DGA monitor measurements and laboratory measurements are calculated as the difference in percentage related to the laboratory measurements.

The differences between TM8 and laboratory results are within 20% except for the ethane and ethylene whose differences are nearly 50%. However, the absolute differences of these two gases are both within the detection limits of the online DGA monitors. The percentage differences of the Transfix measurements of all the gases are higher than the

measurements of TM8 measurements. The reason might be that the method of laboratory DGA measurement is same as the TM8 which is the using the gas chromatography (GC) technique, and it is different from the Transfix which is using the Photo-Acoustic Spectroscopy technique. The extraction methods of all three methods are based on the headspace extraction method. The TM8 is using semi-permeable membrane to extract dissolved gas from the oil. The Transfix is using headspace cell with air bubble purging the dissolved gas from the oil. The different design of headspace methods of the two online DGA monitors might also generate discrepancies in measurement results.

The comparison results between online DGA monitors and laboratory measurements of oil samples after a T3 fault in Gemini X mineral oil are shown in Table 4-8.

Table 4-8 Comparison between laboratory measurements and online DGA measurements (ppm) of Gemini X mineral oil under fault gas level after T3 fault

T3	Syringe 1 (ppm)	Syringe 2 (ppm)	Average (ppm)	TM8 (ppm)	D of TM8	Transfix (ppm)	D of Transfix
CO2	456	449	452.5	458	**1%**	527	**16%**
CO	126	112	119	133	**12%**	102	**-14%**
H2	1330	882	1106	922	**-17%**	1915	**73%**
CH4	1797	1578	1687.5	1555	**-8%**	1265	**-25%**
C2H6	291	261	276	277	**0%**	374	**36%**
C2H4	2534	2290	2416.5	2129	**-12%**	2381	**-1%**
C2H2	129	121	125	118	**-6%**	82	**-34%**

The percentage differences of all gases are within 20%. In general, the percentage differences of the Transfix results are larger than those of the TM8. The percentage differences of the Transfix DGA measurements of the ethane and ethylene are all above 30%. The percentage difference of the hydrogen is more than 70%. The probable reason is that the dissolved hydrogen in the oil is measured by the dissolved hydrogen sensor which is based on different technique from GC measurement.

In conclusion, the DGA measurements of the TM8 are closer to the laboratory measurements compared with the Transfix probably because the TM8 is using similar gas detection technique to the laboratory. Under low concentration levels, i.e. below 10 ppm, the percentage differences are higher than those under normal concentration levels. However, at low concentration levels, the absolute differences are within the low detection limits. In addition, there is a big discrepancy between the hydrogen

measurements between Transfix and laboratory which is possibly because the Transfix is using hydrogen sensor in oil to measure the dissolved hydrogen.

4.12 Summary

In this chapter, it is so far the first time to present the pool boiling phenomenon in the immersed heating DGA experiments in insulating liquids. According to the pool boiling theory, the temperature of the immersed heating element will be saturated at the Nukiyama temperature with large input power increment and followed by an inhomogeneous temperature distribution and localised extremely high temperature. The pool boiling curves of three tested liquids are measured and reported. The Nukiyama temperatures of the Diala S4 ZX-I and MIDEL 7131 are higher than that of the Gemini X, probably due to the different boiling temperatures of the oils. According to the pool boiling theory and phenomenon, the immersed heating element temperature will saturate at the Nukiyama temperature with large input power increment and followed by an inhomogeneous temperature distribution and localised extremely high temperature. Therefore, any immersed heating element with a measured temperature higher than the Nukiyama temperature might actually be in the film boiling region where the actual hotspot temperature might be in a T3 thermal fault level. The results in previous DGA works with immersed heating method might need to be reinterpreted. In addition, the temperature of transformer thermal fault might not cover the whole T2 range if the fault is immersed heating type.

As the immersed heating element temperature is limited by the Nukiyama temperature. The immersed heating method could hardly cover the whole transformer thermal fault range. However, it is still a suggestion for some laboratory DGA experiments where there is little requirement on temperature range, considering this method is flexible, economical and easy to control. In this PhD research work, a DGA thermal fault experimental system is necessary to cover the whole range of transformer thermal fault temperature. Hence, a DGA thermal fault experimental system based on tube heating method has been established which will be introduced in the next chapter.

In this chapter, the online DGA monitors are assessed by comparing the measurements with the laboratory DGA measurements. By comparing between both the TM8 and Transfix give measurement differences lower than 30% on normal gas concentration levels. On low gas concentration levels, the measurements of online DGA monitors are reliable by comparing the absolute differences with the low detection limits. In general, Transfix gives higher measurement differences than TM8, especially on the hydrogen measurements. The probable reason is that the different gas measurement techniques are utilised by the two online DGA monitors.

Chapter 5 DGA Experimental System with Tube Heating Thermal Faults Simulation Method

5.1 Introduction

As discussed in the previous chapters, the conventional immersed heating element could not cover the whole range of transformer thermal faults i.e. 300 – 700 ℃, hence a different heating method is required.

A DGA pyrolysis study of transformer oils with tube heating method is introduced in Chapter 2. In this method, a small portion of oil is heated in a section of tube which is heated by a temperature controlled furnace. According to the pyrolysis study, this method is capable of simulating transformer thermal fault stably at any temperature below 700 ℃.

The temperature of the immersed heating element is limited by the boiling effect. The vaporisation of oil and interaction between vapor and subcooled oil could significantly dissipate the heat energy. In the tube heating system, only tens millilitres of oil is heated in a section of tube. In this situation, once the oil is being heated above the boiling point, there oil will get vaporised. However, there is no subcooled oil surrounded. The heat could only be dissipated inside the tube which is much less efficiency compared with immersed heating method. On the other words, in the tube heating method, the oil could be maintained under vapor state stably in the heating pipe. Therefore, the tube heating method could generate thermal fault stably at the temperature above the boiling point of oil.

A DGA thermal test setup based on tube heating method has been established. In this chapter, the design of the system is introduced as it is based on a novel thermal fault simulation method. Subsequently, several preliminary experimental trials are discussed in order to quantify the characteristics of the established setup. Finally, a series of experimental procedures are designed based on the preliminary trials.

5.2 Experimental Setup Description

5.2.1 Overall System

The whole test system is designed compactly on a portable trolley for flexibility. The TM8 online DGA monitor is connected to the system. As discussed in previous contents, multiple online DGA monitors could operate in parallel by connecting through a check valve. This system could also connect multiple online DGA devices in parallel. Controller of the furnace and a water bath are set on lower level of the trolley. The water bath is used to cool down the oil and pipe outside the heating area during experiments, which will be introduced later in detail. The tube heating based DGA thermal fault test system is shown in Figure 5-1. A photo of the test system is shown in Appendix III.

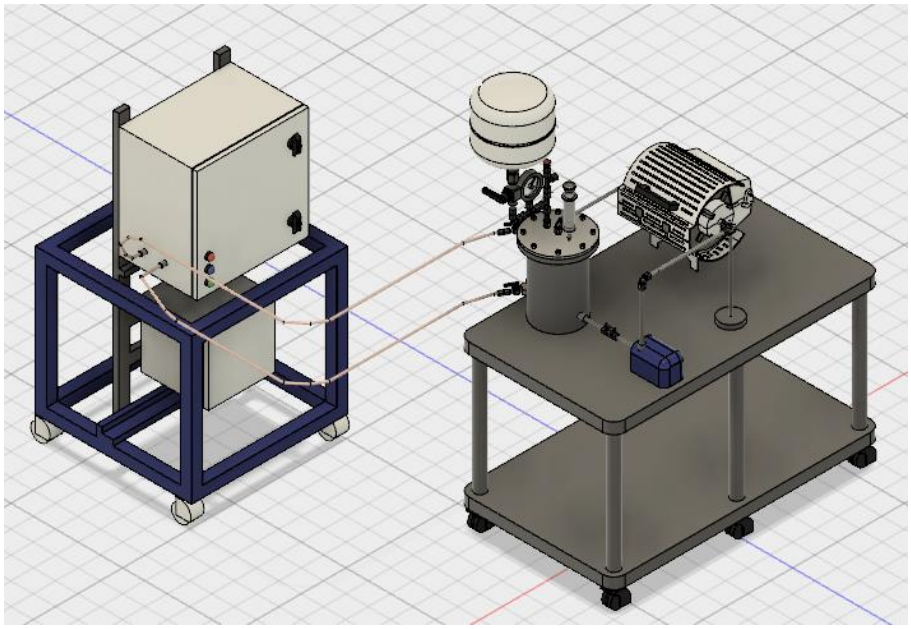

Figure 5-1 Overall tube heating based DGA thermal fault simulation experimental system

5.2.2 Oil Circulation System

The total volume of the oil circulation system is 8.3 litres. It is measured by fully filling the system with water and then measuring the volume of the water. The pump is used to mix the oil in the system by circulating the oil from the bottom of the main vessel and returning it from the top. The online DGA monitor is connected to the system through the

valves on the main vessel. The oil circulation system contains main vessel, circulation pump and heating pipe as shown in Figure 5-2.

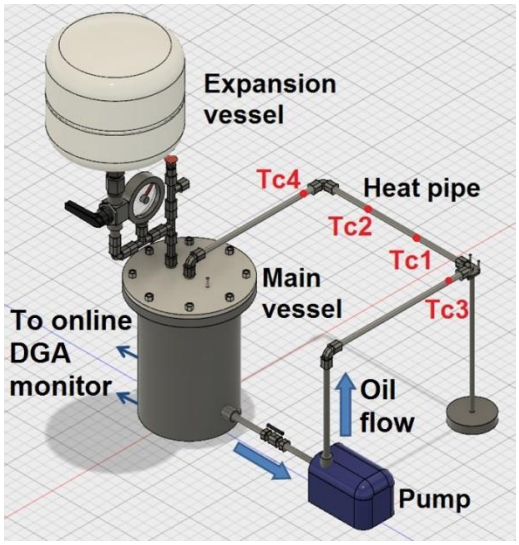

Figure 5-2 Oil circulation system of the tube heating DGA test system

Main Vessel

The geometry of the main vessel is shown in the Figure 5-3.

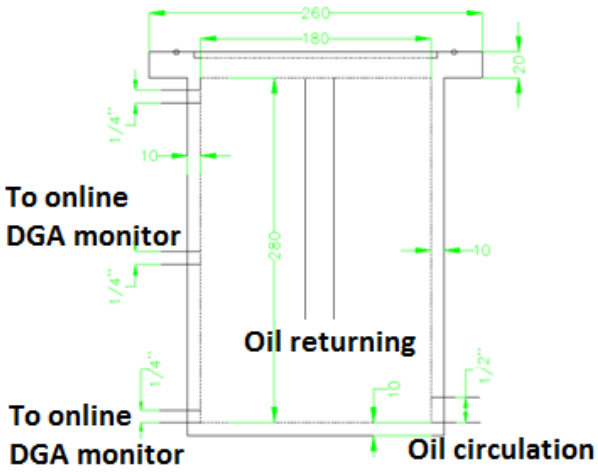

Figure 5-3 Geometrical size of the main vessel

Most of the tested oil is in the main vessel. The total volume of the main vessel is about 7.6 litres. During experiments, tens millilitres of oil are heated in the heating pipe, which would decompose and generate fault gases. Then the fault gases would be dissolved in the oil in main vessel through pump circulation. If the oil volume in the main vessel is too large, the fault gas concentrations could be too small to be detected at lower fault levels.

However, if the oil volume in the main vessel is too small, the fault gas concentrations might be beyond the DGA detection limits. In addition, the bulk oil temperature might be significantly increased by mixing with the heated oil. When the oil is heated at high temperature, e.g. above 600℃, free gases might be strongly evolved. For safety consideration, a certain volume of gas space is necessary in the main vessel. In the experiments, there are 6 litres of oil and 1.6 litres gas headspace in the main vessel. The lid of the vessel is sealed by a rubber gasket. The geometry of the main vessel is shown in the Figure 5-3. The oil is circulated from the oil circulation tube at the bottom of the vessel and returned from the oil returning tube at the top. As shown, the oil returning tube is extended below the oil surface in the vessel which could maintain the oil in the heating pipe rather than flow back to the main vessel. On the opposite side of the oil circulation tube, three valves are connected to the vessel by threads. The top valve leads to the headspace above the oil surface which could be used to purge the air or fill charge gas. The other two valves are used to connect the online DGA monitor. For convenience, the two valves are on the same side. However, the oil is actually circulated from the bottom of the valve and returned to the top oil surface on the far side as shown in Figure 5-3. In this arrangement, the local oil circulation is avoided and the oil sampled by the online DGA monitor is representative. For better sealing performance, these connections are reinforced by silicone sealant.

Circulation Pump

The oil in the heating pipe and main vessel is mixed before and after heating by pump circulation. The Totton® magnetic coupled centrifugal pump is used as circulation pump. The model number is NDP 14/2. There are two reasons to use magnetic coupled pump. First, the impeller is sealed properly in pump body and driven by drive magnet which could ensure a gas tight sealing performance. Second, the magnetic coupled pump is economical which could cover a wide range of flow rate. A needle valve is installed to control the flow rate by manually adjusting the orifice size. In this stage, the oil is static during heating. However, it might be interesting to investigate the gas generation of oil flow through heated pipe. This will be introduced in detail in the future work section.

The pump inlet and outlet ports are connected to the stainless steel tubing with rubber

hose and sealed with Jubilee® clips. To improve the gas tight sealing performance, the connection points between rubber hose and stainless steel tubing are reinforced with silicone sealant. The datasheet of the pump is shown in Table 5-1.

Table 5-1 Data sheet of the circulation pump in the tube heating experimental system

Pump Model	Max pressure	Max capacity	Max head	Temperature range	Max specific gravity
NDP 14/2	1.4 bar	15.5 L/min	2.4 m	-20 ℃ – 85 ℃	1.2

5.2.3 Oil Heating System

The oil heating system contains tube furnace and water bath cooling loop. The heating pipe is heated in the tube furnace chamber in order to generate thermal fault in oil. To maintain the system temperature outside the furnace chamber around room temperature, the two pipes connecting the heating pipe are covered with water circulating loop. The water is continuously circulated during experiments. The temperature of the water is controlled by a water bath.

Tube Furnace

The thermal fault is generated by a Carbolite® tube furnace. The furnace could operate stably at 1100 ℃. The furnace chamber is cylindrical which is made of thermal blockage material to limit heat loss. Most of the input energy is transformed into heat and increase the temperature in the furnace chamber. The chamber diameter is 60 cm and the length is 15 cm. The furnace chamber is shown in Figure 5-4. The maximum power of the furnace is 750 W at which the maximum temperature rising rate is about 100 ℃/minute. During operating, the furnace could maintain the working temperature at the set point by adjusting the output power to be pulsed.

Heating Pipe

Before heating, the heating pipe should be filled with oil. Then the pipe is heated by the furnace. The total length of the heating pipe is 30 cm and the length of the heated area is 15 cm. Considering the temperature distribution in the furnace chamber, the actual hotspot temperature zone might be much shorter than 15 cm. The Swagelok® stainless

steel tubing is used as the heating pipe. The material of the tubing is 316 stainless steel. The major advantage of 316 stainless steel over 304 stainless steel is the better corrosion resistance. Stainless steel has higher hardness than other metal such as copper and aluminium. In addition, in DGA studies copper is not preferred as material of oil container or pipe because the copper might react with dissolved hydrogen. The heating pipe outside diameter of the pipe is 1/2 inch (1.27 cm) and the inside diameter is about 0.4 inch (1.02 cm). The wall thickness of the heating pipe is 0.125 cm. According to the Fourier's law of heat transfer, the maximum temperature difference between the inner and outer surfaces of the heating pipe is only about 10 ℃ when the furnace is working at its maximum 750W output power. Therefore, the hotspot temperature of the thermal fault inside the heating pipe could be considered same as the heating pipe outer surface temperature which is measured by the thermocouple clamped on it. The heating pipe is a section of pipe heated in the furnace as shown in Figure 5-4.

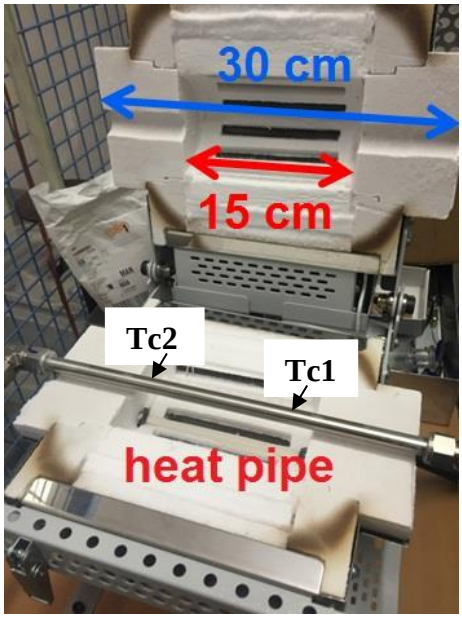

Figure 5-4 Geometry of the heating pipe and the furnace chamber

During heating, the oil natural expansion might introduce pressure in the heating pipe. Although there are gas cushion in headspace and expansion vessel, the localised high pressure during heating could be dangerous. This could be quite severe under high temperature at which the oil would be vaporised rapidly and large amount of free gas

could be accumulated in a short duration. The pipes are connected with Swagelok® tube fittings to guarantee the safety which could withstand 3000 psi (200 bar) positive pressure.

Water Cooling Loop

The cooling pipes connecting between heating pipe and the outside oil system are covered with water cooling loop. The water is circulated through the outside of the two cooling pipes with a water bath which would control the water temperature. The water bath cooling loop is used to accelerate oil condensation. The cooling loop is shown in Figure 5-5.

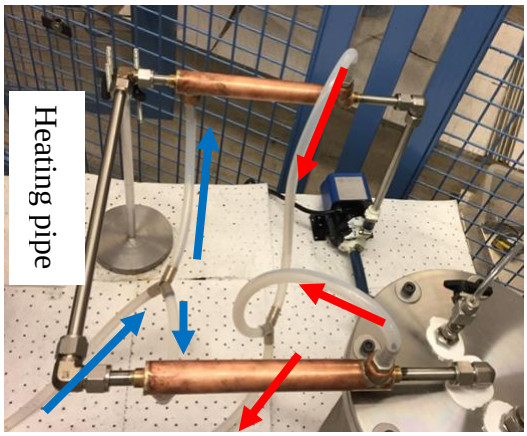

Figure 5-5 Water bath cooling loop

5.2.4 Gas Expansion System

The gas expansion system is consisted of the headspace gas phase in the main vessel above the oil surface, the expansion vessel and the pressure relief valve. The gas phase in the system refers to the gas in the gas in the gas expansion system. The major function of the gas expansion system is to relieve the pressure surge and release overpressure during operating for safety consideration. The volume of the gas phase needs to be determined in order to quantify the total fault gas content in the system.

Nitrogen Filled Headspace

Initially, argon was used as the purge gas to replace air in the headspace. It was then found that the oxygen measurement of TM8 online DGA monitor is interfered by the

dissolved argon in the oil. The reason is that the peak of the argon on the TM8 GC spectrum will slightly overlap with the oxygen peak, and the TM8 would misinterpret the oxygen concentration as 0. On the other words, the TM8 online DGA monitor could not analyse oil with significant amount of dissolved argon. Therefore, the purging gas is changed to nitrogen in the following experiments.

In the main vessel there is 1.6 litres headspace above the oil surface. This headspace gas works as gas cushion to prevent the sudden pressure build-up during heating. The headspace is filled with nitrogen rather than air. There are two reasons. First, the nitrogen blanket could limit the oxygen level in the oil and largely mitigate oil oxidation. Second, prevent oil ignition or explosion in case the hot oil vapour splashes into the headspace during heating. Even at the auto-ignition point of the oil, the oil vapour could not burn without enough oxygen.

The headspace is filled with nitrogen (> 99.999%) from nitrogen gas cylinder. The air in the headspace will be purged out by a vacuum pump. Then the nitrogen will be charged into the system. The vacuum pump could purge the air out up to 0.3 bar absolute pressure. Assuming the system is properly sealed at this pressure level. According to the ideal gas law, only 30% gas would remain in the system after each vacuum purging and nitrogen filling cycle. On the other words, after each vacuum purging and nitrogen filling cycle, 70% of previous gas would be replaced by nitrogen. After n times of vacuum purging and nitrogen filling cycle, the remaining air in the system would be $0.3^n*100\%$ of the initial value. Normally the percentages of oxygen and carbon dioxide in air are 21% and 0.4%, respectively. It can be calculated that the remaining concentrations of oxygen and carbon dioxide in the system headspace after five times vacuum purging cycles would be nearly 510 ppm and 10 ppm, respectively. In the experiments, to remove as much oxygen and carbon dioxide as possible, the vacuum gas purging process should be repeated at least five times.

Expansion Vessel

Although the nitrogen filled headspace could function as gas cushion, during heating the pressure could significantly change due to oil thermal expansion, vaporisation or free gas generation. The expansion vessel is connected to relief the expansion pressure.

The expansion vessel is originally designed for the solar expansion system. The expansion rubber bladder is connected to the main vessel headspace. The bladder rubber is synthetic rubber which has low gas permeability. The bladder is in an expansion tank which works as a secondary vessel to prevent gas leaking into the laboratory if the rubber bladder is exploded. The maximum volume of the bladder is 3 litres. The inside volume of the expansion tank is 15 litres. The bladder is sealed in the expansion tank with a stainless steel flange. The expansion tank is equipped with a Schrader valve at the upper side. The Schrader valve is a type of pneumatic tyre valve widely used on motor vehicle and bicycle. The valve core is a poppet valve assisted by a spring. Therefore, the expansion tank could maintain positive pressure inside. The pressure could also be relieved by pushing the valve stem and opening the valve. A positive pressure could also be injected into the expansion tank through a tyre pump. In addition, when the pressure inside the expansion tank is lower than outside, based on the design of Schrader valve it will naturally open. Therefore, the expansion tank could not maintain negative pressure. The structure of the expansion vessel is shown in Figure 5-6.

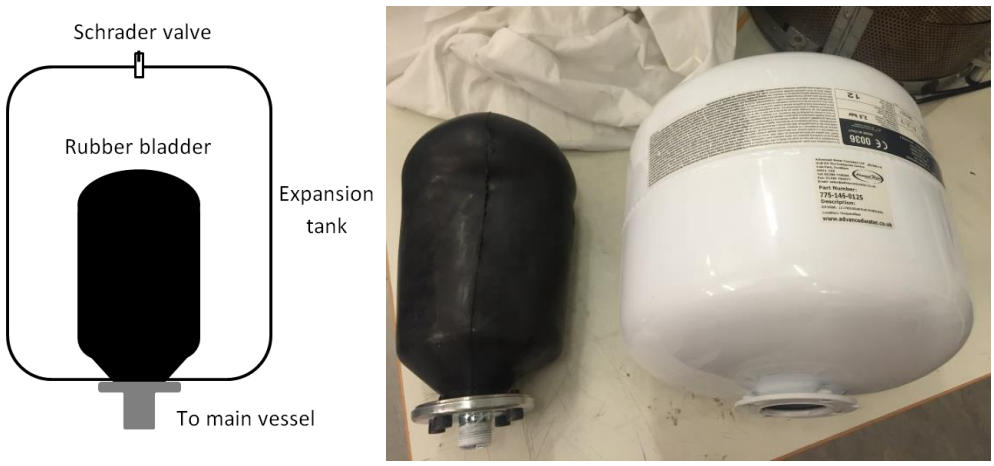

Figure 5-6 Structure of expansion vessel

Pressure Relief Valve

Although the expansion vessel could effectively and safely relieve the expansion pressure, the system inner pressure could still be built up if the volume increment is larger than 3 litres. For example, the free gas generation during experiments might be much larger than 3 litres if the experimental duration is not properly designed. Therefore, a pressure relief valve is fitted as a secondary protection. The pressure relief valve is connected in parallel with the expansion vessel to the headspace of the main vessel.

The Swagelok® pressure relief valve is used in this system. In this system, the operation pressure is set at 10 psig. For safety consideration, a manual operation handle is equipped on the pressure relief valve. The pressure relief valve could be switched on with the manual operation handle even if the pressure in the system is lower than the set pressure.

5.3 Preliminary Trial Tests

After the DGA tube heating experimental system has been established. There are virtually no experiences on its performance and characteristics. Therefore, a series of preliminary trial tests are performed to understand whether the system could be working as its design. A set of detailed experimental procedures could be made based on the preliminary trial test results.

5.3.1 Sealing Test

Dissolved gas analysis is studying the amount and combination of fault gases dissolved in the transformer insulating liquids. Therefore, DGA test system requires gas tight sealing condition. In general, sealing tests should be applied on any containers or test systems related to DGA studies. For example, sealing test is a key step in the online DGA monitors installation before commission. The results might be severely distorted if the system is gas or oil leaking.

The sealing performance of a sealed system could be indicated by measuring the retention

time of a pressure difference in the system. The pressure difference could be either positive or negative. Both the magnitude of the pressure difference and the retention time depend on the sealing requirement of the system.

The tube heating DGA test system is designed to operate under atmosphere pressure for safety consideration. However, due to the design of the expansion vessel, the system might build up positive pressure inside if the free gas is largely generated and accumulated in the expansion bladder. In an assumed extreme case, the initial gas volume in the expansion bladder is 700 mL and the final volume is at the maximum bladder volume which is 3 litres. The initial 700 mL gas volume in the expansion bladder is necessary for sampling proposes and will be explained in the latter section. In this case, the free gas generation volume would be about 2.3 litres under atmosphere pressure. The pressure difference built up in the system is 200 mbar. If the furnace keeps heating, the free gas would be generated more than 2.3 litres and the system pressure would keep increasing until the pressure relief valve is triggered. Hence, the heating duration should be strictly limited to avoid too much free gas generation.

In the sealing test, a positive pressure of 200 mbar is manually injected into the system. The test results are shown in Figure 5-7.

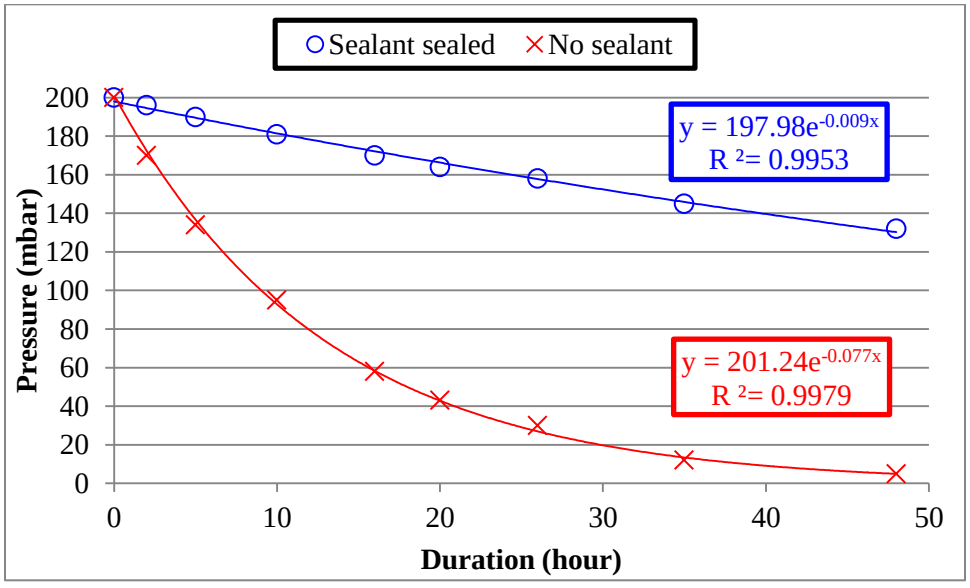

Figure 5-7 Inside pressure with test duration of the system with and without sealant sealed

In the first test, the system is not properly sealed. The sealing test results are shown as the

red curve in Figure 5-7. The pressure decreased to about 5 mbar in 48 hours which shows significant gas leakage. The leakage points were then located by soup water covering all connection points. It was found that the thread connection points on the main vessel were the major leakage points. Those leakage points were then sealed by silicone sealant. More than 130 mbar pressure could be maintained within 48 hours which indicates the sealing condition is largely improved. The relationship between pressure and duration gives an exponential fitting curve. The smaller the exponential parameter is, the better the sealing condition the system is. The curve could also be used to estimate the system sealing performance under different initial pressures and durations.

It needs to be noticed that the leakage in the sealing tests is an extreme case where the system is set under the maximum possible pressure. In experiments, the system is designed to work under atmosphere pressure where the pressure driving force of leakage is negligible.

5.3.2 Flow Rate Test

The oil is circulated by a centrifugal pump. The flow rate of the oil circulation depends on the oil viscosity and the friction loss of the system. The flow rate could be controlled by the needle valve. The orifice size of the needle valve could be adjusted smoothly. The smaller the orifice size is, the larger the friction loss of the system is. And the flow rate could be controlled smoothly up to the maximum speed at which the orifice of the needle valve is at maximum size. Therefore, it is important to determine the maximum flow rates of the circulation in various types of liquids.

The maximum flow rate of the pump is estimated by measuring the volume of circulated liquid in unit time. Firstly, about 5 litres of tested liquid is filled in the main vessel. Then, the return section of the cooling loop is disconnected. The disconnected pipe is the pipe marked with T4 as shown in Figure 5-2. Subsequently, the liquid is pumped from the bottom of the main vessel and flows into a measuring vessel from the heating pipe which is disconnected from the cooling loop. With the needle valve being fully open, by measuring the volume of liquid in the measuring vessel and the pump operation time, the

maximum flow rate can be calculated. It needs to be noticed that the estimated flow rate might be slightly different from the actual flow rate since the system is varied. One section of cooling loop is disconnected so that the friction loss of the measuring system might be smaller than the actual system. However, the difference is negligible since the effect of the friction loss difference between the two setups is quite small. The minimum flow rate refers to the minimum flow rate the needle valve can achieve in the system. If the needle valve is set to a lower flow rate, the circulation would be stopped even with the pump is powered on. The minimum flow rates in various liquids could be measured by the same methods with the needle valve slightly open.

The maximum and minimum flow rates of the system with various types of insulating oils are listed in the Table 5-2.

Table 5-2 Minimum and maximum flow rates of the investigated oils in the system

Liquid type	Minimum flow rate	Maximum flow rate
Gemini X	2.3 mL/sec	60 mL/sec
Diala S4 ZX-I	3 mL/sec	67 mL/sec
MIDEL 7131	1.3 mL/sec	32 mL/sec

The flow rate of MIDEL 7131 is much lower than the other two oils. The volume of the oil in the oil circulation system is about 6 litres. According to the maximum flow rates of the pump in three types of oils, the shortest time durations of a circulation cycle related to the volume of Gemini X, Diala S4 ZX-I and MIDEL 7131 are 1.6 minutes, 1.5 minutes and 3.1 minutes, respectively. Therefore, 10 minutes oil circulation at maximum flow rate would circulate the oil more than 3 times. Considering the oil is also circulated by the TM8 online DGA monitor, 10 minutes oil circulation at maximum flow rate should be enough to mix the oil in the test system.

5.3.3 Gas Sampling Test

As previously discussed, the volume of gas phase and liquid phase in the system should be accurately controlled in order to calculate the gas in total amount. Therefore, the volume of each gas sample and oil sample should be controlled.

The experimental system is gas-tight sealed and operates under atmosphere pressure. A slight positive pressure would be helpful to sample. The positive pressure is created by injecting air into the expansion tank as shown in Figure 5-6. The pressure is injected by a gas pump through the Schrader valve on the expansion tank. The pressure value is monitored by the pressure gauge. According to the preliminary trial, gas and oil samples can be taken easily under 200 mbar positive pressure. This is the reason that there is initial gas injected in the expansion bladder before experiment.

The connection of syringe and gas bag during gas sampling process is shown in Figure 5-8.

Figure 5-8 Gas bag and syringe connection in gas sampling process

A multi-layer foil gas sampling bag is combined with a gas-tight syringe and the valve to the headspace by a three-way Luer valve. The Luer valve could connect any two of the three ports and isolate the other one. During sampling, 50 mL of the gas from the headspace is firstly filled into the syringe by isolating the gas sampling bag. Then the 50 mL gas in the syringe is injected into the sampling bag by isolating the headspace valve. By this process, 50 mL gas sample from the headspace of the main vessel is taken into the gas sampling bag [31].

The gas sample is analysed by laboratory based gas chromatography (GC). In the GC analysis ten millilitres of gas volume is adequate for DGA measurement. However, in free gas DGA measurements, the gas is directly injected into the GC columns by manually squeezing the gas sampling bag without purge gas. On the other words, extra

volume of gas is required to function as purge gas. Therefore, extra volume of free gas needs to be sampled. In this experiment, 150 mL free gas is sampled from headspace which is enough for DGA free gas measurements.

5.3.4 Oil Sampling Test

Glass type gas-tight syringe is commonly used in DGA oil sampling. When sampling with glass type syringe, air bubbles would migrate into the syringe if the plug is strongly pulled. The air migration would cause inaccurate and ineffective DGA results. Therefore, same as gas sampling, oil could be readily sampled with positive inner pressure as the oil would be naturally flow into the syringe. According to preliminary trials, 200 mbar positive pressure in the system is adequate to take both gas and oil samples. Hence, the oil could be sampled after gas sampling. The positive pressure environment is created by the method introduced in previous section. The oil sampling connection is shown in Figure 5-9.

Figure 5-9 Oil sampling connection in oil sampling process

The syringe is connected to the oil sampling valve which is a bypass on the oil sampling loop of the online DGA monitor. The syringe is connected to the sampling valve through a three-way Luer valve. The other connector of the Luer valve leads to a waste oil container. Thus, the oil is sampled from the bottom of the main vessel.

The sampling process follows the IEC standard 60567 [30]. Firstly, the syringe is connected to the sampling valve and filled with 20 to 30 mL of oil. Then, the sampling valve is switched off and the oil in the syringe is disposed into the waste oil container. In this process, the syringe is flushed and air bubbles could be purged out. In addition, the dead oil would be disposed in this process which is trapped in the valve and not involved in the circulation loop. Subsequently, the syringe is connected to the sampling valve and 50 mL of oil is sampled. Then, the sampling operation is repeated for another syringe if necessary. Finally, the syringe is disconnected and the sampling valve is closed. It needs to be noticed that the total volume of oil taken from the system including the oil sampled in the syringe and the oil disposed before sampling. Since the oil volume in the system needs to be accurately monitored to calculate the fault gas amount.

5.3.5 Gas in Bladder Volume Measurement Test

The volumes of total gas phase and liquid phase in the sealed experimental system need to be ascertained accurately in order to calculate the total fault gas amount in the system from the gas-in-gas and gas-in-oil concentrations.

The oil volume in the system can be calculated from the initial oil amount and oil loss amount. The initial oil amount refers to the volume of oil filled into the system before experiments. The oil loss amount refers to the oil purged from the system including the oil sampled for laboratory measurements and the oil loss caused during heating pipe changing process. The volume of oil samples can be measured by the syringe. The oil loss volume during heating pipe changing process needs to be measured. This is introduced in the following section.

The gas volume measurement is more difficult than the oil volume measurement majorly because of the gas volume in the expansion bladder. The total gas in the system contains gas in headspace and gas in bladder. The gas volume in the headspace can be calculated from the volume difference between the total system volume and the oil volume. However, the volume of gas in bladder needs to be measured separately. It needs to be noticed that the gas volume measured should be under atmosphere pressure.

The method to measure the volume of gas in bladder is to purge all the gas out from the bladder and measure the volume. As introduced in the gas sampling method, the gas in the headspace can be sampled by pressurising the expansion tank. In fact, the gas in the bladder is pushed from the bladder into the headspace of the main vessel. Therefore, if all the gas in the bladder is squeezed into the headspace, the gas in bladder could be taken out by isolating the expansion vessel and relieving the headspace pressure. Then the volume of gas in the bladder could be measured.

The gas volume in the bladder needs to be measured in each experiment after the gas samples are taken after faults. During gas volume measurement, firstly, a new 50 mL gas-tight syringe is connected to the gas sampling valve through a three-way Luer valve. Subsequently, the online DGA monitor is isolated by switching off the valves in case the positive pressure in the test system would affect the extractor in the online DGA monitor. Then, the expansion tank is pressurised to squeeze the expansion bladder. In the preliminary trials, it is found that 200 mbar is enough to thoroughly squeeze the expansion bladder. Finally, purge gas out with the syringe. In this step, the syringe is connected to the headspace by switching on the gas sampling valve where the gas would flow into the syringe. Once the syringe is filled with 50 mL gas, the gas sampling valve is switched off. The gas in the syringe is purged out by adjusting the Luer valve. In this procedure, each stroke would purge 50 mL gas out from the system. If this procedure is repeated until the pressure in the system returns to atmosphere pressure (0 mbar on pressure gauge), the volume of the gas in bladder could be calculated from the number of full strokes without the final stroke and the gas volume of the final stroke. The calculation method is shown in equation (8).

$$V = 50mL \times N + V_0 \tag{8}$$

Where, V is the volume of gas in the bladder;

N is the number of full strokes without the final stoke;

V_0 is the gas volume of the final stroke in the syringe;

The syringe connection to the headspace of main vessel during gas volume measurement is shown in Figure 5-10.

Figure 5-10 Syringe connection during gas volume measurement process

In this method, the expansion tank is initially pressurised with 200 mbar pressure which is same as the pressure in the headspace. In this situation, the expansion bladder is squeezed and a part of the gas is pushed into the headspace of the main vessel. With the first stroke of gas purge, the pressure in the system as well as in the expansion tank starts to decrease. More gas in the bladder is pushed into the headspace. The gas in the bladder would all be pushed into the headspace if the pressure in the expansion tank could finally be larger than the pressure in the headspace which is close to the atmosphere pressure. Otherwise, there would be still some gas remaining in the bladder. To guarantee all the gas in the bladder are pushed out, after the final stroke the expansion tank needs to be pressurised again. In this stage, the pressure in the expansion tank is larger than pressure in the main vessel so that all the gas in the bladder should be pushed into the headspace. On the other words, the expansion tank needs to be pressurised again after the final stroke to make sure the bladder is entirely squeezed.

The final stoke occurs where the pressure in the system is atmosphere pressure. The atmosphere pressure can be verified by either the pressure gauge measurement or the syringe plug. When the pressure in the system is 200 mbar, the syringe plug needs to be hold in case it jumps out. When the pressure in the system is close to the atmosphere pressure, the syringe plug would automatically stop. Therefore, it is quite important that the friction between the plug and syringe inner surface is so small that the plug could move freely under small pressure difference. In the gas volume measurements, a new and

cleaned syringe is necessary.

To verify the accuracy of this gas volume measuring method, a certain amount of gas is injected into the bladder whose volume is measured. In the tests, the gas in the expansion bladder is purged out by vacuuming the headspace of the test system with vacuum pump. Subsequently, the headspace of the system is resumed atmosphere pressure with the expansion bladder isolated. A 250-mL gas tight syringe is used to inject 250 mL, 500 mL and 1 litre gases into the system, respectively. Then the volume of the injected gas in the bladder is measured. The tests are repeated three times. The results are listed in the Table 5-3.

Table 5-3 Verification of bladder gas volume measurement method

Injected gas (mL)	Average measurement (mL)	Std of measurements	Relative discrepancy
250	217.3	6.43	-13%
500	450.0	7.21	-10%
1000	890.0	26.46	-11%

The standard deviations of the measurements show good repeatability. The relative discrepancies of the measurements of all three inject gas amounts are from -10% to -13%. The measurement error of 250 mL gas in bladder is slightly larger than those of 500 mL and 1000 mL gases. The discrepancies are all negative which means the volume measurement method would probably under estimate the volume of gas in the expansion bladder. Based on the results, the accuracy of the volume measurement method is about 10%. Considering the volume of the initial gas volume in expansion bladder is 700 mL and 300 mL of gas is sampled during experiments, typical value of gas volume to be measured in the expansion bladder is 400 mL or above. The gas volume measurement error is about 40 mL. This would cause a 2% measurement error on the total 2.1 litres gas volume in the system which includes 1.7 litres in the headspace of the main vessel and 0.4 litres in the expansion bladder. Therefore, the gas volume measurement method is acceptable in measuring the gas volume in the expansion bladder.

5.3.6 Degassing Efficiency Test

As introduced before, the oxygen in the system needs to be removed. There are two major reasons. The first one is to minimise oil oxidation. The second one is to mitigate fire or explosion hazard. The air in the headspace would be replaced with nitrogen as previously introduced. The oxygen in the oil needs to be removed as well. Normally, the dissolved air in the oil could be removed by two methods. The first one is vacuum degassing. And the second one is bubbling with noble gas, for example, argon, helium or nitrogen.

These two degassing methods are tested separately on this system. After the sealing performance is improved with silicone sealant, the tube heating DGA system could withstand negative pressure up to 0.7 bar (0.3 bar absolute pressure). This vacuum pressure is established with the vacuum pump.

In the vacuum degassing method test, 6 litres of MIDEL 7131 with certain amount of dissolved gases are filled in the system. The dissolved gases contents are measured with the TM8 online DGA monitor before degassing. Subsequently, the headspace pressure is maintained at 0.3 bar absolute pressure (-0.7 bar absolute pressure) with the vacuum pump operating continuously for 3 hour. Then the oil is circulated for 10 minutes in order to distribute the dissolved gases evenly. Finally, the dissolved gases contents are measured with the TM8 online DGA monitor after degassing until the measurements are stabilised.

In the bubbling degassing method test, the noble gas is provided from gas cylinder. The gas is injected from the oil sampling valve at the bottom of the main vessel. And the gas is escaped from the gas sampling valve at the top of the main vessel. In this way, the noble gas is bubbled through the bulk oil in the main vessel. The dissolved air and other gases will be replaced by the purging gas. The flow rate of the gas injection is set as 20 – 30 mL/sec by the regulator. The oil is bubbled for 1 hour. Same as the vacuum degassing method test, TM8 online DGA monitor is used to measure the dissolved gas contents before and after oil degassing.

The test results are shown in the Table 5-4. The degassing efficiency is the percentage of the gas removed based on the background gas level.

Table 5-4 Degassing efficiencies of vacuum and bubbling methods

Vacuum	CO2	CO	CH4	C2H6	C2H4
Background (ppm)	484.9	120.1	67.3	225.8	86.9
Efficiency	10%	48%	32%	10%	13%
Bubbling	**CO2**	**CO**	**CH4**	**C2H6**	**C2H4**
Background (ppm)	435.7	63	45.5	202.4	75.7
Efficiency	65%	67%	80%	58%	61%

The bubbling degassing method removes 60% to 80% of dissolved fault gases. It is much more than the vacuum degassing method which removes below 50% of dissolved fault gases. Considering the efficiency of the vacuum degas method is based on 3 hours duration while that of bubbling degassing method is based on 1 hour duration, the degas efficiency of bubbling degassing method is much higher than that of the vacuum degassing method. Therefore, in the experiments the bubbling degassing method is used to remove the dissolved gas in the oil before test.

It needs to be noticed that the much lower efficiency of vacuum degassing method is majorly due to the vacuum pressure. In conventional vacuum degassing, the vacuum pressure should be close to 0. For example, the oil is processed under pressure lower than 5 mbar in vacuum oven to remove the dissolved gases. In Toepler pump based vacuum extraction method, the pressure is as low as 0.01 mbar. In this test, the 0.3 bar pressure is too much higher than the conventional vacuum degassing method. Therefore, the comparison in Table 5-4 only indicates the degassing efficiency of the degassing methods which could be applied on the experimental system rather than the comparison between the vacuum degassing method and bubbling degassing method.

5.3.7 Heating Temperature Test

As previously discussed the maximum temperature difference between the inner and outside surfaces of heating pipe is only about 10 ℃. Therefore, the fault temperature is

measured by two thermocouples tightly clamped on the tube by Jubilee clips. The Jubilee clips are made by stainless steel which could withstand temperature above 800 ℃.

Initially, the system is tested by heating with water instead of oil for safety consideration. The water test is performed to make sure the system could be sealed properly, especially the heating pipe. A series of water tests with tube furnace set point up to 450 ℃ were carried out successfully without and leakage or overpressure which proves the system could work safely with or without circulation.

However, in the water tests, it was found that the heating pipe surface temperature is much lower than the tube furnace setting temperature. For example, when the water is not circulated, the heat pipe surface temperature is only stabilised at 140 ℃ with the furnace working at 450 ℃. In another test, the heating pipe surface temperature is monitored by a clamped thermocouple while another thermocouple is about 1 mm away from the heating pipe which is measuring the air temperature around the heating pipe in the furnace chamber. It was found that the air temperature is quite close to the furnace set temperature, but it is much higher than heating pipe surface temperature. Almost all the temperature gradient falls on the small air gap near the heating pipe outside surface. The phenomenon is known as the thermal boundary layer. In another words, the thermal fault level is determined on the heating pipe surface temperature rather than the furnace working temperature.

The relationship between the furnace set temperature and the heating pipe surface temperature is tested as shown in Figure 5-11. The heating pipe surface temperature is measured as the maximum approachable temperature of the heating pipe surface at a specific furnace working temperature. The system is tested with MIDEL 7131. In the first test, the circulation pump is not working. The oil in the heating pipe is virtually static. The relationship between the heating pipe surface temperature and the furnace set temperature is shown as the blue curve in the Figure 5-11. The second test is for comparison where the oil is circulated through the heating pipe with roughly 250mL/min flow rate. The flow rate is controlled by the needle valve. The results of the second test are shown as the red curve.

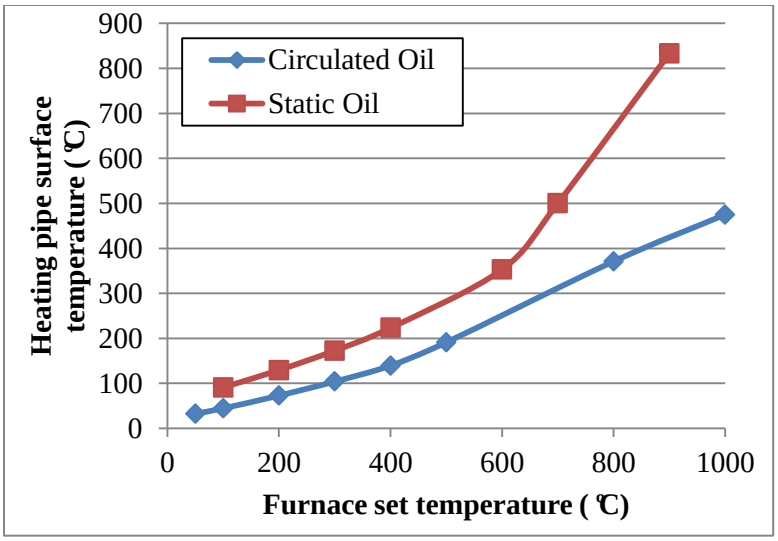

Figure 5-11 Relationship between heating pipe surface temperature and furnace set temperature

The heating pipe surface temperature increases linearly with the furnace set temperature up to about 350 ℃ where the furnace is set at 600 ℃. Then the heating pipe surface temperature rises sharply with furnace set temperature increasing. The reason of the turning point at about 350 ℃ might be due to the boiling phenomenon in the heating pipe. When the temperature of the heating pipe surface is above the boiling point of the oil, the oil close to the heating pipe inner surface is getting vaporized. With the furnace temperature keeps increasing, the vapor temperature could increase easily. Therefore, above the 350 ℃ point, the heating pipe surface temperature increases sharply. This phenomenon is somehow different from the pool boiling phenomenon with the immersed heating element. With the immersed heating element, the input power is constant. With vapor film generated, the heating element temperature would rapidly increase due to the largely decreased heat dissipation efficiency. In the tube heating process, the input power of the furnace is varied with the furnace chamber temperature. On the other words, the heating power is transferred with the temperature difference on the thermal boundary layer. Hence, in the tube heating method, the heating pipe surface temperature would not jump to an extremely high temperature as in the immersed heating method. With oil not circulated, the heating pipe surface temperature could reach 833 ℃ when the furnace set temperature is 900 ℃. However, when the oil is circulated, the heating pipe surface temperature could only reach about 450 ℃ with the furnace working at 1000 ℃. The reason might be that the oil circulation largely improves the heat dissipation in the system.

To simulate thermal fault covering all three thermal fault levels, the oil should not be circulated.

The furnace working temperature could be set according to the relationship in Figure 5-11. However, the relationship as shown in Figure 5-11 is only based on one test with MIDEL 7131 in the system. During experiments, the furnace working temperature should be slightly adjusted if the heating pipe surface temperature is far from the designated fault temperature. In addition, in high temperature thermal fault, i.e. above 650 ℃, the heating pipe surface temperature might exceed the temperature easily. The adjustment of furnace working temperature might be too slow to control the heating pipe surface temperature. Therefore, in high temperature thermal fault experiments, on-off control method is used. For example, in a 650 ℃ thermal fault experiment, the furnace is switched off when the heating pipe surface temperature reaches in between 660 ℃ and 670 ℃, and it needs to be switched on when the temperature of the heating pipe surface decreases in between 630 ℃ and 640 ℃. With this method, the heating pipe surface temperature could be maintained in ±20 ℃ of 650 ℃.

5.3.8 Heating Pipe Changing Trial

As introduced in the previous section, the established experimental system is capable of performing DGA thermal fault experiments stably up to 750 ℃. During experiments, only about 10 mL of oil in the heating pipe is heated and decomposed. After heating, the oil in the heating pipe is totally mixed with the bulk oil by pump circulation. Although the 10 mL heated oil is decomposed and might be different from the new oil, the more than 6 L bulk oil in the main vessel can still be considered as new oil since it is under room temperature during experiments. Therefore, only about 0.15% of total oil is decomposed under thermal fault. It is not necessary to change the bulk oil after each experiment subject to the negligible oil volume in heating tube and to the degas of the oil before each test.

Different from the oil, the heating pipe needs to be changed after each experiment. During heating, the heating pipe inner surface might be attached by carbonisation

products possibly due to the carbonisation of oil or metal. In severe cases, there might be solid carbon generated in the oil. If the heating pipe is not changed, the carbon attached on the heating pipe inner surface might get involved in the following oil decomposition in the next experiment. The carbonised heating pipe inner surface is shown in Figure 5-12. The heating pipe is cut into two pieces after a 750 ℃ preliminary DGA thermal fault experiment. The fault duration is 5 minutes.

Figure 5-12 Carbonised inner surface of heating pipe after a 750 ℃ thermal fault with MIDEL 7131

It can be seen that the whole heating area is covered by carbonisation products. In addition, there is some carbon solid in the pipe which is swept by tissue. Therefore, the heating pipe needs to be changed as the final step in each DGA thermal experiment.

The heating pipe is connected to the other tubing by the Swagelok tube fitting units. The tube fitting units provide good sealing performances and could withstand high pressure if they are correctly installed. The nut and ferrules should be installed on the new heating pipe. The nut needs to be turned one and a quarter turns to make sure the ferrules is stuck on the pipe. Then the replaced heating pipe is taken down and new heating pipe is installed with new nut and ferrules. Considering the good sealing behaviour of the Swagelok tube fitting units, a two-day sealing test is not necessary after the heating pipe is changed. However, for safety consideration, the sealing condition can be simply checked during nitrogen filling process. In nitrogen filling procedure, the headspace of the main vessel would be vacuumed to 0.3 bar absolute pressure in order to purge air out and re-fill nitrogen in. In this procedure, the first vacuum could be intensively remained for couple of minutes. If the pressure is not significantly changed, the new heating pipe is successfully installed.

It is worth noting that the oil loss during heating pipe changing procedure should be measured as it is related to the oil volume calculation and total gas amount calculation. Therefore, two small measuring beakers are put below the two connection nuts on the replaced heating pipe in order to collect any oil leaking when the replaced heating pipe is taken down. In addition, the headspace in the main vessel could be slightly vacuumed before changing the heating pipe. When the replaced heating pipe nut is loosen, air would be sucked into the system other than the oil flow out, which could largely minimise the oil loss during heating pipe changing. It also needs to be noticed is that the nuts and joint units need to be cleaned thoroughly after the new heating pipe is installed. Otherwise, any oil residue on the connection parts might generate smoke and even cause fire risks, as the joint units might under high temperature during experiment.

5.4 Experimental Procedures

According to the preliminary trials discussed in section 5.3, the tube heating DGA test system is improved from the initial design. In addition, operational procedures are established such as sealing performance test, oil degas, oil and gas sampling procedures and so on. In this section, the experimental procedures are introduced related to the tube heating test system step by step. The experimental procedures are established based on the design principle of the experimental system and the preliminary trials. The designed experimental procedures are listed in Table 5-5.

Table 5-5 Experimental procedures of the established tube heating DGA system

Step I	System assembly
Step II	Oil filling
Step III	Background DGA measurements
Step IV	Thermal fault generation
Step V	After fault DGA measurements
Step VI	Preparation for next experiment/system disassembly

Step I – System assembly

In this step, the system is firstly assembled according to Figure 5-1. After assembly, the sealing condition of the system needs to be tested. The detailed introduction of the sealing test process is in section 6.3. The system is required properly sealing within 48 hours.

Step II – Oil filling

In this step, 6.6 litres of tested oil are pumped into the system with the circulation pump of the TM8 online DGA monitor. The top gas sampling valve is open during oil filling in for air bleeding. After all the oil is filled in, the oil is degassed by nitrogen bubbling and the headspace air is replaced with nitrogen by vacuum the headspace and charge with nitrogen. The air in the expansion bladder is all purged out. Finally in this step, 700 mL nitrogen is manually injected into the bladder.

Step III – Background DGA measurements

In this step, the dissolved gas contents are measured as the background gas level. The TM8 online DGA monitor starts continuously measurements for couple of hours until the dissolved gas concentrations of the oil remain stable. The oil and gas in the system are sampled right after the last online DGA measurement for laboratory measurements.

Step IV – Thermal fault generation

In this step, the thermal fault is generated by furnace operating. Initially, the water bath circulates the water through the cooling loop. The heating pipe in the furnace chamber is heated to a designated thermal fault level. The thermal fault level is determined by the thermocouples measurements on the heating pipe. When the thermocouples measurements are in ±20 ℃ of the target temperature, the designated thermal fault level is assumed to be achieved where the timer starts. Once the thermal fault reaches the expected duration, the furnace is powered off. It is worth noting that the temperature around the furnace chamber and heating pipe during experiments might be several hundreds of degree Celsius. The safety needs to be considered during the whole

experiment including burning hazard and fire risk the mitigation methods are given in the risk assessment form given in Appendix V.

Step V – After fault DGA measurements

In this step, the oil in the system is circulated for 10 minutes by the system circulation pump in order to distribute the fault gas evenly in the system. Then the TM8 online DGA monitor starts analysing dissolved gas in the oil. For thermal faults where virtually no free gases generated, it takes five to six hours after fault DGA measurements. However, for thermal faults where free gases are significantly generated, it takes up to 24 hours of after fault DGA measurements when the dissolved gas concentrations get stabilised. After the final online DGA measurement, the oil and gas in the system are sampled for laboratory DGA measurement.

Step VI – Preparation for next experiment/system disassembly

If the oil does not need to be changed for the next experiment, the system only needs degas. Firstly, the heating pipe is changed. Then the oil is bubbled with nitrogen and the headspace is vacuumed and charged with nitrogen. If the oil needs to be change for the next experiment, then the oil should be purged out from the system with the circulation pump of TM8 online DGA monitor. Then the system needs to be disassembled and each oil circulation component needs to be flushed with the replaced oil at least two times.

5.5 Summary

The thermal fault temperature is limited by the immersed heating method in laboratory based DGA experiments. To investigate the fault gas generation characteristics under the whole thermal fault range, a tube heating method based DGA thermal fault experimental system is established.

The experimental system is consisted of oil circulation, oil heating system and gas expansion system. The bulk of oil is in the main vessel. The oil is circulated from the bottom of the main vessel through a section of heating pipe which is heated in a tube

furnace chamber. The two parts of the oil circulation tubing are covered with water cooling loop whose temperature is maintained by water bath. The headspace in the main vessel is connected to an expansion vessel in order to relieve the thermal expansion during heating and hold the generated free gases.

To understand how the established system operates, a series of trials are performed. The sealing condition of the system is investigated in the sealing test. Flow rate test indicates the required oil circulation duration. Gas and oil sampling methods are established in the gas and oil sampling tests. The volume of gas in the expansion bladder could be measured in order to calculate the whole gas phase volume. Two types of degas methods are tested in which the bubbling method is much more efficient than the vacuum degas method. Heating temperature test indicates that the furnace working temperature might be much higher than the heating pipe surface temperature. After each experiment, the heating pipe can be changed. The experimental procedures of the established tube heating DGA experimental system are designed based on the preliminary trials.

Chapter 6 DGA Experimental Results with Tube Heating Fault Simulation Method

6.1 Introduction

In this chapter, the DGA thermal fault experimental results from the tube heating test system will be presented. The experiments are all performed based on the experimental procedures introduced in the previous chapter.

Initially, the experimental phenomenon is introduced including the temperature distribution around the heating pipe and the pipe photos after experiments. As previously introduced, when the heating pipe surface temperature is below 650 ℃, the fault temperature is stabilised with the furnace temperature working at a set point. When the heating pipe surface temperature is 650 ℃ or above, on-off control is required to maintain the fault temperature fluctuating within the designated temperature range. The effect of on-off control could be observed in the temperature distribution profile. The heating pipe surface temperature is within ±20 ℃ of the designated fault temperature. During experiments, the heating pipe is changed after each fault temperature. Each pipe is cut into two pieces after changing in order to observe the inner surface. After some experiments, the inner surface is obviously carbonised.

The experimental system is consisted of oil phase and headspace gas phase. The oil phase includes the oil in the online DGA monitor and the oil in the test system. The oil is adequately mixed with the circulation of the system pump and online DGA monitor. To calculate the fault gas amount in the system, both the fault gas concentrations in the headspace gas phase and in the oil phase are required. In addition, the volumes of these two phases need to be accurately monitored. During the experiments, the dissolved gas concentration in the oil is measured by the online DGA monitors hourly. The oil is also sampled for conventional laboratory measurements. In the laboratory DGA measurements, two extraction methods are utilised which are vacuum extraction method and headspace extraction method. The gas from the headspace of the main vessel is

sampled as well. The fault gas concentration in the gas phase is measured by analyse the gas samples directly in the laboratory.

Through the fault gas concentration measurements of the gas and the oil, the total fault gas in the system could be calculated according to the known volumes of the two phases. In the gas in total calculation, Ostwald coefficients of the investigated liquid type need to be considered. The thermal fault gas generation patterns under various fault temperatures could be plotted according to the calculated total gas concentration. The thermal fault gas generation patterns of the three tested oils give more detailed diagnostic information of thermal faults than the conventional DGA data interpretation methods.

6.2 Measurement Procedures

The experimental profiles of the DGA tube heating experiments of three tested liquids in the established tube heating DGA test system are shown in the Table 6-1.

Table 6-1 Experimental profiles of the DGA tube heating experiments of three tested liquids

Fault level (℃)	**250**	**350**	**450**	**550**	**650**	**750**
Duration	24 h	12 h	5 h	1 h	5 min	1 min
Oil type	**Free gas generation (mL)**					
Gemini X	0	0	0	0	90	700
MIDEL 7131	0	0	0	0	100	900
Diala S4 ZX-I	0	0	0	0	80	670

The temperature of the simulated thermal fault ranges from 250 ℃ to 750 ℃ with 100 ℃ interval. The fault duration gradually decreases with the fault temperature increasing from 24 hours under thermal fault at 250 ℃ to 1 minute under thermal fault at 750 ℃. The aim is to generate proper amount of dissolved gas concentrations which are within the detection ranges of both the TM8 online DGA monitor and the laboratory measurement.

In this thesis, the dissolved gases are measured by laboratory and online DGA monitor. The laboratory measurement refers to the DGA result which is carried out by external analytic laboratory where either headspace extraction or vacuum extraction methods are applied. The online DGA measurement refers to the DGA result analysed by the online

DGA monitor which is the TM8 measurement in this chapter. The major difference between two DGA measurement methods is that the laboratory measurement requires manual oil sample and transportation while the online DGA measurement analyse the oil by circulation through the experimental system and could obtain the results within 1 hour.

The DGA measurement accuracies of the methods used in this chapter are listed in Table 6-2. The low concentration level refers to the dissolved gas concentrations are below 10 ppm and the medium concentration level refers to gas concentrations above 10 ppm. The Lab with Headspace and Lab with Vacuum refer to the laboratory DGA measurement with headspace and vacuum extraction methods, respectively. The Online with TM8 refers to the measurement carried out with TM8 online DGA monitor. LDL is the low detection limits of the TM8 which are provided in Table 4-1.

Table 6-2 Accuracies of the DGA measurement methods used in this chapter [5]

Method	**Accuracy (%)**	
	Low concentration	**Medium concentration**
Lab with Headspace	37	18
Lab with Vacuum	30	13
Online with TM8	5 or LDL	5

The original DGA measurements from TM8 online DGA monitor during a 550℃ experiment in MIDEL 7131 are shown as an example in Figure 6-1.

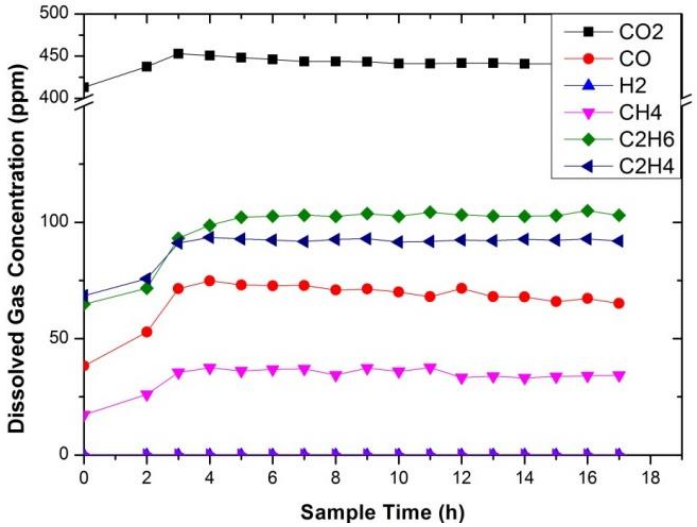

Figure 6-1 Original DGA measurements from TM8 in a 550℃ thermal fault experiment

The measurements of the initial sample hour show the background gas level in the oil. The oil and gas are sampled from the system and headspace, respectively. After experiment, the oil is analysed by the TM8 hourly. It can be seen that the gas level increases in the initial three hours and then stabilised where the system probably reaches equilibrium. Once the gas level measured by the online DGA monitor reaches equilibrium state after three to four hours of thermal fault, the oil and gas samples are taken to measure the gas contents after fault.

The original DGA measurements from TM8 online DGA monitor during a 650 ℃ experiment in MIDEL 7131 are shown as an example in Figure 6-2.

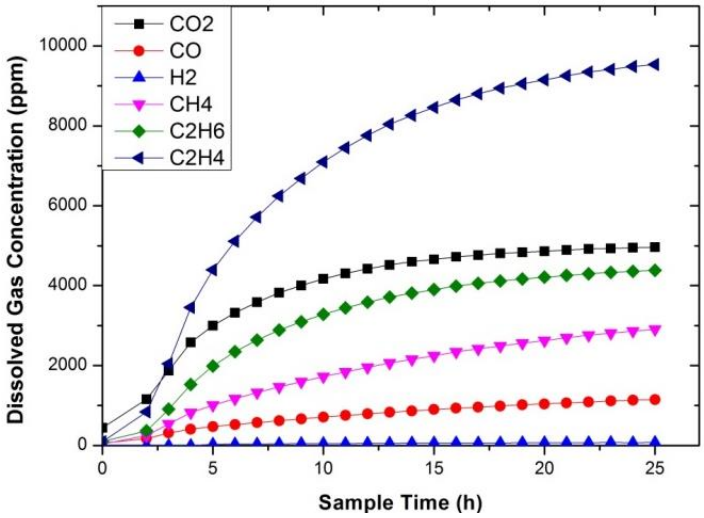

Figure 6-2 Original DGA measurements from TM8 in a 650 ℃ thermal fault experiment

The initial hour shows the background gas level. Different from the measurements after 550 ℃ thermal fault experiment, the gas concentrations after experiment start increasing rapidly and then slowly increasing. It takes almost 24 hours of the gas concentrations to become stabilised after experiment, which is quite different from the stabilising duration of the gas concentrations after the 550 ℃. The reason might be that a part of fault gases are generated as free gas in the 650 ℃ and focused in the headspace which would take longer time to dissolved back into the oil. Therefore, with free gas generated, the system would take much longer time to reach stable dissolved gas concentration.

In the DGA thermal fault with immersed heating element, significantly amount of free gas is also generated in the film boiling region. When the immersed heating element is in

film boiling, the localised hotspot temperature might be above 1000 ℃ where observable free gas bubbles are formed. After experiments, the free gas volume is measured. It was found that the free gas generation rate is about 1 to 3 mL/sec or even larger depending on the film boiling hotspot area. Due to the experimental system design, the free gas is limited on the top of the test cell where the oil is circulated through. In the immersed heating experiments, the gas concentration in the oil reaches stable after 3 to 5 hours even with free gas generated. However, with the free gas generation in the tube heating experiments, it takes much longer duration for the dissolved gas concentration to reach stable. The reason might be the different oil flow arrangement. In the immersed heating test system, the oil flow through the free gas which largely accelerates the free gas being dissolved back into the oil. In the tube heating test system, the free gas is mixed with the gas in the headspace which takes much longer time to be dissolved back into the oil.

As the system is properly sealed, the concentrations of the gas phase and oil phase could give the total fault gas amount with known volumes. However, the total fault gas amount could have errors if the oil and gas are not adequately mixed. Therefore, the gas and oil should be sampled after the system reaches stable state, i.e. the fault gas transfer between the two phases are minimised. This could be determined by the dissolved gas concentration in the oil becomes stabilised. For experiments below 650 ℃, the oil and gas could be sampled 4 to 5 hours after thermal fault injection. However, for 650 ℃ experiments or above, the oil and gas should be sampled 24 hours after thermal fault injection due to the largely generated free gas.

6.3 Experimental Observations

6.3.1 Temperature Profile

The temperature distribution profile of the heating pipe during a 550 ℃ thermal fault experiment with MIDEL 7131 synthetic ester oil in the system is shown as an example in Figure 6-3. The four thermocouples (Tc1, Tc2, Tc3 and Tc4) are used to monitor the temperature continuously.

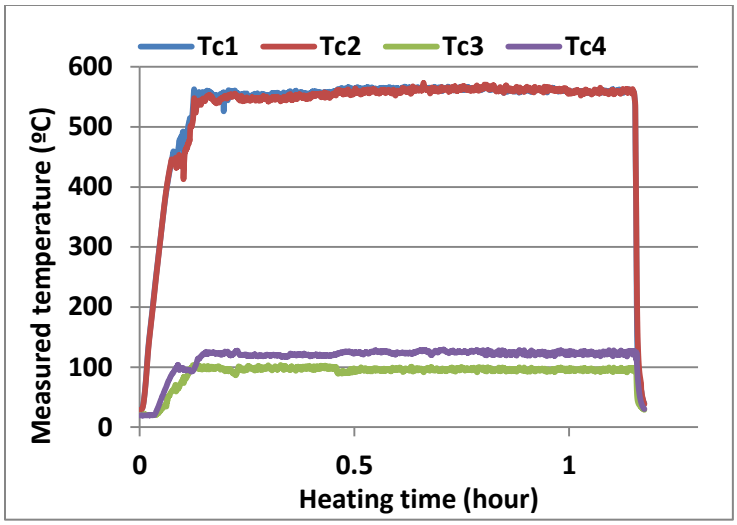

Figure 6-3 Temperature distribution of the heating pipe in a 550 ℃ experiment

The locations of four thermocouples are shown in Figure 5-2 in which the thermocouples Tc1 and Tc2 are on the two boundaries of the heating zone as shown in Figure 5-4. The thermocouple Tc1 and thermocouple Tc2 give almost similar temperature measurements which take less than 10 minutes to reach 550 ℃ from initial room temperature. Then the temperatures are almost constant with the furnace working at set temperature. After the designated fault duration, the furnace is power off and the oil is circulated by the system pump. It can be found that the temperatures on the heating pipe decreases sharply. According to Figure 5-4, the heating pipe length is 30 cm of which a section of 15 cm is in the furnace chamber and the other two sections of 7.5 cm each are outside the heating chamber but still in the furnace thermal blockage unit. The temperature measurements from thermocouples Tc3 and Tc4 are used to understand the temperature gradient of the sections in the furnace thermal blockage unit. The temperatures of Tc3 and Tc4 are about 97 ℃ and 125 ℃, respectively. Therefore, there is more than 400 ℃ temperature gradient on the heating pipe sections which are outside the furnace chamber. There is about 30 ℃ difference between the temperatures measured by thermocouples Tc3 and Tc4 which is probably due to the thermocouple of Tc3 is not in good contact with the pipe surface as the system should be symmetric.

During experiments there would be a portion of fault gases generated under lower fault temperature than the heating pipe. For example, in the 550 ℃ thermal fault experiment, there is a portion of oil in the pipe sections in the furnace thermal blockage unit whose

temperature ranges from 125 ℃ to 550 ℃. On the other words, this portion of oil is under thermal fault with temperature lower than 550 ℃ which might generate fault gases with different gas patterns. In this work, these gases are neglected. The first reason is that the temperature gradient on the heating pipe sections outside the furnace chamber is inevitable. This temperature gradient might also occur in real thermal fault in transformer which is being simulated in this work. The second reason is that the fault gas generation rate increases exponentially with fault temperature. The amount of fault gases generated in the oil outside the furnace chamber is much less than that in the furnace chamber. Due to the similar reason, the gas generation in the temperature increasing stage is also negligible.

The temperature distribution profile of the heating pipe during a 650 ℃ thermal fault experiment with MIDEL 7131 synthetic ester oil in the system is shown as another example in Figure 6-4.

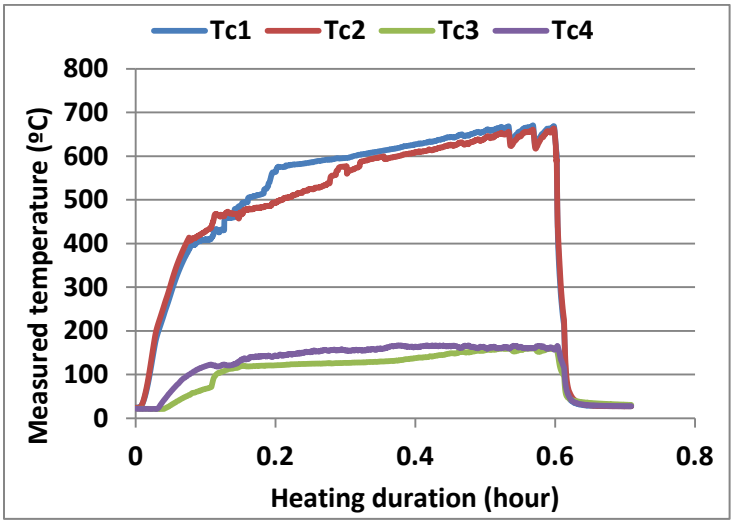

Figure 6-4 Temperature distribution of the heating pipe in a 650 ℃ experiment

The heating pipe temperature increases rapidly initially and then slowly increase. In the slow increasing stage, there is a temperature difference up to about 100 ℃ between the measurements of thermocouple Tc1 and Tc2. This is probably because during heating in this test the oil in the heating pipe has localised convection which causes the temperature unsymmetrical distribution on the heating pipe. With the temperature increasing the difference becomes smaller. It takes more than 20 minutes for the heating pipe temperature to reach 600 ℃. When the heating pipe surface temperature measured by the

two thermocouples approaches 670℃, the furnace is power off until the temperature approaches 630℃ where the furnace is switched on. This is the on-off control which aims to maintain the heating pipe surface temperature in ±20℃ of the designated fault temperature in high temperature thermal fault experiments. The reason is that the heating pipe surface temperature is difficult to maintain with the furnace working at a high temperature levels which is discussed in detail in the previous chapter. The heating pipe temperature decreases sharply after experiment with the forced circulation of oil which is similar to the 550℃ experiment. The temperatures measured by the thermocouples Tc3 and Tc4 are about 160℃ during heating which is higher than in the 550℃ experiment. Although the temperature gradient on the heating pipe section outside the furnace chamber is larger than in the 550℃ experiment, the gas generated in this part is negligible due to the same reason as previously discussed. The gas generation in the temperature increasing stage is also neglected.

6.3.2 Heating Pipe after Experiment

After each thermal fault experiment, the heating pipe is changed with a brand new section of tubing. Each of the tested heating pipes is cut from the central in order to observe the heating pipe inner surface. The inside and outside surfaces of replaced heating pipes after 250℃, 550℃ and 750℃ experiments with MIDEL 7131 synthetic ester liquid are shown in Figure 6-5 as examples.

After the 24 hours of 250℃ thermal fault experiment, both the heating pipe inside and outside surfaces are not carbonised which are all similar to the condition of new tubing as shown in the Figure 6-5 (a). From 350℃ thermal fault experiment, the outside surface of the heating pipe starts to be carbonised with brownish and black mark which is getting stronger with the increasing of thermal fault temperature. However, the inside surface of the heating pipe is not carbonised. The phenomenon is shown as in the Figure 6-5 (b). With the thermal fault temperature reaches 750℃, both the inside and outside surfaces of the heating pipe are heavily carbonised as shown in Figure 6-5 (c).

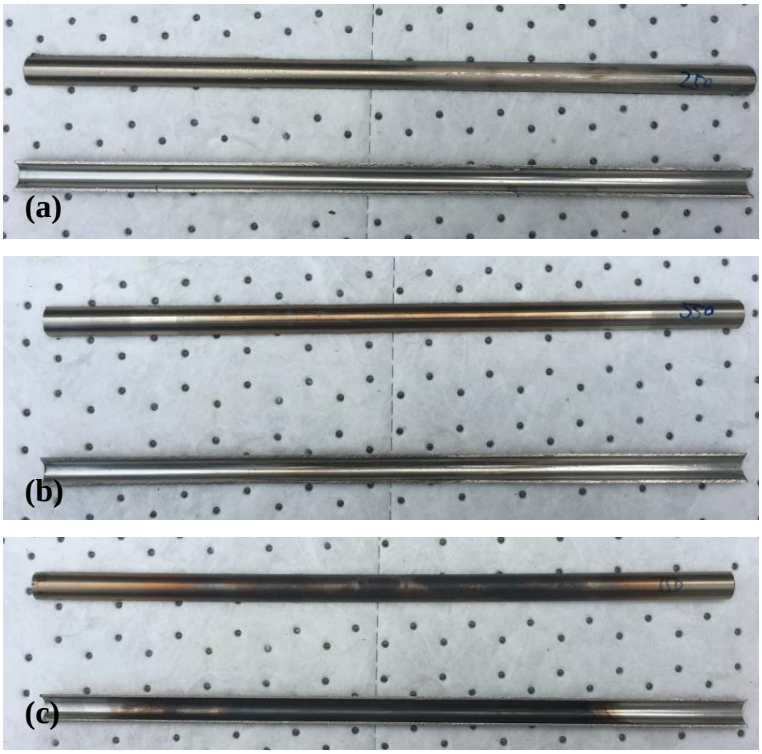

Figure 6-5 Heating pipe inside and outside surface after various temperatures of thermal fault experiments: (a) pipe surfaces after 250 ℃ experiment; (b) pipe surfaces after 550 ℃ experiment; (c) pipe surfaces after 750 ℃ experiment.

According to the carbonisation phenomenon of the heating pipe surfaces, the heating pipe material is easily to get carbonised in air above 350 ℃. The carbonisation might be from the oxidation products of some elements alloyed in the heating pipe material. However, as the inside surface is covered by oil in which the oxygen level is much lower than in air, the heating pipe inside surface is hardly oxidized. On the other words, the heating pipe inside surface with oil is virtually not carbonised due to heating. Therefore, the carbonisation products attached on the heating inside surfaces are mostly generated from the oil under the thermal fault, which means these carbonisation products are generated from the oil under 750 ℃ thermal faults. In addition, below 750 ℃ no visible carbon is generated. The same phenomenon is found in the experiments with the other two types of oils where only at 750 ℃ the heating pipe inside surface is attached with carbonisation products.

6.4 Gas-in-Total (GIT) Calculation

The fault gas contents in the system are composed of the dissolved gas in the oil and the free gas in the headspace gas phase. The dissolved gas contents are measured by the gas in oil concentrations. The free gas contents in the gas phase are measured by the gas in gas concentrations. The total amount of fault gas in the system could be calculated. However, in DGA study the relative gas amount is widely accepted, i.e. the gas concentration in ppm value. Hence, the total fault gas is described by the gas concentration value in ppm which is related to the total oil volume. The gas in total can be calculated as the equation (9).

$$C_{git} = \frac{C_{gio} \times V_o + C_{gig} \times V_g}{V_o} \tag{9}$$

Where, C_{gio} is the gas in oil concentration of the fault gas dissolved in the oil phase;
C_{gig} is the gas in gas concentration of the fault gas focused in the gas phase;
V_o is the volume of total oil phase;
V_g is the volume of the total gas phase;
C_{git} is the gas in total concentration of the fault gas related to the total oil volume.

It needs to be noticed that the calculated gas in total concentration is the value which is assumed all the fault gas in the system is dissolved in the oil. It has no physical meaning and different from the gas in oil concentration which describes the dissolved gas concentration, although both of them are concentration value in ppm related to the oil volume. Considering there might be considerable amount of fault gas in the headspace gas phase, the calculated gas in total concentration might be significantly larger than the theoretical maximum gas concentration under saturation level.

In the experiments, the fault gas amounts dissolved in the oil are measured by three methods: TM8 online DGA monitor measurement, laboratory measurement with vacuum extraction and laboratory measurement with headspace extraction. The TM8 online DGA monitor extracts the dissolved gases from the oil by semi-permeable membrane which is similar to headspace extraction method. It is calibrated by gas in oil standard during manufacturing. The TM8 online DGA monitor is equipped with calibration gas to

calibrate the GC system. In DGA measurement, the TM8 online DGA monitor measures the gas in gas concentration and reports the gas in oil results by calculating with the embedded mineral oil Ostwald coefficients. The laboratory DGA facilities are calibrated with gas in oil standard of mineral oil. On the other words, mineral oil is the default oil type for all these three DGA measurement methods. When alternative insulating liquids are analysed, the DGA results need to be corrected based on the Ostwald coefficients of the tested liquid and the mineral oil.

The gas in oil concentration results from the TM8 online DGA monitor are calculated from the gas in gas concentrations which are directly measured by the GC system. Therefore, when the alternative insulating liquids are analysed by the TM8, the gas in oil concentrations of the fault gases need to be calculated according to the equation (10). The Ostwald coefficients of the mineral oil which are embedded in the TM8 algorithm are same as the Ostwald coefficients from IEEE standard listed in Table 3-1.

The Ostwald coefficients under room temperature of the Diala S4 ZX-I and 25 ℃ of the MIDEL 7131 used in the calculation are listed in Table 3-6 and Table 3-3, respectively. As the TM8 is operating under room temperature, the Ostwald coefficients of the alternative liquids under room temperature are used in the calculation.

$$C_{gio}^{a} = \frac{C_{gio}^{min} \times K_{a}^{RT}}{K_{min}^{RT}} \tag{10}$$

Where, C_{gio}^{a} is the real concentration of the fault gas dissolved in the oil;

C_{gio}^{min} is the concentration calculated with the mineral oil Ostwald coefficient;

K_{a}^{RT} is the Ostwald coefficient of the alternative liquid under room temperature;

K_{min}^{RT} is the mineral oil Ostwald coefficient embedded in the TM8.

There might be difference between the equilibrium temperature of the TM8 extractor and the temperature of the Ostwald coefficients. For example, the Diala S4 ZX-I Ostwald coefficients are measured under 28 ℃ but the MIDEL 7131 Ostwald coefficients are under 25 ℃. The TM8 extraction equilibrium temperature might vary between 25 ℃ and 28 ℃ depending on the environmental condition. In this work, the change of the Ostwald coefficients caused by the temperature difference is neglected as the temperature

variation range is small.

In the laboratory DGA measurement with headspace extraction method, the DGA facility is calibrated with mineral oil gas in oil standard. There are no Ostwald coefficients embedded in the system. The gas in oil concentration is obtained directly from the GC area and calibration curves. Therefore, the information of the Ostwald coefficients and the phase ratio of in the headspace vial are both contained in the measurement results. In addition, the headspace extraction in the laboratory is under 70 ℃ instead of room temperature. The calculation method for alternative liquids is shown in the equation (11). The Ostwald coefficients of mineral oil are from IEC standards under 70 ℃ which are given in Table 3-1. The Ostwald coefficients of Diala S4 ZX-I and MIDEL 7131 under 70 ℃ are given in Table 3-4 and Table 3-3, respectively.

$$C_{gio}^{a} = \frac{C_{gio}^{min} \times (K_{a}^{70} + \beta)}{K_{min}^{70} + \beta} \tag{11}$$

Where, C_{gio}^{a} is the real concentration of the fault gas dissolved in the oil;

C_{gio}^{min} is the concentration calculated with the mineral oil Ostwald coefficient;

K_{a}^{70} is the Ostwald coefficient of the alternative liquid under room temperature;

K_{min}^{70} is the mineral oil Ostwald coefficient embedded in the TM8;

β is the phase ratio of the headspace vial in the laboratory DGA measurement.

In the laboratory DGA measurement with vacuum extraction method, the DGA measurement system is calibrated with mineral oil gas in oil standard as well. In the method, the Toepler pump is used to extract the dissolved gas. In the extraction process, only one cycle is performed. The extraction is partial degas extraction. The degas efficiency might be as low as 60% [30]. Therefore, the Ostwald coefficients need to be considered in correcting the results of alternative insulating liquids measured in this laboratory DGA system. The correcting method is similar to that of the laboratory DGA system with headspace extraction method except for the phase ratio and temperature of Ostwald coefficients. In this method, the Ostwald coefficients are under room temperature which is same as those in the correction equation (12) of TM8 measurement. The phase ratio is the phase ratio in the whole Toepler pump during extraction.

$$C_{gio}^{a} = \frac{C_{gio}^{min} \times (K_a^{RT} + \beta)}{K_{min}^{RT} + \beta} \tag{12}$$

Where, C_{gio}^{a} is the real concentration of the fault gas dissolved in the oil;

C_{gio}^{min} is the concentration calculated with the mineral oil Ostwald coefficient;

K_a^{RT} is the Ostwald coefficient of the alternative liquid under room temperature;

K_{min}^{RT} is the mineral oil Ostwald coefficient under room temperature;

β is the phase ratio in the Toepler pump in the laboratory DGA measurement.

The correct of DGA measurement results with Ostwald coefficients for alternative insulating liquids are necessary. However, there are several factors in the correction method which might cause errors. The major factor is the inaccurate Ostwald coefficient values. As previously discussed, there are discrepancies in Ostwald coefficients of mineral oil from different publications. The TM8 online DGA monitor is embedded with mineral oil Ostwald coefficients from IEEE standard. The synthetic ester oil Ostwald coefficients are from the IEC standard. The measurement methods of these Ostwald coefficients are not given. However, the Ostwald coefficients of the gas to liquid insulating oil are laboratory measured with the phase ratio variation method. The different Ostwald coefficient measurement methods might give significantly different results. In addition, although the experimental system is under room temperature, the actual temperature in the TM8 extractor might be slightly different from 25 ℃ or 28 ℃ under which the Ostwald coefficients of the mineral oil and gas to liquid insulating oil are measured. The Ostwald coefficients of mineral oil from the publications might also be measured with other types of mineral oil rather than Gemini X which is used in this work. In summary, although being corrected, the gas in oil results of alternative transformer oils might be inaccurate. The accuracy primarily depends on the Ostwald coefficients used in the calculation.

6.5 DGA Measurements of Gemini X Mineral Oil

6.5.1 Original Measurement Results of Gemini X Mineral Oil

The DGA measurement results of Gemini X mineral oil before and after 250 ℃ are listed in the Table 6-3. The first part of the table is classified as "Before" which gives the background gas level. They are the dissolved gas concentrations before thermal fault generation. The second part of the table is "After" which gives the gas concentrations after thermal fault generation. There are four types of DGA measurements. The "TM8" gives the dissolved gas concentration measurement from the TM8 online DGA monitor. The "Vacuum" and "Headspace" give the dissolved gas concentration measurements of the oil samples from laboratory DGA facility with vacuum extraction method and headspace extraction method, respectively. The "Gas in gas" gives the DAG investigated gas concentrations of the gas sample from the headspace gas phase. The oil and gas samples related to the measurements are all taken right after the TM8 measurement cycle completion. And the samples of gas and oil are taken virtually simultaneously. Therefore, all the three types of measurements in the table can be regarded as coinstantaneous DGA measurements of the test system. The following tables of the DGA measurements give the same information.

Table 6-3 DGA measurements (ppm) before and after 250 ℃ thermal fault in Gemini X

Before	**CO2**	**CO**	**H2**	**CH4**	**C2H6**	**C2H4**	**C2H2**	**O2**	**N2**
TM8	13.1	0	0	0	0	5.2	0	175	74753.6
Vacuum	14	1	0	3	2	6	0	2341	47234
Headspace	19	1	0	4	2	5	0	3985	77662
Gas in gas	80	2	0	1	2	0	0	10270	982233
After	**CO2**	**CO**	**H2**	**CH4**	**C2H6**	**C2H4**	**C2H2**	**O2**	**N2**
TM8	27.8	0	0	0	0	0	0	306.2	73833.6
Vacuum	29	2	0	2	3	2	0	2049	49234
Headspace	19	1	0	1	2	4	0	1434	73087
Gas in gas	121	5	0	2	1	3	0	17771	976683

From the "Before" TM8 results in Table 6-3, the background fault gases are all 0 except for the CO2 and C2H4 which are 13.1 ppm and 5.2 ppm, respectively. The dissolved oxygen level is 175 ppm which means the oil is thoroughly degassed. Due to oil is degassed with nitrogen bubbling and the headspace gas is filled with nitrogen, the oil is nearly nitrogen saturated whose concentration is more than 70000 ppm. The oil is

sampled and measured by laboratory DGA facility. The laboratory measurements give similar amount of CO2 in both extraction methods. Trace amounts of other gases are found in laboratory measurements, such as CO, CH4 and C2H6, which probably indicates that the laboratory DGA measurement is more sensitive than the online DGA monitor for very low dissolved gas concentrations. The laboratory gives higher dissolved O2 concentrations which might be due to the air ingression during oil sampling and sample transportation. The gas concentrations in headspace gas phase are larger than the dissolved gas in oil. It needs to be noticed that they are not in equilibrium state according to the Ostwald coefficients of mineral oil listed in Table 3-2. More gases are in the gas phase than those which should be dissolved in the oil.

After fault, the dissolved CO2 concentration increased by 14.7 ppm measured by TM8. The concentration of C2H4 decreases from 5.4 ppm to 0 which means in the experiment the generation of C2H4 is negative. As the 5.4 ppm of background C2H4 concentration might be cause by the measurement fluctuation of TM8 at low gas levels. Therefore, the negative gas generation values are neglected. It needs to be noticed that the oxygen level measured by TM8 increases. The reason might be due to the air ingression into the test system during oil sampling, gas sampling and nitrogen re-charging. As the oxygen content in the system is at very low level, and small portion of air ingression might cause significant oxygen increasing.

The DGA measurement results before and after 350 ℃ thermal fault in Gemini X mineral oil are listed in the Table 6-4 which follows the same format.

Table 6-4 DGA measurements (ppm) before and after 350 ℃ thermal fault in Gemini X

Before	**CO2 (ppm)**	**CO (ppm)**	**H2 (ppm)**	**CH4 (ppm)**	**C2H6 (ppm)**	**C2H4 (ppm)**	**C2H2 (ppm)**	**O2 (ppm)**	**N2 (ppm)**
TM8	27.8	0	0	0	0	0	0	306.2	73833.6
Vacuum	29	2	0	2	3	2	0	2938	43924
Headspace	19	1	0	1	2	4	0	1434	73087
Gas in gas	121	5	0	2	1	3	0	17771	976683
After	**CO2 (ppm)**	**CO (ppm)**	**H2 (ppm)**	**CH4 (ppm)**	**C2H6 (ppm)**	**C2H4 (ppm)**	**C2H2 (ppm)**	**O2 (ppm)**	**N2 (ppm)**
TM8	65	7.4	0	7.1	5.8	0	0	921	74288.2
Vacuum	67	7	0	6	4	5	0	3018	44681
Headspace	62	6	0	5	6	5	0	2360	76407
Gas in gas	147	24	0	10	3	4	0	24177	963097

In this specific test, due to the TM8 online DGA monitor is breakdown, the after fault gas

levels from Table 6-3 are taken as the background gas levels. Also only in this specific test, the system is not degassed before experiment.

It can be seen that the CO2 is significantly generated. CO, CH4 and C2H6 are slightly increased, but the increments are all above the low detection range of the TM8. From gas in gas results, the CO2, CO and CH4 are generated by 26 ppm, 19 ppm and 8 ppm. The oxygen level after fault is larger than that before thermal fault probably due to the air ingression which is discussed in the previous context. It is also noticed that the gas between the oil and headspace phases are not in equilibrium state. More CO2 is in headspace gas phase than it should be dissolved in the oil. However, after fault more CO and CH4 are in the oil phase than it should be in the gas phase. This phenomenon verifies that the CO and CH4 are generated in the oil and small portion is transferred into the gas phase. Hence, more CO and CH4 are in oil than it should be in the gas phase.

The DGA measurements before and after 450 ℃ thermal fault experiments in Gemini X mineral oil are listed in the Table 6-5. The laboratory gas in oil measurements for background oil samples are missing.

Table 6-5 DGA measurements (ppm) before and after 450 ℃ thermal fault in Gemini X

Before	**CO2 (ppm)**	**CO (ppm)**	**H2 (ppm)**	**CH4 (ppm)**	**C2H6 (ppm)**	**C2H4 (ppm)**	**C2H2 (ppm)**	**O2 (ppm)**	**N2 (ppm)**
TM8	80.6	6.9	0	0	6.4	5.5	0	1314.2	73978.5
Vacuum	-	-	-	-	-	-	-	-	-
Headspace	-	-	-	-	-	-	-	-	-
Gas in gas	152	25	0	10	2	3	0	23999	961503
After	**CO2 (ppm)**	**CO (ppm)**	**H2 (ppm)**	**CH4 (ppm)**	**C2H6 (ppm)**	**C2H4 (ppm)**	**C2H2 (ppm)**	**O2 (ppm)**	**N2 (ppm)**
TM8	117.6	19.2	0	21.2	15.4	10.4	0	2171.9	72431.1
Vacuum	121	17	0	20	16	9	0	4664	84429
Headspace	229	16	0	19	16	9	0	4574	49455
Gas in gas	211	49	0	39	3	4	0	34871	935959

According to Table 6-5, C2H4 is generated along with the gases generated under 350 ℃ thermal fault. The two phases in the system are not in equilibrium as well. More fault gases are focused in the oil than they should be in the gas phase.

The DGA measurement results before and after 550 ℃ thermal fault experiment in Gemini X mineral oil are shown in Table 6-6.

Table 6-6 DGA measurements (ppm) before and after 550 ℃ thermal fault in Gemini X

Before	CO2 (ppm)	CO (ppm)	H2 (ppm)	CH4 (ppm)	C2H6 (ppm)	C2H4 (ppm)	C2H2 (ppm)	O2 (ppm)	N2 (ppm)
TM8	122	6	0	0	14.3	6.2	0	2085.9	71083
Vacuum	143	6	0	7	15	7	0	4237	85882
Headspace	268	8	0	6	13	6	0	2075	47723
Gas in gas	158	11	0	10	5	3	0	15709	967573
After	**CO2 (ppm)**	**CO (ppm)**	**H2 (ppm)**	**CH4 (ppm)**	**C2H6 (ppm)**	**C2H4 (ppm)**	**C2H2 (ppm)**	**O2 (ppm)**	**N2 (ppm)**
TM8	148.8	15.3	0	56.8	38.3	34.1	0	1890.8	65924.3
Vacuum	149	15	0	59	44	38	0	4839	86205
Headspace	249	10	0	55	38	34	0	4681	50021
Gas in gas	202	32	0	79	21	30	0	22259	953660

Comparing the background gas level of 550 ℃ experiment with the after fault gas level of 450 ℃ listed in Table 6-5, the background gas concentrations are significantly lower. In addition, the gas in gas concentration in Table 6-6 also decreases from the after fault level of 450 ℃. This phenomenon shows the effect of degas procedure during experiment. As introduced in the previous chapter, to control the background gas level of the oil, the system needs to be degassed before each thermal fault experiment. The degas procedure has significant effect on CO and CH4 as they are less soluble than the other gases such as C2H6 and C2H4.

In the 550 ℃ thermal fault experiment, the generated gas types are same to those generated in 450 ℃ experiment. Considering the experimental duration of the 450 ℃ is four times larger than that of 550 ℃ experiment, the gas generation rate of 550 ℃ thermal fault is much larger than that of 450 ℃. The O2 concentration after fault is lower than before by about 195 ppm which is less than 10%. Hence, the oxygen decreasing after fault is within the accuracy range of TM8 online DGA monitor rather than oxygen consumption.

The DGA measurements before and after 650 ℃ thermal fault experiment in Gemini X mineral oil are shown in Table 6-7.

Table 6-7 DGA measurements (ppm) before and after 650 ℃ thermal fault in Gemini X

Before	CO2 (ppm)	CO (ppm)	H2 (ppm)	CH4 (ppm)	C2H6 (ppm)	C2H4 (ppm)	C2H2 (ppm)	O2 (ppm)	N2 (ppm)
TM8	148.8	7.3	0	11.8	28.3	10.1	0	1890.8	65924.3
Vacuum	161	6	0	13	27	10	0	3953	70817
Headspace	262	5	0	11	24	8	0	3570	39433
Gas in gas	135	5	0	6	7	4	0	11031	971148
After	**CO2 (ppm)**	**CO (ppm)**	**H2 (ppm)**	**CH4 (ppm)**	**C2H6 (ppm)**	**C2H4 (ppm)**	**C2H2 (ppm)**	**O2 (ppm)**	**N2 (ppm)**
TM8	134.4	6.5	9.1	267.4	264.9	300.1	5.4	1251.1	71273.9
Vacuum	157	5	6	287	286	365	5	3437	86347
Headspace	221	4	5	222	239	286	7	2389	44808
Gas in gas	261	213	394	704	147	394	2	15655	967237

The background gas concentrations are lower than the after fault gas level in the previous 550 ℃ experiment due to the degas procedure. In the 650 ℃ experiment, hydrogen is found in both oil phase and gas phase after fault which means H2 starts generating in Gemini X mineral oil from 650 ℃. In addition, the other gases generated in the previous 550 ℃ experiment are all generated.

After the 650 ℃ thermal fault experiment, a significant amount of generated fault gases are focused in the gas phase. The CH4 and C2H6 seem to be in equilibrium state between the headspace gas phase and oil phase. For CO, H2 and C2H4, more gases are in the gas phase than those dissolved in the oil. As previously discussed, if the fault gas is generated in the oil, the system is not in equilibrium state and more gas is dissolved in the oil as in the gas phase. Therefore, in the 650 ℃, more fault gases are generated with free gas generation and focused in the headspace gas phase than those dissolved in the oil.

The DGA measurements before and after 650 ℃ thermal fault experiment in Gemini X mineral oil are shown in Table 6-8.

Table 6-8 DGA measurements (ppm) before and after 750 ℃ thermal fault in Gemini X

Before	CO2 (ppm)	CO (ppm)	H2 (ppm)	CH4 (ppm)	C2H6 (ppm)	C2H4 (ppm)	C2H2 (ppm)	O2 (ppm)	N2 (ppm)
TM8	138.6	5.7	5	215.4	248.2	272.6	0	1406.5	60697.8
Vacuum	131	3	6	161	186	236	0	3444	55777
Headspace	230	3	4	157	208	239	0	3650	38973
Gas in gas	144	4	555	83	53	80	0	16313	966075
After	**CO2 (ppm)**	**CO (ppm)**	**H2 (ppm)**	**CH4 (ppm)**	**C2H6 (ppm)**	**C2H4 (ppm)**	**C2H2 (ppm)**	**O2 (ppm)**	**N2 (ppm)**
TM8	125.9	5	310.6	4188.1	4843.6	7456	24.1	885.3	69739.3
Vacuum	139	2	378	4795	5211	8543	30	2159	85314
Headspace	201	1	369	3508	4303	6848	**0**	2406	43210
Gas in gas	188	90	11202	11489	2351	4987	14	16496	939662

In the 750 ℃ thermal fault experiment, large amount of free gas and dissolved fault gas are generated. It needs to be noticed that the "Headspace" measurement of C2H2 for oil samples after fault is highlighted because it might not be correct.

Apart from the fault gas types generated in the previous 650 ℃ thermal fault experiment, C2H2 is generated. The generation of carbon oxides are smaller compared with the hydrocarbon gases. Similar to the 650 ℃ experiment, more fault gases are in the gas phase than those dissolved in the oil after 750 ℃ thermal fault, especially CO and H2. In addition, in both the 650 ℃ and 750 ℃ experiments the dissolved CO2 and O2 concentrations significantly decrease. The reason might be that a portion of the dissolved CO2 and O2 are diffused into the headspace due to the free gas generation. On the other words, the depletion of dissolved CO2 indicates that the CO2 generation from the oil under high temperature thermal fault is negligible comparing with CO and other fault gases. Besides, the generation of CO and CO2 from mineral oil might also consume small amount of oxygen as there are virtually no oxygen atom in the oil molecules.

6.5.2 Comparison between Online DGA Monitor and Laboratory Measurements of Gemini X Mineral Oil

The dissolved gases in oil in the system are analysed by three methods. In laboratory DGA measurements, the dissolved gases are extracted by either vacuum extraction method or headspace method and then detected by the GC equipment. In the TM8 online DGA monitor, the oil is circulated continuously through the extractor where the dissolved gases are extracted through a semi-permeable membrane. The gases are also analysed by

the laboratory grade GC system. Therefore, the major difference among these three methods is from the oil sample and extraction method.

The laboratory measurements of dissolved gases are plotted against the TM8 online DGA measurements of the same oil. The CO, H2 and C2H2 measurements are not included in this comparison because the dissolved CO concentrations are at very low level and there are limited numbers of H2 and C2H2 measurements. The CO2 and O2 measurements are not included as well because the air ingression might distort the laboratory measurements of these two gases. On the other words, only the results of CH4, C2H6 and C2H4 are used in the comparison. The plot of CH4 measurements in Gemini X mineral oil is shown in Figure 6-6 as an example. The plots of C2H6 and C2H4 give similar conclusion.

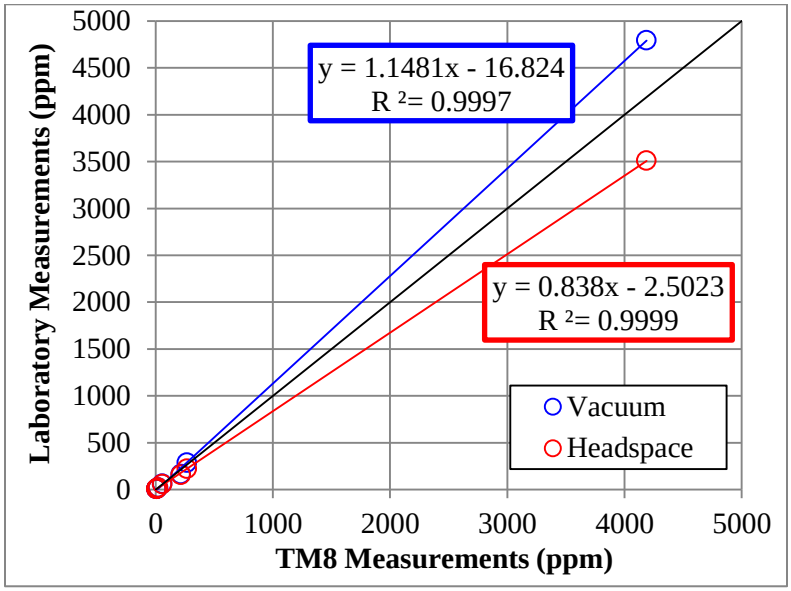

Figure 6-6 Laboratory measurements of methane (CH4) in Gemini X mineral oil against the TM8 online DGA measurements

In general, all three methods give close CH4 measurement results. Both the two laboratory measurement methods give linear relationship of dissolved CH4 concentration against the TM8 measurements, which means these three measurement methods in general are in linear relationship. The slope values from the linear regression of the two laboratory methods are slightly different. The slope of the laboratory vacuum extraction method is slightly larger than unit while that of headspace extraction method is smaller than unit.

In summary, the laboratory DGA measurement with vacuum extraction method is more sensitive than the TM8 online DGA monitor which is more sensitive than the laboratory DGA measurement with headspace extraction method. The intercept values of these two linear regression curves o the laboratory methods are all negative values, which means the laboratory methods might have lower detection limit than the TM8. On the other words, the laboratory DGA methods are more sensitive to oil samples with very low dissolved gas concentrations.

6.6 DGA Measurements of Diala S4 ZX-I GTL Oil

6.6.1 Original Measurement Results of Diala S4 ZX-I GTL Oil

The DGA measurements of Diala S4 ZX-I before and after the 250℃ and 350℃ experiments are listed in the Table 6-9 and Table 6-10, respectively.

Table 6-9 DGA measurements (ppm) before and after 250℃ thermal fault in Diala S4 ZX-I

Before	**CO2 (ppm)**	**CO (ppm)**	**H2 (ppm)**	**CH4 (ppm)**	**C2H6 (ppm)**	**C2H4 (ppm)**	**C2H2 (ppm)**	**O2 (ppm)**	**N2 (ppm)**
TM8	190.4	0.0	0.0	0.0	0.0	0.0	0.0	5003.7	281571.2
Vacuum	55	1	0	1	1	0	0	3806	59785
Headspace	6	1	0	0	1	1	0	13386	71464
Gas in gas	173	3	0	0	1	0	0	19472	973009
After	**CO2 (ppm)**	**CO (ppm)**	**H2 (ppm)**	**CH4 (ppm)**	**C2H6 (ppm)**	**C2H4 (ppm)**	**C2H2 (ppm)**	**O2 (ppm)**	**N2 (ppm)**
TM8	220.0	0.0	0.0	13.2	0.0	0.0	0.0	4018.8	283350.8
Vacuum	90	2	0	6	2	1	0	2927	61733
Headspace	9	2	0	5	2	2	0	12290	69292
Gas in gas	227	7	0	2	1	1	0	26679	964476

Table 6-10 DGA measurements (ppm) before and after 350 ℃ thermal fault in Diala S4 ZX-I

Before	CO2 (ppm)	CO (ppm)	H2 (ppm)	CH4 (ppm)	C2H6 (ppm)	C2H4 (ppm)	C2H2 (ppm)	O2 (ppm)	N2 (ppm)
TM8	210.2	0.0	0.0	0.0	0.0	0.0	0.0	4774.5	287652.6
Vacuum	78	2	0	1	1	1	0	3792	61334
Headspace	23	2	0	0	2	2	0	12955	64504
Gas in gas	222	19	0	11	8	0	0	28333	966757
After	**CO2 (ppm)**	**CO (ppm)**	**H2 (ppm)**	**CH4 (ppm)**	**C2H6 (ppm)**	**C2H4 (ppm)**	**C2H2 (ppm)**	**O2 (ppm)**	**N2 (ppm)**
TM8	227.3	20.1	0.0	27.0	61.1	10.8	0.0	4253.2	286385.6
Vacuum	100	4	0	14	15	5	0	3975	66931
Headspace	27	5	0	11	23	6	0	11858	66446
Gas in gas	261	20	0	33	7	3	0	34556	954475

Similar to the measurements in Gemini X mineral oil, the gas generation amounts under these two thermal fault levels are low in both oil phase and gas phase. The laboratory measurements seem to be more sensitive for low gas concentrations.

There are significant discrepancies between the atmospheric gases (CO2, O2 and N2) concentrations among the TM8 and laboratory measurements. This is also found in the following Diala S4 ZX-I results. The probable reason might be the errors in the Ostwald coefficients and also the air ingression, which are discussed in the latter context.

The DGA measurements of Diala S4 ZX-I before and after the 450 ℃ and 550 ℃ experiments are listed in the Table 6-11 and Table 6-12, respectively.

Table 6-11 DGA measurements (ppm) before and after 450 ℃ thermal fault in Diala S4 ZX-I

Before	CO2 (ppm)	CO (ppm)	H2 (ppm)	CH4 (ppm)	C2H6 (ppm)	C2H4 (ppm)	C2H2 (ppm)	O2 (ppm)	N2 (ppm)
TM8	264.4	0.0	0.0	15.0	120.7	11.4	0.0	4215.5	285157.6
Vacuum	120	2	0	7	40	5	0	4274	67953
Headspace	40	2	0	6	50	5	0	12616	66480
Gas in gas	229	12	0	21	17	3	0	26705	956968
After	**CO2 (ppm)**	**CO (ppm)**	**H2 (ppm)**	**CH4 (ppm)**	**C2H6 (ppm)**	**C2H4 (ppm)**	**C2H2 (ppm)**	**O2 (ppm)**	**N2 (ppm)**
TM8	291.8	0.0	0.0	76.2	341.4	36.8	0.0	4818.2	284506.9
Vacuum	94	3	0	20	69	14	0	3650	59407
Headspace	46	3	0	27	141	18	0	12815	66830
Gas in gas	234	19	0	22	17	3	0	27012	968979

Table 6-12 DGA measurements (ppm) before and after 550 ℃ thermal fault in Diala S4 ZX-I

Before	CO2 (ppm)	CO (ppm)	H2 (ppm)	CH4 (ppm)	C2H6 (ppm)	C2H4 (ppm)	C2H2 (ppm)	O2 (ppm)	N2 (ppm)
TM8	164.2	0.0	0.0	15.8	186.4	13.4	0.0	4268.3	281274.3
Vacuum	73	2	0	9	61	5	0	8318	89113
Headspace	17	1	0	10	89	7	0	14000	74978
Gas in gas	193	1	0	11	5	15	0	24392	936431
After	**CO2 (ppm)**	**CO (ppm)**	**H2 (ppm)**	**CH4 (ppm)**	**C2H6 (ppm)**	**C2H4 (ppm)**	**C2H2 (ppm)**	**O2 (ppm)**	**N2 (ppm)**
TM8	167.0	0.0	0.0	118.5	491.2	71.9	0.0	3536.9	283619.8
Vacuum	80	2	0	38	167	27	0	4168	68289
Headspace	0	2	0	42	216	34	0	11373	67457
Gas in gas	202	7	0	76	66	18	0	24103	930553

Under these two fault levels, the fault gases are obviously generated. Similar to the Gemini X, more fault gases are generated in the oil phase than those should be in the headspace gas phase under equilibrium state, especially the CH4, C2H6 and C2H4 results after faults as they are the dominant gases under thermal faults. It needs to be noticed that the 450 ℃ experiment is not following the previous 350 ℃. Therefore, the background levels of some gases in Table 6-11 is more than the after fault levels in Table 6-10. However, from the degas effect could be found obviously between the background gas level of 550 ℃ experiment and the after fault gas level of 450 ℃ as shown in Table 6-12 and Table 6-11.

The DGA measurement results from 650 ℃ and 750 ℃ experiments are shown in Table 6-13 and Table 6-14, respectively. The measurements with laboratory headspace method in Table 6-14 were lost.

Table 6-13 DGA measurements (ppm) before and after 650 ℃ thermal fault in Diala S4 ZX-I

Before	CO2 (ppm)	CO (ppm)	H2 (ppm)	CH4 (ppm)	C2H6 (ppm)	C2H4 (ppm)	C2H2 (ppm)	O2 (ppm)	N2 (ppm)
TM8	90.2	0.0	0.0	15.0	216.0	27.4	0.0	1520.8	288665.2
Vacuum	26	1	0	7	44	14	0	2721	61841
Headspace	**0**	1	0	7	94	13	0	13681	75063
Gas in gas	165	3	0	21	32	7	0	20590	973446
After	**CO2 (ppm)**	**CO (ppm)**	**H2 (ppm)**	**CH4 (ppm)**	**C2H6 (ppm)**	**C2H4 (ppm)**	**C2H2 (ppm)**	**O2 (ppm)**	**N2 (ppm)**
TM8	124.4	0.0	0.0	296.2	628.1	306.2	0.0	2397.4	283847.8
Vacuum	62	2	0	121	245	162	0	3751	65446
Headspace	0	2	0	120	289	149	0	12716	70662
Gas in gas	167	9	0	387	112	96	0	23648	959381

Table 6-14 DGA measurements (ppm) before and after 750 ℃ thermal fault in Diala S4 ZX-I

Before	CO2 (ppm)	CO (ppm)	H2 (ppm)	CH4 (ppm)	C2H6 (ppm)	C2H4 (ppm)	C2H2 (ppm)	O2 (ppm)	N2 (ppm)
TM8	394.9	0.0	0.0	290.1	1085.8	831.2	0.0	6804.8	283888.7
Vacuum	159	2	0	99	367	324	0	5883	73136
Headspace	74	1	0	103	451	371	0	11619	63912
Gas in gas	238	8	0	308	175	247	0	30579	946096
After	**CO2 (ppm)**	**CO (ppm)**	**H2 (ppm)**	**CH4 (ppm)**	**C2H6 (ppm)**	**C2H4 (ppm)**	**C2H2 (ppm)**	**O2 (ppm)**	**N2 (ppm)**
TM8	442.3	0.0	3266.8	4871.3	17463.9	9994.6	36.6	8723.4	282927.3
Vacuum	125	2	475	1990	9255	5590	24	15193	70036
Headspace	-	-	-	-	-	-	-	-	-
Gas in gas	247	16	10147	4547	3028	3182	9	33401	908032

The CO2 measurement of laboratory headspace method in background gas level in Table 6-13 is highlighted because the measurement is probably not correct. The background gas levels of 750 ℃ experiment are in general higher than the after fault gas level of 650 ℃ because these two experiments are not in sequence and there is another experiment in between them.

Similar to the gas generation in Gemini X mineral oil, in the 650 ℃ and 750 ℃ experiments, the fault gases are significantly generated. More fault gases could be found in the gas phase than it should be dissolved in the oil under equilibrium state after faults. This might be due to the same reason in the Gemini X where the fault gases are generated with free gas generation under high levels of thermal faults.

6.6.2 Comparison between Online DGA Monitor and Laboratory Measurements of Diala S4 ZX-I GTL Oil

The laboratory measurements of dissolved gases in Diala S4 ZX-I with two extraction methods are plotted against the TM8 online DGA measurements. In this analysis, only CH4, C2H6 and C2H4 are investigated. The reason is same as previously discussed in the comparison of Gemini X mineral oil. Comparisons of all the three gases give similar conclusion. Therefore, only comparison of CH4 in Diala S4 ZX-I is shown as an example in Figure 6-7.

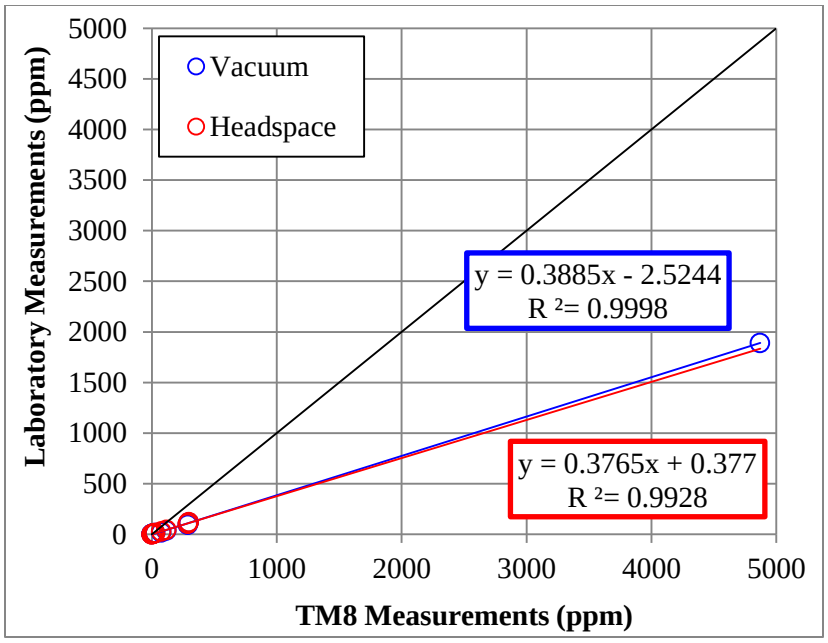

Figure 6-7 Laboratory measurements of methane (CH4) in Diala S4 ZX-I gas to liquid insulating oil against the TM8 online DGA measurements

Similar to the measurements in Gemini X mineral oil, the laboratory measurements of CH4 with both two extraction methods are in linear relationship with the TM8 measurements. However, the slope values of the linear regression curves are all about 0.38 which is quite smaller than 1, which means there is significant discrepancy between laboratory measurement and TM8 online DGA measurement on same Diala S4 ZX-I oil sample. The slope values of CH4, C2H6 and C2H4 are all in between 0.3 and 0.4. Hence, the laboratory measurements in general give less than half of the values from TM8 online DGA measurements. The similar phenomenon is found in CO2 and H2 measurement results. Especially in H2 measurement, the TM8 measurement is much larger than the laboratory measurement as shown in Table 6-14. Similar to the Gemini X mineral oil, the laboratory measurements of CO2 and O2 might be distorted due to air ingression.

The reason for the significant discrepancy might be due to the significantly different hydrogen Ostwald coefficients between mineral oil and Diala S4 ZX-I. In the correction for laboratory measurements, the phase ratio values in the laboratory headspace extraction method and the Toepler pump vacuum extraction method are 1.13 and 8.38, respectively. Although the hydrogen Ostwald coefficients of the mineral oil and Diala S4 ZX-I are quite different, they are both very small compared with the phase ratios.

Therefore, the correction calculation for laboratory measurements of Diala S4 ZX-I virtually does not change the results. However, for TM8 online DGA measurement, the results are corrected proportionally with the Ostwald coefficient variation. As previously discussed, the difference between Ostwald coefficients of Diala S4 ZX-I and conventional mineral oil might be enlarged as the measurement methods might be different. The inaccurate Ostwald coefficients might distort the results from TM8 but have limited effect on laboratory measurements. On the other hand, the larger the phase ratio in the extraction system, the smaller effects the errors in Ostwald coefficients might cause.

Besides, as the extraction systems of these DGA measurements are designed based on mineral oil, the gas phase and oil phase inside might not be able to reach equilibrium with alternative insulating liquids. On the other words, the degas efficiency of the gas extraction system might be lower with alternative insulating liquid than that with mineral oil. This would cause the partition coefficients different from the Ostwald coefficients. Calibration with gas in oil standards could mitigate this issue. Therefore, it is suggested that a DGA measurement system should be calibrated consistently with gas in oil standard rather than calibrate with gas in gas standard and calculate the results with Ostwald coefficients.

6.7 DGA Measurements of MIDEL 7131 Synthetic Ester Liquid

6.7.1 Original Measurement Results of Midel 7131 Synthetic Ester Liquid

The DGA measurements of fault gases before and after 250 ℃ and 350 ℃ experiments are listed in the Table 6-15 and Table 6-16, respectively. The laboratory measurement with headspace method for the background gas level in Table 6-15 is lost.

Table 6-15 DGA measurements (ppm) before and after 250 ℃ thermal fault in MIDEL 7131

Before	CO2 (ppm)	CO (ppm)	H2 (ppm)	CH4 (ppm)	C2H6 (ppm)	C2H4 (ppm)	C2H2 (ppm)	O2 (ppm)	N2 (ppm)
TM8	77.0	0.0	0.0	0.0	25.6	31.7	0.0	569.2	84876.4
Vacuum	90	2	0	1	2	2	0	9343	44226
Headspace	-	-	-	-	-	-	-	-	-
Gas in gas	78	3	0	2	5	7	0	10348	999528
After	CO2 (ppm)	CO (ppm)	H2 (ppm)	CH4 (ppm)	C2H6 (ppm)	C2H4 (ppm)	C2H2 (ppm)	O2 (ppm)	N2 (ppm)
TM8	239.9	35.2	0.0	8.6	39.8	56.8	0.0	1012.1	86712.6
Vacuum	65	4	0	1	3	2	0	9658	56478
Headspace	228	35	0	8	40	39	0	10107	56995
Gas in gas	180	59	0	10	10	9	0	20021	954369

Table 6-16 DGA measurements (ppm) before and after 350 ℃ thermal fault in MIDEL 7131

Before	CO2 (ppm)	CO (ppm)	H2 (ppm)	CH4 (ppm)	C2H6 (ppm)	C2H4 (ppm)	C2H2 (ppm)	O2 (ppm)	N2 (ppm)
TM8	17.1	0.0	0.0	0.0	0.0	8.4	0.0	172.0	91971.5
Vacuum	18	2	0	0	1	1	0	1509	15896
Headspace	27	4	0	2	1	1	0	2080	43919
Gas in gas	163	4	0	0	1	1	0	23524	943593
After	CO2 (ppm)	CO (ppm)	H2 (ppm)	CH4 (ppm)	C2H6 (ppm)	C2H4 (ppm)	C2H2 (ppm)	O2 (ppm)	N2 (ppm)
TM8	96.6	23.4	0.0	0.0	21.8	15.4	0.0	574.5	90200.6
Vacuum	43	3	0	1	2	1	0	8807	67440
Headspace	153	26	0	3	19	11	0	9043	14832
Gas in gas	169	23	0	15	5	4	0	22800	939210

Similar to the measurements for the other two oils, laboratory measurements are more sensitive than the online DGA monitor. Compared with the other two oils, MIDEL 7131 generates gases more under these two thermal fault levels. CO2 and CO are significantly generated. For hydrocarbon gases, CH4 is virtually not generated but C2H6 and C2H4 are significantly generated. The O2 and N2 measurements among these three methods are quite different which might be due to the air ingression in laboratory measurement process.

The DGA measurements of MIDEL 7131 before and after the 450 ℃ and 550 ℃ experiments are listed in the Table 6-17 and Table 6-18, respectively.

Table 6-17 DGA measurements (ppm) before and after 450 ℃ thermal fault in MIDEL 7131

Before	CO2 (ppm)	CO (ppm)	H2 (ppm)	CH4 (ppm)	C2H6 (ppm)	C2H4 (ppm)	C2H2 (ppm)	O2 (ppm)	N2 (ppm)
TM8	149.2	10.2	0.0	0.0	17.5	16.5	0.0	1972.3	83260.1
Vacuum	46	3	0	1	1	2	0	8901	43792
Headspace	196	21	0	1	15	11	0	11473	33177
Gas in gas	138	7	0	2	3	4	0	15750	950611
After	**CO2 (ppm)**	**CO (ppm)**	**H2 (ppm)**	**CH4 (ppm)**	**C2H6 (ppm)**	**C2H4 (ppm)**	**C2H2 (ppm)**	**O2 (ppm)**	**N2 (ppm)**
TM8	240.5	70.1	0.0	13.2	48.6	32.6	0.0	1782.6	85319.6
Vacuum	54	5	0	3	4	3	0	10943	68593
Headspace	288	92	0	12	42	26	0	8443	142609
Gas in gas	158	48	0	11	11	10	0	20741	956612

Table 6-18 DGA measurements (ppm) before and after 550 ℃ thermal fault in MIDEL 7131

Before	CO2 (ppm)	CO (ppm)	H2 (ppm)	CH4 (ppm)	C2H6 (ppm)	C2H4 (ppm)	C2H2 (ppm)	O2 (ppm)	N2 (ppm)
TM8	88.4	7.1	0.0	0.0	12.1	8.4	0.0	505.6	99557.1
Vacuum	44	4	0	1	2	2	0	3708	31958
Headspace	204	5	0	1	2	2	0	11021	-
Gas in gas	176	5	0	1	2	2	0	41631	927801
After	**CO2 (ppm)**	**CO (ppm)**	**H2 (ppm)**	**CH4 (ppm)**	**C2H6 (ppm)**	**C2H4 (ppm)**	**C2H2 (ppm)**	**O2 (ppm)**	**N2 (ppm)**
TM8	253.3	105.2	0.0	36.2	102.8	54.7	0.0	722.3	90713.4
Vacuum	67	25	0	6	11	7	0	10415	41044
Headspace	257	90	0	19	86	46	0	13213	12787
Gas in gas	152	99	0	30	22	18	0	14725	944010

Some nitrogen measurements are lost which are not given due to the operation error of the laboratory GC system. Under these two fault levels, more fault gases are generated. Similar to the other two oils, more fault gases are generated in the oil phase than those should be in the headspace gas phase under equilibrium state, especially the CO, CH4, C2H6 and C2H4 results after faults as they are the dominant gases under thermal faults. The similar degas effects could be found in these results.

The 550 ℃ test has been repeated in order to verify the repeatability of the experiments. In addition, the two samples of gas and oil are taken and measured in several tests with MIDEL 7131 in order to evaluate the gas and oil sampling reliability. The results of these verification tests are provided in Appendix IV. From the results, it can be seen that the DGA experiments performed with the tube heating experimental system are repeatable. The gas and oil sampling methods are reliable.

The DGA measurement results from 650 ℃ and 750 ℃ experiments are shown in Table 6-19 and Table 6-20, respectively.

Table 6-19 DGA measurements (ppm) before and after 650 ℃ thermal fault in MIDEL 7131

Before	CO2 (ppm)	CO (ppm)	H2 (ppm)	CH4 (ppm)	C2H6 (ppm)	C2H4 (ppm)	C2H2 (ppm)	O2 (ppm)	N2 (ppm)
TM8	151.7	45.9	0.0	11.9	54.3	28.1	0.0	723.4	84663.6
Vacuum	29	7	0	2	5	3	0	1353	16486
Headspace	101	16	0	5	7	4	0	14074	-
Gas in gas	87	16	0	5	8	4	0	11017	944748
After	**CO2 (ppm)**	**CO (ppm)**	**H2 (ppm)**	**CH4 (ppm)**	**C2H6 (ppm)**	**C2H4 (ppm)**	**C2H2 (ppm)**	**O2 (ppm)**	**N2 (ppm)**
TM8	420.5	263.3	0.0	134.7	316.3	178.8	0.0	629.3	83865.0
Vacuum	85	54	0	21	43	23	0	29879	50468
Headspace	374	212	0	80	271	153	0	20180	48293
Gas in gas	198	296	0	115	83	63	0	11753	949826

Table 6-20 DGA measurements (ppm) before and after 750 ℃ thermal fault in MIDEL 7131

	CO2 (ppm)	CO (ppm)	H2 (ppm)	CH4 (ppm)	C2H6 (ppm)	C2H4 (ppm)	C2H2 (ppm)	O2 (ppm)	N2 (ppm)
TM8	137.6	34.5	0.0	18.0	106.6	52.5	0.0	521.4	105500
Vacuum	29	6	0	3	10	8	0	2375	23408
Headspace	222	35	0	14	92	44	0	19019	71630
Gas in gas	146	33	0	18	25	14	0	14873	963969
After	**CO2 (ppm)**	**CO (ppm)**	**H2 (ppm)**	**CH4 (ppm)**	**C2H6 (ppm)**	**C2H4 (ppm)**	**C2H2 (ppm)**	**O2 (ppm)**	**N2 (ppm)**
TM8	19674.1	3388.8	422.3	9369.8	9772.6	29204.8	232.5	653.2	84815.5
Vacuum	3670	606	253	1618	1336	6145	52	1401	22031
Headspace	10338	2555	336	786	8333	29247	216	17109	56062
Gas in gas	6804	35295	10647	29773	3751	18151	43	23500	839184

Large amount of fault gases are generated from the 750 ℃ experiment. Similar to the other two oils, under these two fault levels where free gas is generated more fault gases are focused in the gas phase compared with lower fault levels. It also needs to be noticed that the carbon oxides (CO2 and CO) generation amounts are significant and comparable with the hydrocarbon gases.

6.7.2 Comparison between Online DGA Monitor and Laboratory Measurements of Midel 7131 Synthetic Ester Liquid

The comparison between online DGA measurements and laboratory measurements are performed following the similar procedures are in the other two oils. The laboratory measurements with both vacuum extraction method and headspace extraction method are plotted against the TM8 measurement on the same oil. The atmosphere gases (CO2, O2 and N2) are not included in this comparison as significant discrepancies are found in the measurements of these gases probably due to the air ingression in sample transportation

and laboratory measurement procedures. In addition, H2 and C2H2 are not included in the comparison as the sample numbers which contain these two gases are too few to analyse. The R-square values and the slope values of the other fault gases are listed in the Table 6-21.

Table 6-21 R-square and slope values of the linear regression curves of the laboratory measurements related to the TM8 measurements of MIDEL 7131

		CO	CH4	C2H6	C2H4
Vacuum Extraction	R-square	0.9995	1	1	1
	Slope	0.1787	0.1727	0.1369	0.2105
Headspace Extraction	R-square	0.9997	0.9929	1	1
	Slope	0.7518	0.0827	0.8532	1.0019

Similar to the comparison results of the other two oils, the laboratory measurements of CO, CH4, C2H6 and C2H4 in MIDEL 7131 are in linear relationship to the TM8 online DGA measurements where the R-square values are in general quite close to unit. For CO, C2H6 and C2H4, the slope values of vacuum extraction are close or lower than 0.2 while those of headspace extraction are above 0.75. Therefore, for CO, CH4 and C2H4, the laboratory measurements with headspace extraction method give closer results from TM8 online DGA measurements, but there are significant discrepancies between laboratory measurements with vacuum extraction method and online DGA measurements. There are two possible reasons for this phenomenon. One is that the vacuum extraction method has very low degassing efficiency when facing with synthetic ester liquid. The other one is that the Ostwald coefficients of MIDEL 7131 used in the correction calculation might be higher than real values therefore the gas amounts measured with headspace extraction method are overestimated. It needs to be noticed that the slope value of CH4 measurements with headspace extraction method is even lower than half of the vacuum extraction method. This might indicate that there is a huge difference between Ostwald coefficient of CH4 and the true value. Therefore, based on the experimental results, the online DGA measurements and laboratory measurements of MIDEL 7131 could not be unified. It is suggested that the DGA system for MIDEL 7131 needs to be calibrated with gas in oil standards. Besides, more efforts should be focused on the Ostwald coefficient determination.

6.8 Experimental Results of Fault Gas Generation

6.8.1 Fault Gas Generation Results of Gemini X Mineral Oil

The total fault gas generation results of Gemini X mineral oil are listed in Table 6-22. It needs to be noticed that the ppm values in the table are only calculated to indicate the total fault gas amount rather than the dissolved gas concentration values.

Table 6-22 Total fault gas generation results of Gemini X in the tube heating DGA experiments

Fault temperature (℃)	CO2 (ppm)	CO (ppm)	H2 (ppm)	CH4 (ppm)	C2H6 (ppm)	C2H4 (ppm)	C2H2 (ppm)
250	29.2	1.1	0.0	0.0	0.0	0.0	0.0
350	45.7	14.2	0.0	9.9	6.4	0.4	0.0
450	56.7	20.7	0.0	31.4	9.1	5.1	0.0
550	40.5	16.7	0.0	81.0	29.2	37.2	0.0
650	32.9	77.6	157.6	515.0	285.5	432.6	6.1
750	19.4	40.0	5355.9	9212.0	5533.6	9270.7	29.9

The fault gas generation rates of Gemini X mineral oil under thermal faults are calculated and plotted in Figure 6-8 in logarithmic scale. Generation rates of all fault gases generally increase exponentially with the fault level increasing. The generation rates of CO and CH4 under 250 ℃ and C2H4 under 350 ℃ might be inaccurate as the generation amounts of them during experiments are near the low detection limit of the TM8 online DGA monitor. An extended experimental duration might give more accurate gas generation rates for these gases with trace amount of generation.

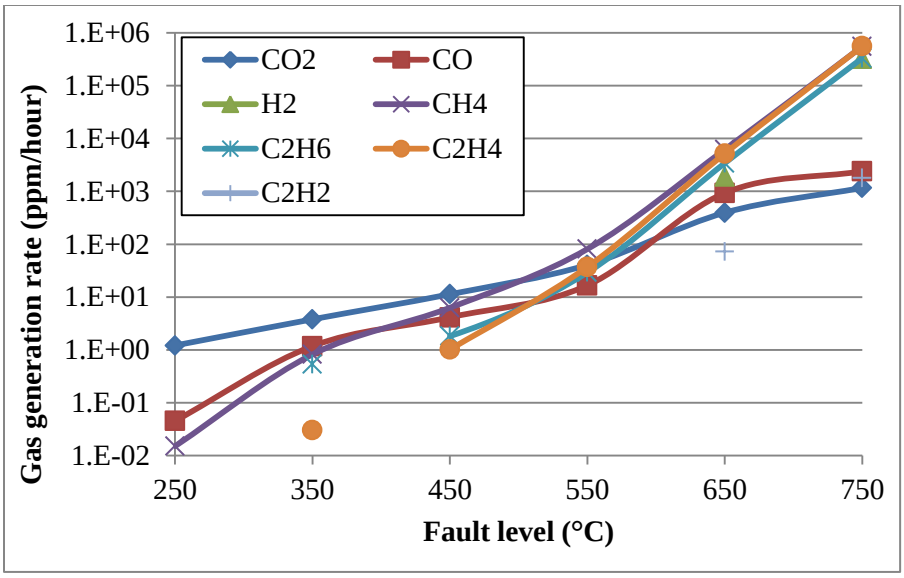

Figure 6-8 Gas generation rates (ppm/hour) of Gemini X mineral oil under various levels of thermal faults

Carbon oxides generation rates are more slowly increasing compared with the generation rates of hydrocarbon gases, such as CH4, C2H6 and C2H4. This might verify that the generation mechanism of carbon oxides from Gemini X mineral oil under thermal faults is not same as that of hydrocarbon gases. The mineral oil molecules are composed of carbon and hydrogen atoms which virtually contain no oxygen atoms. Therefore, the carbon oxides might be generated from the reactions between oil molecules and dissolved oxygen or catalytic reactions with metal. On the other hand, the generation of hydrocarbon gases are from oil molecules decomposition and recombination.

The fault gas generation combinations of Gemini X mineral oil under thermal faults are shown in Figure 6-9. It needs to be noticed that the combination patterns is based on the fault gas generation rather than dissolved gas patterns which are widely used in the conventional DGA data interpretation techniques.

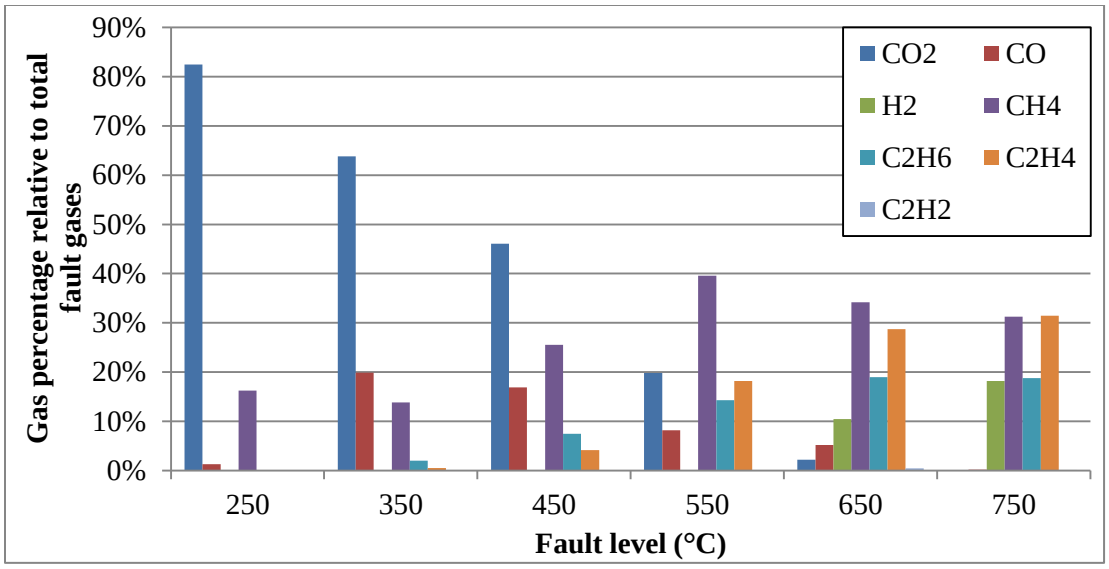

Figure 6-9 Fault gas generation patterns of Gemini X mineral oil under thermal faults

At 250℃, the CO2 is mostly generated and its percentage decreases with fault level increasing. There are about 15% of CH4 and small portion of CO in the 250℃ gas generation pattern. However, as previously discussed, the generation amounts of these two gases are very low at this gas level and might be inaccurate. The CO percentage reaches peak value of about 20% at 350℃ and then decreases with temperature increasing. The CH4 percentage reaches the peak value of about 40% at 550℃ and then decreases. The C2H6 percentage increases with fault level until it reaches peak value of about 20% at 650℃. The C2H4 starts to be obviously generated at 450℃ and keeps increasing with fault level. At 750℃, the percentage of C2H4 is more than 30% which is the maximum. The H2 starts generation from 650℃ and at 750℃ its percentage is approaching 20%. The C2H2 is only found in 750℃ with a small percentage. However, as the C2H2 is the gas generated under high fault energy, the absolute C2H2 generation value is of significance which could indicate a high level thermal fault.

The percentage values of the fault gas generation combination are listed in the Table 6-23.

Table 6-23 Fault gas percentage combination of Gemini X mineral oil under thermal faults

Fault level	250 ℃	350 ℃	450 ℃	550 ℃	650 ℃	750 ℃
CO2	82%	64%	46%	20%	2%	0%
CO	**1%**	20%	17%	8%	5%	0%
H2	0%	0%	0%	0%	10%	18%
CH4	**16%**	14%	26%	40%	34%	31%
C2H6	0%	2%	7%	14%	19%	19%
C2H4	0%	**1%**	4%	18%	29%	31%
C2H2	0%	0%	0%	0%	0%	0%

The percentages of CO and CH4 at 250 ℃ and C2H4 at 350 ℃ are highlighted as they might be inaccurate values. The percentage figures in the Table 6-23 are only based on the experimental results of Gemini X mineral oil in the tube heating test system. The variation of oil types might have different percentage figure. The fault scenario might also affect the gas generation. In real transformers, the fault scenario might be much more complicated than the laboratory simulated system. For example, there might be cellulose material involved in the fault. Therefore, the Table 6-23 is suggested to use as supplement method of fault diagnostic methods rather than take the percentage figures directly to be used as diagnostic technique.

It needs to be noticed that the fault gas combination patterns are based on fault gas generation values rather than the dissolved gas patterns of the oil samples which are widely accepted in the conventional DGA diagnostic methods. It is more reasonable to analyse the gas generation from the transformer rather than the absolute dissolved gas concentrations. With the widely installation of online DGA monitors, the fault gas generations in transformers could be acquired easily. There are also some transformers with frequent DGA measurement periods. For these transformers with known gas generation rates or patterns, the Table 6-23 and Figure 6-9 give effective information for fault diagnosis on condition that these transformers are mineral oil immersed.

6.8.2 Fault Gas Generation Results of Diala S4 ZX-I GTL Oil

The total fault gas generation results of Diala S4 ZX-I GTL oil are shown in Table 6-24.

Table 6-24 Total fault gas generation results of Diala S4 ZX-I in the tube heating DGA experiments

Fault temperature (℃)	CO2 (ppm)	CO (ppm)	H2 (ppm)	CH4 (ppm)	C2H6 (ppm)	C2H4 (ppm)	C2H2 (ppm)
250	32.7	1.5	0.0	6.2	0.0	0.4	0.0
350	21.0	6.1	0.0	19.3	62.8	6.4	0.0
450	13.2	2.5	0.0	25.9	102.6	12.4	0.0
550	3.4	2.2	0.0	66.6	163.8	29.8	0.0
650	18.8	2.3	0.0	255.5	222.2	170.8	0.0
750	45.2	4.5	5133.2	3889.1	8894.4	5825.8	23.4

The gas generation rates of Diala S4 ZX-I under thermal faults are shown in Figure 6-10. The gas generation rates increase exponentially with fault level rising. The increasing trends of carbon oxides are different from those of hydrocarbon gases which indicate that the generation mechanism of carbon oxides is different from hydrocarbon gas generation for the same reason in Gemini X mineral oil. All gas generation rates are similar to those in mineral oil except for the CO which generates much less than in Gemini X.

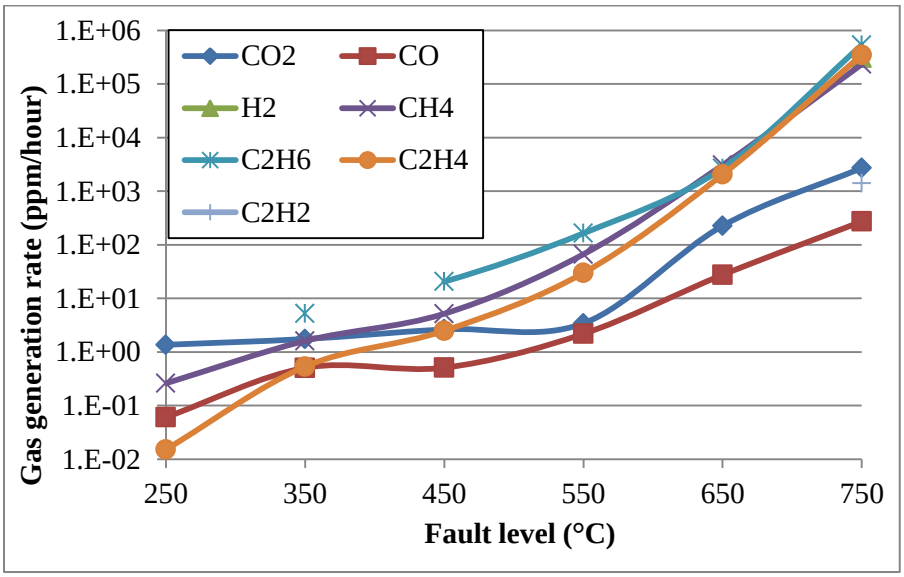

Figure 6-10 Gas generation rates (ppm/hour) of Diala S4 ZX-I under various levels of thermal faults

The percentage combinations of gas generation of Diala S4 ZX-I under thermal faults are shown in Figure 6-11.

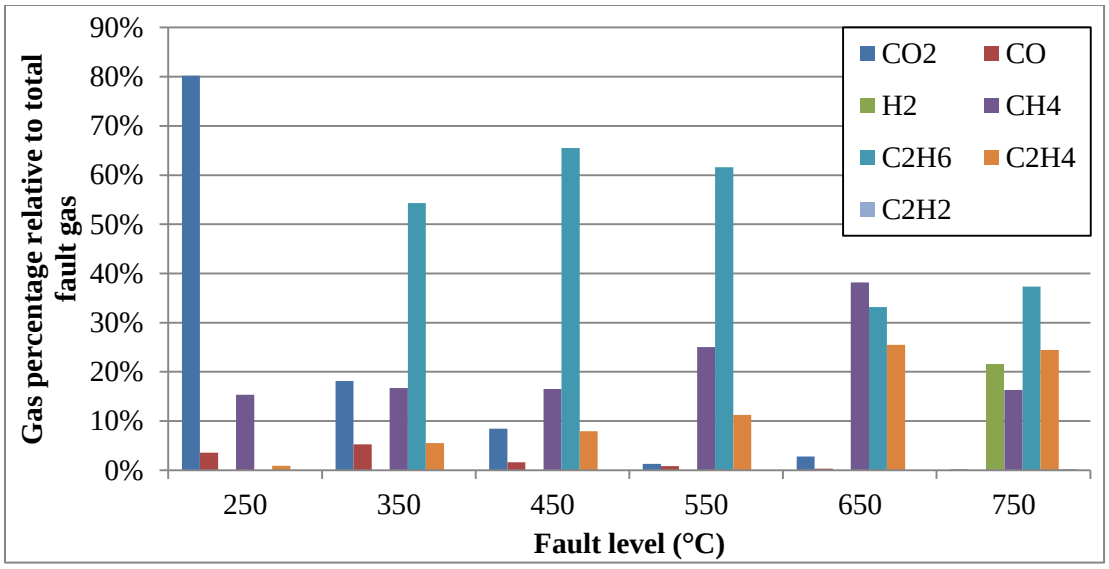

Figure 6-11 Fault gas generation patterns of Diala S4 ZX-I under thermal faults

The CO2 takes about 80% at 250 ℃ and sharply decreases with fault level increasing. Same as in the mineral oil, the CO percentage reaches peak value at 350 ℃ which is only 5% and then decreases. The peak percentage of CH4 appears at 650 ℃. The generation of H2 and C2H2 starts at 750 ℃. The percentage of C2H2 is also negligible but the absolute concentration value is important for diagnosis. It needs to be noticed that the C2H6 dominates the gas generation from 350 ℃ to 550 ℃, the percentages of which are 54%, 65% and 62%. This is the major difference of Diala S4 ZX-I gas generation from that of Gemini X mineral oil.

For diagnostic purposes, the figures of the percentage combination patterns of Diala S4 ZX-I gas generation under thermal faults are listed in the Table 6-25.

Table 6-25 Fault gas percentage combination of Diala S4 ZX-I under thermal faults

Fault level	250 ℃	350 ℃	450 ℃	550 ℃	650 ℃	750 ℃
CO2	80%	18%	8%	1%	3%	0%
CO	4%	5%	2%	1%	0%	0%
H2	0%	0%	0%	0%	0%	22%
CH4	15%	17%	17%	25%	38%	16%
C2H6	0%	54%	65%	62%	33%	37%
C2H4	1%	6%	8%	11%	26%	24%
C2H2	0%	0%	0%	0%	0%	0%

Same as the percentage figures of Gemini X fault combination, these figures are not strictly regulating the fault gas generation patterns. Instead, they should be regarded as

supplement information for fault diagnosis.

It also needs to be noticed that the percentage combination patterns are for gas generation rather than absolute dissolved gas concentration patterns which are widely used in the conventional diagnostic methods. In Table 6-25, the percentage combinations are based on results from the established experimental system. Therefore, the combinations are valid only with the same DGA measurement condition, such as consistent Ostwald coefficients and similar fault condition. As previously discussed, the DGA results of Diala S4 ZX-I might be somehow inaccurate as the results are established based on the measured Ostwald coefficients and calculation for correction. In real cases, the DGA measurement method might change. For example, the DGA measurement system might be calibrated with Diala S4 ZX-I gas in oil standard, or the Ostwald coefficients measured are varied. The percentage figures of the fault gas combination might change. Therefore, it is suggested that the utility dealing with transformers filled with Diala S4 ZX-I should build up consistent DGA measurement system and repeat the thermal fault experiments in order to establish their internal gas generation patterns.

6.8.3 Fault Gas Generation Results of MIDEL 7131 Synthetic Ester Liquid

The total fault gas generation results of MIDEL 7131 synthetic ester liquid are shown in Table 6-26.

Table 6-26 Total fault gas generation results of MIDEL 7131 in the tube heating DGA experiments

Fault temperature (℃)	CO2 (ppm)	CO (ppm)	H2 (ppm)	CH4 (ppm)	C2H6 (ppm)	C2H4 (ppm)	C2H2 (ppm)
250	196.3	55.1	0.0	11.4	15.4	24.9	0.0
350	80.2	30.0	0.0	5.5	22.9	7.8	0.0
450	95.0	73.7	0.0	16.3	33.3	17.8	0.0
550	152.3	130.7	0.0	46.2	96.4	51.3	0.0
650	305.8	319.7	0.0	162.5	285.8	170.4	0.0
750	22289.2	20887.1	5733.0	23947.8	11236.2	37337.7	247.0

The gas generation rates of MIDEL 7131 under thermal faults are shown in Figure 6-12.

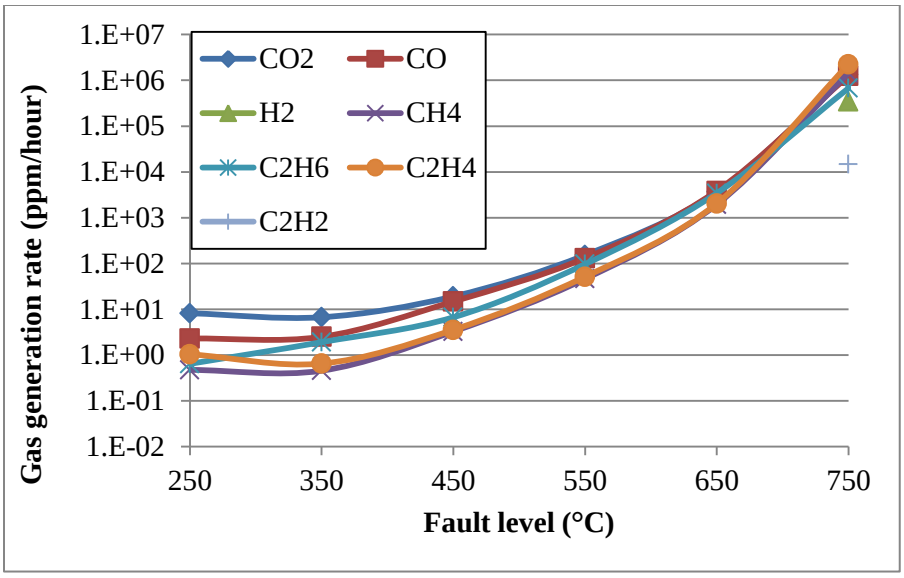

Figure 6-12 Gas generation rates of MIDEL 7131 synthetic ester liquid under various levels of thermal faults

The fault gas generation rates are in general increasing exponentially. However, secondary decomposition could be observed as the increments of gas generation rates under low thermal fault levels are smaller than those under high thermal fault levels. H2 and C2H2 are generated under 750 ℃. It needs to be noticed that the generation rates of carbon oxides (CO2 and CO) are in similar trends of the other gases which is different from the other two tested liquids. This verifies that the carbon oxides are generated in the molecule decomposition process of MIDEL 7131 under thermal faults as the MIDEL 7131 contains oxygen atom in the oil molecules. Therefore, in the fault diagnosis of MIDEL 7131, carbon oxides should be regarded as key fault indicators. The fault diagnosis of cellulose involved transformer faults in MIDEL 7131 filled transformers should apply different CO2/CO standards from the mineral oil filled transformers.

The percentage combinations of gas generation of MIDEL 7131 under thermal faults are shown in Figure 6-13.

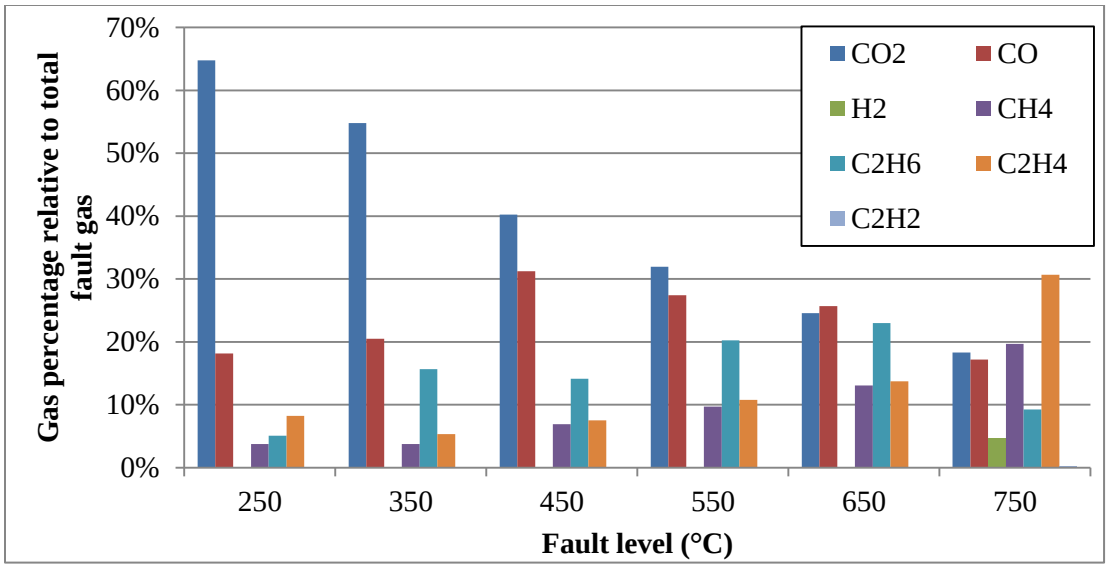

Figure 6-13 Fault gas generation patterns of MIDEL 7131 under thermal faults

The percentage of CO2 decreases with fault level increasing. At 750 ℃, there is still 18% of CO2 in the fault gas generation combination. The CO percentage increases from 18% to 31% at 450 ℃ and then decreases with temperature increasing. At 750 ℃, there is still 17% of CO in the fault gas combination. Therefore, the percentages of CO2 and CO should be noticed in fault diagnosis in MIDEL 7131 filled transformers as they might not only be generated from cellulose involved faults. Similar to the Diala S4 ZX-I, C2H6 is the key fault indicator which is the dominant generated hydrocarbon gases from 350 ℃ to 650 ℃ followed with C2H4. It needs to be noticed that the C2H4 percentage is even larger than those of CH4 and C2H6 which might be regarded as high temperature thermal fault in mineral oil. There are two methods to distinguish 250 ℃ and 750 ℃. The first one is comparing total hydrocarbon gases with carbon oxides. At 250 ℃, carbon oxides are mostly generated while at 750 ℃ the percentage of hydrocarbon gases is larger than carbon oxides. The second one is to observe the generation of H2 and C2H2 which could only be generated under 750 ℃ or above. However, the fault gas generation patterns discussed here are for thermal faults with oil only cases. If considerable amount of cellulose materials are involved in the faults, the largely generated carbon oxides from cellulose might interfere with the fault diagnosis for MIDEL 7131. Therefore, more efforts should be focused on investigation of fault gas generation in MIDEL 7131 with cellulose material involved.

For diagnostic purposes, the figures of the percentage combination patterns of MIDEL 7131 gas generation under thermal faults are listed in the Table 6-27.

Table 6-27 Fault gas percentage combination of MIDEL 7131 under thermal faults

Fault level	250 ℃	350 ℃	450 ℃	550 ℃	650 ℃	750 ℃
CO2	65%	55%	40%	32%	25%	18%
CO	18%	20%	31%	27%	26%	17%
H2	0%	0%	0%	0%	0%	5%
CH4	4%	4%	7%	10%	13%	20%
C2H6	5%	16%	14%	20%	23%	9%
C2H4	8%	5%	8%	11%	14%	31%
C2H2	0%	0%	0%	0%	0%	0%

Same as the percentage figures of the other two oils, these figures are not strictly regulating the fault gas generation patterns. Instead, they should be regarded as supplement information for fault diagnosis. The percentage values are based on the fault gas generation patterns rather than the absolute dissolved gas concentration patterns. Therefore, the combination of the gas generation patterns might be different from the conventional DGA diagnostic methods.

Similar to the Diala S4 ZX-I, the fault gas generation patterns are based on the dissolved gas measured by TM8 online DGA monitor and gas in gas concentration measured by laboratory GC facility. As the gas in oil concentration is calculated according to the Ostwald coefficients of MIDEL 7131, errors might be introduced. Therefore, it is suggested that the DGA measurement system should be calibrated with gas in oil standard. In addition, it is also suggested that the MIDEL 7131 users should test the oil with their own DGA measurement system in order to form their own diagnostic patterns.

6.9 Summary

Based on the established tube heating DGA experimental system, three investigated liquids are tested. The fault gas generation characteristics under thermal fault from 250 ℃ to 750 ℃ are tested with 100 ℃ interval. The concentrations of dissolved gases in the oil are measured by both laboratory measurements with either headspace extraction method or vacuum extraction method and TM8 online DGA measurement. The DGA

measurement results of alternative insulating liquids are calculated based on the Ostwald coefficients and known phase ratio in the extraction system.

For Gemini X mineral oil, the laboratory DGA measurements with two extraction methods give comparable results to the TM8 online DGA measurement. However, for the other two tested alternative insulating liquids, there are significant discrepancies between laboratory measurements and TM8 online DGA measurement probably due to the inaccurate Ostwald coefficients used in the calculation. It is thusly suggested that the DGA measurement system should be calibrated with gas in oil standard.

With the measured fault gas generation results, the fault gas generation patterns of three tested liquids are plotted. In Gemini X and Diala S4 ZX-I, the carbon oxides generation mechanism might be different from that in MIDEL 7131. The key hydrocarbon gases for the Gemini X are CH4 under lower fault level range and C2H4 under high fault level range. The key hydrocarbon gases for Diala S4 ZX-I and MIDEL 7131 are C2H6 under lower fault level range and C2H4 under high fault level range. Considerable amount of carbon oxides are generated from MIDEL 7131 under thermal faults. To mitigate the error introduced by the inaccurate Ostwald coefficients or the variation of DGA measurement system, it is also suggested that the alternative liquids users should test and build their own fault gas generation patterns and diagnostic standards with their own DGA measurement system.

Chapter 7 Conclusion and Future Work

7.1 Conclusion

7.1.1 General

This thesis is mainly focused on the methodology on how to simulate transformer thermal fault in laboratory for experimentally studying gas generation characteristics. This methodology has been applied on alternative insulating liquids. Through experimental investigations and data analysis, the research objectives are achieved and some valuable conclusions and findings are made.

There are three research topics in this thesis. The first is to study the methodology of laboratory thermal fault simulation in DGA experiments. The second is to study the fault gas generation characteristics of investigated liquids under laboratory simulated thermal faults. The third is to compare the measurements between online DGA techniques and laboratory DGA methods.

There are five major contributions in this PhD research work which are reported in this thesis:

1 Two novel DGA laboratory based experimental systems to simulate thermal faults have been established with two fault simulation methods.
2 Experimental studies of three different types of transformer insulating liquids have been carried out by the established experimental systems.
3 The Ostwald coefficients of the Gas to Liquid (GTL) transformer oil have been determined for the first time.
4 The pool boiling phenomenon and boiling curves for the three types of insulating liquids were found and reported in this thesis for the first time.
5 Experimental results of gas generation characteristics for the three types of transformer insulating liquids under various levels of thermal faults have been obtained using the established experimental systems.

7.1.2 Summary of Results and Main Findings

(i). Methodology of laboratory thermal fault simulation in DGA experiments

In this thesis, an experimental platform with immersed heating element was established. It was found that the heating element temperature would increase with input power rising up to the Nukiyama temperature of the oil at which the heating element temperature is almost constant with input power largely increasing.

The phenomenon is verified by the fact that the fault gas generation rates are virtually stable with input power significantly increasing in the nucleate boiling regime. Then the heating element temperature distribution would become inhomogeneous and localised hotspot temperature might be extremely high with a slight input power increment. This phenomenon is similar as the pool boiling phenomenon in water.

The Nukiyama temperature depends on the liquid nature and it varies from liquid type. The Diala S4 ZX-I and MIDEL 7131 have higher Nukiyama temperatures than Gemini X probably due to their higher boiling point. The pool boiling phenomenon in the immersed heating method somehow limits the thermal fault temperature which could not cover the range between the Nukiyama temperature and the burnout temperature. In other words, the immersed heating method could not cover the whole range of the thermal fault level due to the pool boiling phenomenon.

In addition, a tube heating method based DGA experimental system is established which could generate thermal fault in laboratory covering the whole thermal fault temperature range. It is consisted of oil heating, oil circulation and gas expansion components. The oil volume in the system is accurately controlled. The gas volume in the expansion bladder could be measured. By the known volumes of the two phases and the measured gas concentrations, the total fault gas contents can be quantified. The dissolved gas in oil is measured by both the laboratory measurements and online DGA measurement.

(ii). Gas generation characteristics of investigated liquids under thermal faults

The dissolved gas measurement devices are calibrated based on mineral oil. For

alternative insulating liquids, the Ostwald coefficients are used to correct the dissolved gas concentration results. The gas concentration in headspace is measured by the laboratory GC facility directly. The tube heating method could generate thermal fault covering the whole transformer thermal fault level range in three tested liquids.

The fault gas generation charts of three investigated liquids under various levels of thermal faults are plotted. In Gemini X mineral oil, the carbon oxides take up majority percentage but decrease with fault level increasing. The key hydrocarbon gas is methane which reaches peak value at 550 ℃ and decreases with ethylene increasing. Hydrogen and acetylene generations are found only at 750 ℃. In Diala S4 ZX-I GTL insulating oil, the fault gas generation characteristics are similar to the Gemini X except for the ethane which is dominantly generated. In MIDEL 7131 synthetics ester liquid, the key hydrocarbon gas is also ethane. Besides, considerable portions of carbon monoxide and carbon dioxide are generated. It is difficult to directly compare gas generation results between different types of oils primarily because the physical and chemical properties and molecular compositions of the three tested oils are different which might lead to different gas generation results.

(iii). Comparison between online DGA measurements and laboratory DGA measurements

The two online DGA monitors, SERVERON TM8 and GE Transfix are tested. For comparison, the oil is sampled and sent to laboratory for conventional DGA measurements. There are two extraction methods used in the laboratory DGA measurements which are vacuum extraction method and headspace method. Based on the laboratory measurements of Gemini X mineral oil samples after T1 and T3 faults, TM8 gives closer results to the laboratory than Transfix. The reason might be that the both the TM8 and laboratory use GC system to detect gases while the Transfix uses PAS system.

The percentage differences between online DGA monitor and laboratory measurements are larger at lower gas concentrations where the low detection limits of online DGA monitors need to be considered. At regular concentration levels, the percentage differences of TM8 are in general within 20%. The percentage differences of Transfix are in general within or near 30% except for hydrogen. The reason might be that it is

measured by a separate hydrogen sensor.

Comparing with different extraction methods, the TM8 measurements are close to the laboratory for Gemini X mineral oil. For Diala S4 ZX-I gas to liquid insulating oil, the TM8 gives about two times of the laboratory measurements. For MIDEL 7131 synthetic ester liquid, the vacuum extraction method gives much lower results than the TM8. There are two possible reasons. The first is that the Ostwald coefficients used in the correction are inaccurate. The second is that the extraction efficiencies in the laboratory measurements for alternative insulating liquids are less than mineral oil. In DGA analysis, the measurement method needs to be consistent and it needs to be considered when the DGA data are cross compared with others.

7.2 Future work

In this thesis, some useful conclusions are made on the laboratory methodology of DGA studies and fault gas generation under thermal faults. Meanwhile there are new questions raised and more work could be done in the future study.

For pool boiling phenomenon in transformer oil

i. The Nukiyama temperature depends on oil nature which is largely related to the boiling point. The Nukiyama temperatures for alternative insulating liquids need to be determined as it might affect the immersed thermal fault temperature range in transformers.

ii. The relationship between Nukiyama temperature and pressure needs to be determined. In large transformers, the oil pressure might vary significantly. Therefore, the thermal fault temperature range might be related to the depth of the fault location. The deeper thermal fault location might have higher thermal fault temperature in nucleate boiling region.

For fault gas generation patterns

i. The fault gas generation patterns obtained in this thesis are based on the experiments. Variation of experimental environment might affect the gas generation characteristics. For example, changing the size of heating tube might change the temperature gradient in the heating pipe. Therefore, the results need to be verified under various experimental conditions, for example, various oil and headspace volumes, various heating pipe size and so on.

ii. The fault gas generation patterns also depend on the Ostwald coefficients. As the Ostwald coefficient measurements are unreliable, the various DGA measurement methods are suggested to be calibrated with gas in oil standards of the tested liquids in which the accuracy of the Ostwald coefficients could be verified. In addition, the Ostwald coefficients of the alternative insulating liquids are suggested to be measured with different methods to mitigate the error introduced from the measurement process.

For representative transformer insulation system

i. In this thesis, the fault gas generation patterns of oil only are obtained. However, in real transformers, the faults are usually accompanied with other materials, such as metals or cellulose. To understand the gas generation of more realistic transformer insulation system, cellulose material such as cellulose paper or pressboard should be tested. Gas generation characteristic under fault with paper and pressboard involved is necessary to investigate in this platform. The established platform is capable of simulating transformer electrical or thermal fault in oil, with or without paper and pressboard. Several classic types of online DGA devices will be connected and operating in parallel. The cellulose paper or pressboard could be inserted into the heating pipe to compose the oil-paper insulation system. In addition, paper wrapped conductor could be inserted into the heating pipe to investigate the fault gas generation from the oil-paper-conductor system.

ii. This study could also be performed in the immersed heating method where the

cellulose paper could be wrapped on the heating element. In a preliminary study, the conventional Kraft paper for transformer insulation is wrapped on the heating element. It is found that with the paper wrapped, the heating becomes quite inhomogeneous. A part of the paper might be totally carbonised while other part still remains normal condition. This is one of the major challenges in this work. Carbon oxides are found generated from the paper with hydrocarbon gases which might be generated from the oil in the hotspot area. Extended efforts are required on this part of work.

iii. It has been found that a portion of fault gases are dissolved in the pressboard. With the temperature variation, the proportion of the gas content in the oil and in the pressboard might change. In an experimental study, the CO concentration in the oil would increase from 6000 ppm to 8000 ppm from 30℃ to 80℃. The migration phenomenon of CO2 is much stronger than CO [69]. It is quite necessary to study the situation where the gas generated from thermal faults might migrate between the oil phase and pressboard or cellulose paper. In transformer filled with MIDEL 7131, considerable amount of carbon oxides are formed under faults. The gas migration with temperature might distort the DGA results. The relationship between the fault gas distribution and temperature could be investigated by embed adequate amount of pressboard in the experimental system. The temperature of the oil in the system could be controlled by wrapped heater. Theoretically, the gas generation under faults is much faster than the gas migration between the oil and pressboard. Therefore, this migration phenomenon might not affect the online condition monitoring but affect the fault diagnosis for the transformer.

iv. The experimental results could be compared with DGA data from real transformers that subjected to a thermal fault. The oil types should be the same. The thermal fault level of a real transformer is normally identified by visual inspection through which the accurate hotspot temperature of the fault is difficult to be determined. The fault gas generation patterns and fault gas combination ratios need to be compared. It need to be noticed that the DGA results from real transformer represent the gas

combination at the time the oil is sampled. In comparison with laboratory DGA works, the gas generation should be used rather than absolute gas combination. For example, for a transformer which experiences a thermal fault on a certain day, the difference of DGA result after the thermal fault and the most recent result before the fault should be calculated and used to compare with the laboratory DGA results under the similar level of thermal fault.

Reference

[1] "Mineral oil-impregnated electrical equipment in service — Guide to the interpretation of dissolved and free gases analysis," in *IEC Std 60599*, ed, 2016.

[2] R. R. Rogers, "IEEE and IEC codes to interpret incipient faults in transformers, using gas in oil analysis," *IEEE Transactions on Electrical Insulation*, pp. 349-354, 1978.

[3] "Guide for The interpretation of the analysis of gases in transformers and other oil-filled electrical equipment in service," in *IEC Std 599-1978*, ed, 1978.

[4] M. Duval and A. DePabla, "Interpretation of gas-in-oil analysis using new IEC publication 60599 and IEC TC 10 databases," *IEEE Electrical Insulation Magazine*, vol. 17, pp. 31-41, 2001.

[5] M. Duval, "New techniques for dissolved gas-in-oil analysis," *IEEE Electrical Insulation Magazine*, vol. 19, pp. 6-15, 2003.

[6] M. Duval, "Dissolved gas analysis: It can save your transformer," *IEEE Electrical Insulation Magazine*, vol. 5, pp. 22-27, 1989.

[7] T. O. Rouse, "Mineral insulating oil in transformers," *IEEE Electrical Insulation Magazine*, vol. 14, pp. 6-16, 1998.

[8] Nynas, "Nytro Gemini X Safety Data Sheet," *Available: www.nynas.com*, 2006.

[9] M. Shirai, S. Shimoji, and T. Ishii, "Thermodynamic study on the thermal decomposition of insulating oil," *IEEE Transactions on Electrical Insulation*, pp. 272-280, 1977.

[10] A. Sierota and J. Rungis, "Electrical insulating oils. I. Characterization and pre-treatment of new transformer oils," *IEEE Electrical Insulation Magazine*, vol. 11, pp. 8-20, 1995.

[11] I. Fofana, "50 years in the development of insulating liquids," *IEEE Electrical Insulation Magazine*, vol. 29, pp. 13-25, 2013.

[12] P. Smith, "The benefits of inhibited transformer oils using the latest gas-to-liquids based technology," in *Euro Techcon*, United Kingdom, 2013.

[13] M. Ghalkhani, I. Fofana, A. Bouaicha, and H. Hemmatjou, "Influence of aging byproducts on the gassing tendency of transformer oils," in *Conference on Electrical Insulation and Dielectric Phenomena (CEIDP)*, 2012, pp. 870-873.

[14] "IEEE Guide for the Interpretation of Gases Generated in Oil-Immersed Transformers," in *IEEE Std C57.104-2008*, ed, 2009, pp. 1-36.

[15] CIGRÉ296, "Recent developments in DGA interpretation," *CIGRÉ Joint Task Force D1.01/A2-11*, 2004.

[16] H. Ding, R. Heywood, J. Lapworth, and S. Ryder, "Learning from success and failure in transformer fault gas analysis and interpretation," *IET Conference on Reliability of Transmission and Distribution Networks (RTDN)*, pp. 1-6, 22-24 Nov. 2011 2011.

[17] "IEEE Guide for the Interpretation of Gases Generated in Oil-Immersed Transformers," in *IEEE Std C57.104-1991*, ed, 1992.

[18] Z. Wang, X. Yi, J. Huang, J. V. Hinshaw, and J. Noakhes, "Fault gas generation in natural-ester fluid under localized thermal faults," *IEEE Electrical Insulation Magazine*, vol. 28, pp. 45-56, 2012.

[19] T. A. Prevost and T. V. Oommen, "Cellulose insulation in oil-filled power transformers: Part I - history and development," *IEEE Electrical Insulation Magazine*, vol. 22, pp. 28-35, 2006.

[20] "Mineral oil-impregnated electrical equipment in service — Guide to the interpretation of dissolved and free gases analysis," in *IEC Std 60599*, ed, 1999.

[21] W. D. Halstead, "A thermodynamic assessment of the formation of gaseous hydrocarbons in faulty transformers," *Journal of the Institute of Petroleum*, vol. 59, pp. 239-41, 1973.

[22] "Transformer maintenance," *Hydroelectric research and technical services group, USA*, 2000.

[23] T. V. Oommen, R. A. Ronnau, and R. S. Girgis, "New mechanism of moderate hydrogen gas generation in oil-filled transformers," *Cigre 21, rue d'Artois, F-75008 Paris*, vol. 12-206, 1998.

[24] E. Casserly and J. M. Rasco, "Stray gassing of refinery streams and transformer oil produced from them," in *IEEE International Conference on Dielectric Liquids (ICDL)*, 2014, pp. 1-4.

[25] I. Hohlein, "Unusual cases of gassing in transformers in service," *IEEE Electrical Insulation Magazine*, vol. 22, pp. 24-27, 2006.

[26] S. Besner, J. Jalbert, and B. Noirhomme, "Unusual ethylene production of in-service transformer oil at low temperature," *IEEE Transactions on Dielectrics and Electrical Insulation*, vol. 19, pp. 1901-1907, 2012.

[27] D. Martin, N. Lelekakis, J. Wijaya, M. Duval, and T. Saha, "Investigations Into the Stray Gassing of Oils in the Fault Diagnosis of Transformers," *IEEE Transactions on Power Delivery*, vol. 29, pp. 2369-2374, 2014.

[28] "Fluids for electrotechnical applications — Unused mineral insulating oils for transformers and switchgear," in *IEC Std 60296*, ed, 2012.

[29] CIGRÉ526, "Oxidation Stability of Insulating Fluids," *CIGRÉ Working Group D1.30*, 2013.

[30] "Oil-filled electrical equipment — Sampling of gases and analysis of free and dissolved gases — Guidance," *IEC Std 60567*, 2011.

[31] "Method of sampling insulating liquids," *IEC Std 60475*, 2011.

[32] A. Abu-Siada, S. Hmood, and S. Islam, "A new fuzzy logic approach for consistent interpretation of dissolved gas-in-oil analysis," *IEEE Transactions on Dielectrics and Electrical Insulation*, vol. 20, pp. 2343-2349, 2013.

[33] A. D. Ashkezari, T. K. Saha, C. Ekanayake, and H. Ma, "Evaluating the accuracy of different DGA techniques for improving the transformer oil quality interpretation," in *Australasian Universities Power Engineering Conference (AUPEC)*, 2011, pp. 1-6.

[34] N. A. Bakar, A. Abu-Siada, and S. Islam, "A review of dissolved gas analysis measurement and interpretation techniques," *IEEE Electrical Insulation Magazine*, vol. 30, pp. 39-49, 2014.

[35] S. A. Ward, "Evaluating transformer condition using DGA oil analysis," in *Conference on Electrical Insulation and Dielectric Phenomena,* , 2003, pp. 463-468.

[36] D. Zhou, N. Azis, G. Y. Yang, Z. D. Wang, D. Jones, B. Wells, *et al.*, "Examining acceptable Dissolved Gas Analysis level of in-service transformers," in *International Conference on High Voltage Engineering and Application (ICHVE)*, 2012, pp. 612-616.

[37] W. He-Xing, Y. Qi-Ping, and Z. Qun-Ming, "Artificial neural network for transformer insulation aging diagnosis," in *Third International Conference on Electric Utility Deregulation and Restructuring and Power Technologies (DRPT),*, 2008, pp. 2233-2238.

[38] N. A. Muhamad, B. T. Phung, T. R. Blackburn, and K. X. Lai, "Comparative study and analysis of DGA methods for transformer mineral oil," in *IEEE Power Tech*, 2007, pp. 45-50.

[39] M. Duval, "Fault Gases Formed in Oil-Filled Breathing EHV Power Transformers – The Interpretation of Gas Analysis Data," *IEEE Transaction on Power Apparatus and Systems,* vol. 104, pp. 477-487, 1974.

[40] M. Duval, "The duval triangle for load tap changers, non-mineral oils and low temperature faults in transformers," *IEEE Electrical Insulation Magazine,* vol. 6, pp. 22-29, 2008.

[41] H. Molavi, A. Zahiri, and K. Anvarizadeh, "Condition assessment and fault diagnosis of two load tap changers using dissolved gas analysis," in *22nd International Conference and Exhibition on Electricity Distribution (CIRED)*, 2013.

[42] P. J. Griffin, L. Lewand, R. C. Peck, N. A. Letendre, D. Frieze, and J. Johnson, "Load tap changer diagnostics using oil tests–a key to condition-based maintenance," *report from Doble Engineering Company,* pp. 1-21, 2005.

[43] H. Borsi, "Gassing behaviour of different insulating liquids for transformers," *ELECTRA-CIGRE-*, pp. 21-42, 2000.

[44] U. K. Imad, Z. D. Wang, I. Cotton, and S. Northcote, "Dissolved gas analysis of alternative fluids for power transformers," *Electrical Insulation Magazine, IEEE*, vol. 23, pp. 5-14, 2007.

[45] M. Duval and L. Lamarre, "The duval pentagon-a new complementary tool for the interpretation of dissolved gas analysis in transformers," *IEEE Electrical Insulation Magazine*, vol. 30, pp. 9-12, 2014.

[46] H. Borsi, K. Durnke, and E. Gockenbach, "Relation between faults and generated gases in transformer liquids," in *IEEE International Conference on Dielectric Liquids (ICDL)*, 1999, pp. 487-490.

[47] M. Jovalekic, D. Vukovic, and S. Tenbohlen, "Gassing behavior of various alternative insulating liquids under thermal and electrical stress," in *IEEE International Symposium on Electrical Insulation*, 2012, pp. 490-493.

[48] M. Jovalekic, D. Vukovic, and S. Tenbohlen, "Dissolved gas analysis of alternative dielectric fluids under thermal and electrical stress," in *Dielectric Liquids (ICDL), 2011 IEEE International Conference on*, 2011, pp. 1-4.

[49] M. Jovalekic, D. Vukovic, and S. Tenbohlen, "Dissolved gas analysis of natural ester fluids under electrical and thermal stress," in *report by University of Stuttgart*, 2009.

[50] D. H. C. Clair Claiborne, Donald B. Cherry and George K. Frimpong, "Understanding Dissolved Gas Analysis – Part 2: Thermal Decomposition of Ester Fluids," in *TechCon*, Chicago, Illinois, 2012.

[51] Y. Liu, J. Li, and Z. Zhang, "Gases dissolved in natural ester fluids under thermal faults in transformers," in *IEEE International Symposium on Electrical Insulation (ISEI)*, 2012, pp. 223-226.

[52] N. A. Muhamad, B. T. Phung, and T. R. Blackburn, "Dissolved gas analysis for common transformer faults in soy seed-based oil," *IET electric power applications*, vol. 5, pp. 133-142, 2011.

[53] R. Hughes, W. Schubert, and R. Buss, "Solid‐State Hydrogen Sensors Using Palladium‐Nickel Alloys: Effect of Alloy Composition on Sensor Response," *Journal of The Electrochemical Society*, vol. 142, pp. 249-254, 1995.

[54] G. Ma, J. Jiang, C. Li, H. Song, Y. Luo, and H. Wang, "Pd/Ag coated fiber Bragg grating sensor for hydrogen monitoring in power transformers," *Review of Scientific Instruments*, vol. 86, p. 045003, 2015.

[55] "Standard Test Method for Analysis of Gases Dissolved in Electrical Insulating Oil by Gas Chromatography," *ATSM D3612-02*, 2004.

[56] J. Jalbert, R. Gilbert, P. Tétreault, and M. A. E. Khakani, "Matrix effects affecting the indirect calibration of the static headspace-gas chromatographic method used for dissolved gas analysis in dielectric liquids," *Analytical Chemistry*, vol. 75, pp. 5230-5239, 2003.

[57] CIGRÉ443, "DGA in Non-Mineral Oils and Load Tap Changers and Improved DGA Diagnosis Criteria," *CIGRÉ Working Group D1.32*, 2010.

[58] J. Jalbert, R. Gilbert, and M. A. E. Khakani, "Comparative Study of Vapor-Liquid Phase Equilibrium Methods to Measure Partitioning Coefficients of Dissolved Gases in Hydrocarbon Oils," *Chromatographia*, vol. 56, pp. 623-630, 2002.

[59] "TMx Training Slides Part 1," *SERVERON*, 2007.

[60] CIGRÉ409, "Report on Gas Monitors for Oil-Filled Electrical Equipment," 2010.

[61] D. Skelly, "Photo-acoustic spectroscopy for dissolved gas analysis: Benefits and Experience," in *International Conference on Condition Monitoring and Diagnosis (CMD)*, 2012, pp. 29-43.

[62] Z. Qi, Y. Yi, W. Qiaohua, W. Zhihao, and L. Zhe, "Study on the online dissolved gas analysis monitor based on the photoacoustic spectroscopy," in *International Conference on Condition Monitoring and Diagnosis (CMD), ,* 2012, pp. 433-436.

[63] F. Wan, W. Chen, X. Peng, and J. Shi, "Study on the gas pressure characteristics of photoacoustic spectroscopy detection for dissolved gases in transformer oil," in *International Conference on High Voltage Engineering and Application (ICHVE), ,* 2012, pp. 286-289.

[64] G. Belanger and M. Duval, "Monitor for hydrogen dissolved in transformer oil," *IEEE Transactions on Electrical Insulation*, vol. EI-12, October, 1977.

[65] Qualitrol, "SERVERON TM8 product brochure," *www.qualitrolcorp.com*, 2017.

[66] R. Peltier, "Monitoring key gases in insulating oil keeps transformers healthy," *available: http://www.powermag.com/*, 2006.

[67] S. Nukiyama, "The maximum and minimum values of the heat Q transmitted from metal to boiling water under atmospheric pressure," *International Journal of Heat and Mass Transfer,* vol. 9, pp. 1419-1433, 1966.

[68] A. Mills and J. Fry, "Rate of evaporation of hydrocarbons from a hot surface: Nukiyama and Leidenfrost temperatures," *European Journal of Physics,* vol. 3, p. 152, 1982.

[69] H. Kan and T. Miyamoto, "Proposals for an improvement in transformer diagnosis using dissolved gas analysis (DGA)," *IEEE Electrical Insulation Magazine,* vol. 6, pp. 15-21, 1995.

[70] J. G. Collier and J. R. Thome, "Convective boiling and condensation," *Clarendon Press,* 1994.

Appendix I List of Publications

Journal Paper:

[1] X.F. Wang, Z.D. Wang, Q. Liu, P. Mavrommatis and P. Dyer, "Dissolved Gas Analysis (DGA) for Immersed Thermal Faults in Transformer Liquids," IEEE Transaction on Dielectrics and Electrical Insulation (TDEI), October, 2018. [Submitted].

International Conference Papers:

[2] X.F. Wang, Z.D. Wang, Q. Liu, G. Wilson, D. Walker and P.W.R. Smith, "Dissolved Gas Analysis (DGA) of Mineral Oil under Thermal Faults with Tube Heating Method," IEEE International Conference on Dielectric Liquids (ICDL), Manchester, United Kingdom, 25-29 June, 2017, pp. 1363.

[3] X.F. Wang, Z.D. Wang, Q. Liu, G. Wilson, P. Jarman and D. Walker, "Evaluation of Mass Transfer Rate of Dissolved Gases in Transformer Oils," IEEE International Conference on Condition Monitoring and Diagnosis (CMD), Xi'an, China, 25-28 Sept, 2016, pp. 475-478.

[4] X.F. Wang, Z.D. Wang, Q. Liu, Ch. Krause, P.W.R. Smith and D. Walker, "Dissolved Gas Analysis of a Gas to Liquid hydrocarbon transformer oil under thermal faults," International Symposium on High Voltage Engineering (ISH), Pilsen, Czech Republic, 23-28 Aug 2015, pp. 424.

Appendix II Pool Boiling Phenomenon in Water

Pool boiling is defined as boiling from a heated surface submerged in a large volume of stagnant liquid. The immersed heating in the DGA thermal experiments is a pool boiling process. The pool boiling theory could be explained by immersed heating in water as an example. The relationship between heating element surface heat flux and the heater temperature is defined as the "boiling curve". The boiling curve of heating in water is shown in Figure A-1. There are in general four regimes on the boiling curve.

The first regime is natural convection region AB where the heat energy is dissipated by water natural convection. The second regime is nucleate boiling region BC where the difference between temperature of heating element surface and water saturation temperature is sufficient to initialize vapor nucleation. As the vaporization normally absorbs large amount of energy, in this regime the surface heat flux increases rapidly. The point of critical heat flux (CHF) indicates the upper limit of nucleate boiling regime. The temperature at the CHF point is known as the Nukiyama temperature. The third regime is transition boiling region CD. In this regime, the heater temperature exceeds the CHF point. The strong interaction between vapor stream and water around the heater restricts the adequate supply of subcooled water to dissipate the heating energy. Therefore, the heat dissipation efficiency starts to decrease. On the boiling curve, the temperature increases with surface heat flux decreasing. In the transition boiling region, the heater surface is covered by unstable vapor bubbles. The fourth region is film boiling region DE. In this region, the heater is covered by a stable vapor film. The heat is transferred through the vapor film and it is dominated by radiation heat transfer. Therefore, the heater temperature would significantly increase with increasing surface heat flux [70].

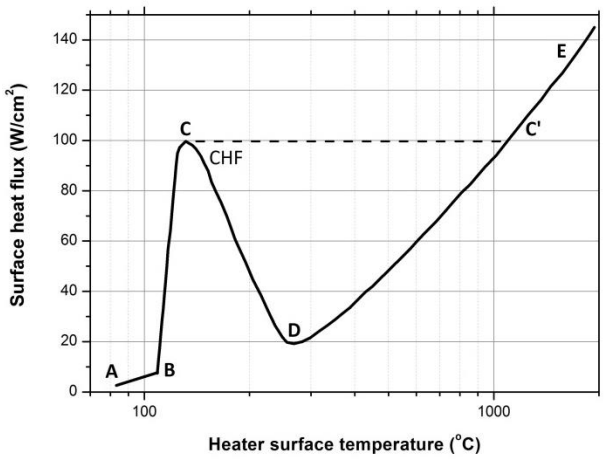

Figure A-1 Pool boiling curve of water

In practical situation, if the input power of heater is individually controlled, the heating process will follow the first and second regimes of the boiling curve, i.e. from A to C. Once it reaches the CHF point C, the heater temperature is 35℃ higher than water saturation temperature. Any small increment of input power might cause a sudden jump of heater temperature to the C'. The C' is the next practical stable point after C. On the other words, the boiling curve would jump from C to C' and the transition boiling regime is actually missing. At the C' point, the heater temperature is the next stable point after C where the heater temperature is nearly 1150℃. In many investigations of the boiling curves of water, heater failures are caused due to extreme high temperature at C' point which is also named as "burnout" [67, 70].

In summary the temperature range of transition boiling regime is "missing" in the immersed heating process. The upper limit of stable temperature is limited by the Nukiyama temperature at the critical heat flux (CHF) point which depends on the boiling point of the liquid. Beyond the CHF point , the heater temperature will suddenly jump to film boiling regime at temperature higher than 1000℃ where most heaters might burnout. If the melting point of the heater is higher than the temperature at the C' point, the material could survive at this point. It should be noticed that the temperature distribution could be quite inhomogeneous in the practical film boiling regime.

Appendix III Tube Heating Experimental System

Overall of the tube heating experimental system

Appendix IV Verification DGA Tests

Table A. 1 Repeated 550℃ DGA experiment of MIDEL 7131 with the tube heating test system

Before	CO2 (ppm)	CO (ppm)	H2 (ppm)	CH4 (ppm)	C2H6 (ppm)	C2H4 (ppm)	C2H2 (ppm)	O2 (ppm)	N2 (ppm)
TM8	802.7	0.0	0.0	0.0	0.0	8.7	0.0	30950.0	60069.1
Vacuum	138	3	0	1	0	1	0	11288	38339
Headspace	-	-	-	-	-	-	-	-	-
Gas in gas	363	12	0	4	3	7	0	23756	62763
After	**CO2 (ppm)**	**CO (ppm)**	**H2 (ppm)**	**CH4 (ppm)**	**C2H6 (ppm)**	**C2H4 (ppm)**	**C2H2 (ppm)**	**O2 (ppm)**	**N2 (ppm)**
TM8	990.2	134.5	0.0	54.9	167.6	77.4	0.0	0.0	84268.3
Vacuum	176	19	0	9	18	12	0	6667	21913
Headspace	-	-	-	-	-	-	-	-	-
Gas in gas	473	328	0	82	41	34	0	34563	93502

Table A. 2 Laboratory DGA measurements with vacuum extraction method of two sample oil samples

	CO2 (ppm)	CO (ppm)	H2 (ppm)	CH4 (ppm)	C2H6 (ppm)	C2H4 (ppm)	C2H2 (ppm)	O2 (ppm)	N2 (ppm)
Vacuum 1	26	7	0	2	5	3	0	1351	16461
Vacuum 2	27	8	0	2	5	3	0	1764	19773

Table A. 3 Laboratory DGA measurements with headspace extraction method of two sample oil samples

	CO2 (ppm)	CO (ppm)	H2 (ppm)	CH4 (ppm)	C2H6 (ppm)	C2H4 (ppm)	C2H2 (ppm)	O2 (ppm)	N2 (ppm)
Headspace 1	196	34	0	8	49	41	0	9932	55781
Headspace 2	281	32	0	8	42	51	0	11868	148042

Table A. 4 Laboratory DGA measurements of two sample gas samples

	CO2 (ppm)	CO (ppm)	H2 (ppm)	CH4 (ppm)	C2H6 (ppm)	C2H4 (ppm)	C2H2 (ppm)	O2 (ppm)	N2 (ppm)
Gas in gas 1	169	23	0	15	5	4	0	22800	939210
Gas in gas 2	154	23	0	16	5	4	0	15820	948333

Appendix V Risk Assessment of Tube Heating DGA Experiments

The University of Manchester

University of Manchester National Grid Power Systems Research Centre Laboratories

Title of Experiment / Test:-	DGA of insulating oils under thermal faults simulated by tube furnace
Location:-	B20-HV Cage 3
Project Supervisor (must be SAE):-	Prof. Zhongdong Wang

The Project Supervisor will usually be the Academic Supervisor when the person carrying out the experiment is a student experimenter.

Name Of Person Carrying Out Expt:-	Xiongfei Wang

Safety Documents Valid From:- 10 Oct 2016 To:- 10 Apr 2017

For continuous periods of experimentation only. Re-validation of this document is required for breaks in experimentation greater than one month or when test circuit is dismantled and re-assembled.

Level Of Supervision (to be completed by Academic Supervisor/HV Laboratories Manager):

- ●Experimentation to be carried out in presence of student's Academic Supervisor □
- ●Experimentation to be carried out in the presence of a SAE □
- ●Experimentation to be carried out only with other Authorised Experimenters/Authorised Student Experimenters present in laboratory □
- ●Experimentation may be carried out providing an SAE is in the Centre √

A SAE (in area of competence) must always be in the Centre to permit experimentation to take place in the Centre.

Safety Key No. (for all HV experiments and any others requiring this): -None

Main Point of Isolation:-at the back of the cage

Special Precautions/Instructions:-None

SANCTION TO EXPERIMENT

EXPERIMENTER DECLARATION: I understand the contents of these safety documents. I am aware that any change in the experiment beyond that identified in these safety documents means that work must stop, the Risk Assessment reviewed and permission to resume has been given and countersigned by the Project Supervisor or HV Laboratories Manager.

Name: Xiongfei Wang Signed: _____ Date: _____

Name of SAE 1, Validation:-_____ Signed:-_____

Name of SAE 2, Check:-_____ Signed:-_____

Two SAEs must be identified and sign here having confirmed the safety documents to be satisfactorily completed.

Document Cancelled: Date: _____ Name: _____ Signature:_____

METHOD STATEMENT

Title of Experiment / Test:-	DGA of insulating oils under thermal faults simulated by tube furnace		
Prepared by:-	Xiongfei Wang	**Date:-**	10 Oct 2016

A. Purpose of Experiment:

1. to investigate the types and amounts of fault gases formed under thermal faults from T1 (< 300 ℃) to T3 (> 700 ℃) levels.

2. to generate a chart of fault gas generation against temperature of three types of transformer insulating oils (Gemini X, Diala S4 ZX-I, MIDEL 7131).

3. to compare the measurement between laboratory DGA measurements and online DGA monitors measurements under same oil samples.

B. Equipment Being Used / Circuit Diagram (where appropriate):

1. Carbolite EVT 12/300 tube furnace.

Working temperature range: ≤ 1200 ºC.

2. Thermocouples and thermometer.

The thermocouples are mineral insulated and sheathed with stainless steel. They are capable of measuring temperature below 1100 ºC. The thermocouple tips will be attached to the measuring pipe by a metal sheet. They will be covered with ceramic wool in order to prevent heat dissipation at the measuring point and obtain accurate measurements.

The temperature measuring points are marked as the red circles in Fig 1. These thermocouples measure the temperatures of the cold oil, hot oil, the entrance and exit of the heat pipe, respectively.

3. Online DGA monitors

In the experiments, two online DGA monitors will be connected on the system to continuously measure the dissolved gas content.

Serveron TM8 is a GC based online DGA monitor. It continuously circulates the oil. The extracted gas is injected into the GC column with Helium carrier gas. The carrier gas is stored in a high pressure Helium cylinder.

GE Transfix is a PAS based online DGA monitor. It only pumps the oil before detection. The extracted gas is sent into detector by air as carrier gas.

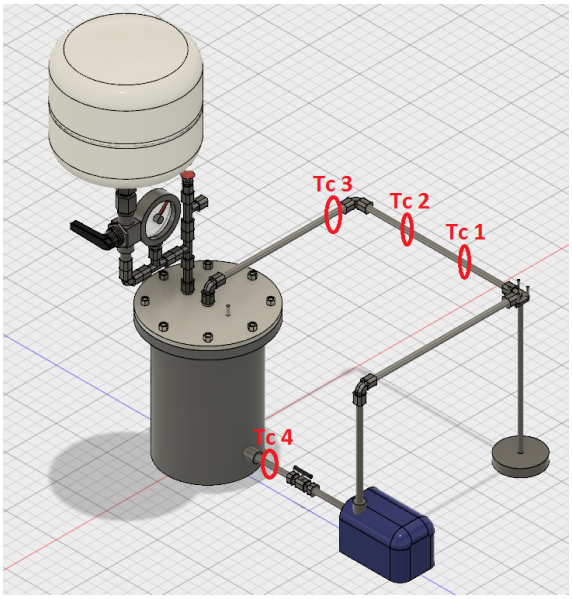

Fig 1 Circulation system and thermocouple location

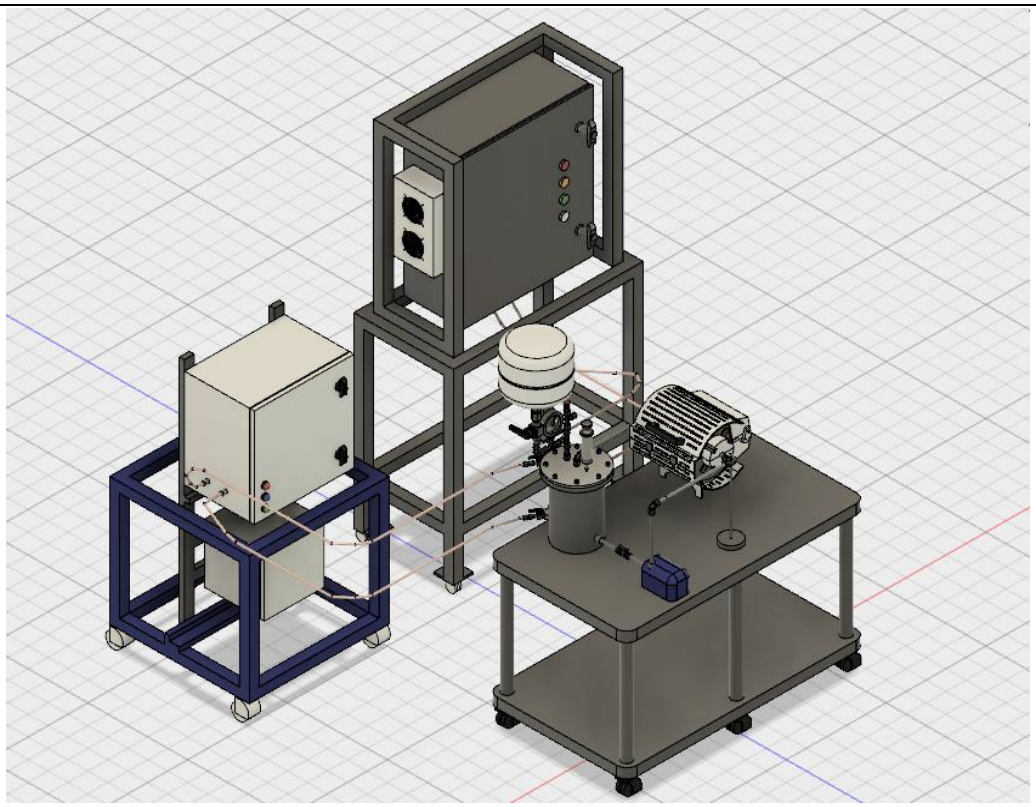

Fig 2 Overall system

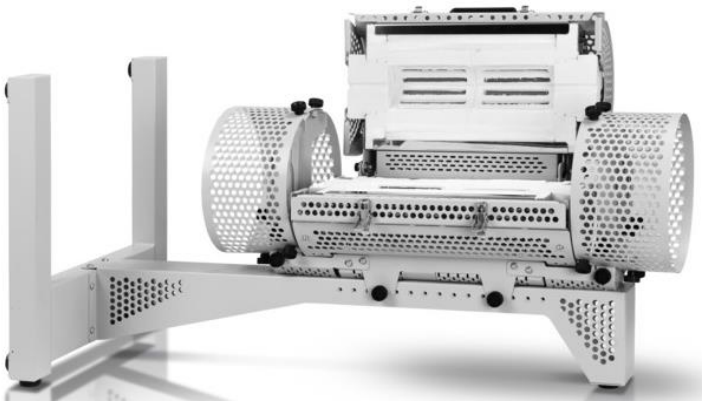

Fig 3 Furnace oven for thermal fault simulation

Fig 4 Expansion bladder (left) and expansion vessel tank (right)

C. Experimental Procedure:

1. Assemble the system according to Fig 1. Make sure all the connections are properly sealed.

1) Check the sealing condition by pressurising the system to 5 psig;

2) If the pressure doesn't change in 1 hour, the system is properly sealed. Otherwise, the leakage points should be detected by soup water and sealed by silicon sealant.

2. Fill the tested oil in the system. The oil and gas volumes in the system should be controlled. In this section, a few steps will be done to control the oil and gas volume.

1) Open the lid and pour 6.3 litres of new oil into the main vessel;

2) Put the tubings of TM8 and Transfix into a beaker with 2 litres of new oil;

3) Circulate the oil for 10 minutes so that the two monitors are filled with oil;

4) Connect the online DGA monitors to the test system as Fig 2. So far, the oil volume in the system is controlled as 7 litres.

5) Pressurise the expansion tank with a manual gas pump and there is no gas in the expansion bladder;

6) Release the excessive gas until the system returns atmosphere pressure;

7) Release the pressure of expansion tank to atmosphere pressure;

8) Manually inject 600 mL gas in to the system with syringe. By this way, the gas volume in the system is controlled as 1.6 litres.

3. Measure the background gas contents in the system. Since the DGA investigated gas will exist in both gas phase and oil phase, the gas in headspace of the system will be sampled for

laboratory measurement. Dissolved gas in oil phase will be measured by online DGA monitors and sampled for laboratory measurement as well.

1) Circulate the oil through the system and measure the dissolved gas content with the online DGA monitors;

2) Once the online DGA monitors show stable dissolved gas values, stop measurement and oil circulation;

3) Sample 50 mL of gas and oil samples each with syringes. These samples will be delivered and analysed in professional laboratory and marked as "background".

4. Generate thermal fault. The pipe in the furnace will be heated to a certain temperature (heat pipe). The surface temperature of the heat pipe will be measured.

1) Isolate the online DGA monitors from the system by the ball valves;

2) Switch on the furnace at set temperature. The set temperature will follow the red curve in Fig 5. For example, if a 500 ºC thermal fault is applied, the furnace will be set working at 700 ºC. During heating, the temperatures at four thermocouple locations will be monitored as shown in Fig 1;

3) If a T1 or T2 fault (< 700 ℃) is generated, heating will be stopped after 15 minutes and the oil will be circulated for 3 minutes. Then the heating will be repeated. This step is to balance the outside system temperature. The heating profile is shown in Fig 6 below. Heating will be stopped once the total heating time reaches the designated duration;

4) If a T3 fault (> 700 ℃) is generated, the heating duration is shorter than 10 minutes. Therefore, the periodic cooling is not necessary. Once the heat pipe reaches the target temperature, the furnace will be stopped. The temperature will maintain until the designated duration. Then the oil will be circulated and heat pipe will be cooled down.

5. Measure the fault gas content. The fault gas is generated during fault. After fault, the gas will be either in gas phase or in oil phase. The DGA measurements here are similar to those for background measurements.

1) Connect the online DGA monitors back to the system;

2) Circulate the oil and start measuring dissolved gas content with online DGA monitors;

3) Once the online DGA monitors show stable dissolved gas values, stop measurement and oil circulation;

4) Sample 50 mL of gas and oil samples each with syringes. There samples will be delivered and analysed in professional laboratory and marked as "after fault";

5) Pressurise the expansion tank with a manual gas pump and there is no gas in the expansion bladder;

6) Release the excessive gas through a syringe until the system returns atmosphere pressure. Record the number of syringe strokes from which the gas volume in the bladder can be calculated. The difference from the initial gas volume is the free gas generation volume.

7) The total gas generation amount can be calculated as:

$$gas\ generation\ (\mu L) = cgig*Vg+cgio*Vo$$

Where, $cgig$ and $cgio$ are the concentration of gas-in-gas and gas-in-oil, respectively; Vg and Vo are the volume of gas phase and oil phase, respectively.

6. Clean the system. In this section, the procedures after a test and preparing for another test are introduced.

1) Drain the tested oil into waste oil container;

2) Disconnect the online DGA monitors and put the tubing into beaker with new oil;

3) Circulate the oil through DGA monitors in order to flush and dilute the old oil;

4) Open the lid of main vessel, pour about 3 litres new oil into the system;

5) Circulate the oil through the system in order to flush and dilute the old oil.

7. Repeat test. After the system is cleaned, test with another thermal fault temperature will be performed.

1) Drain the flushing oil in the system and online DGA monitors;

2) Repeat section 2 to section 6 with another fault temperature. The thermal fault temperature varies from 250 ℃ to 750 ℃ with 100 ℃ interval.

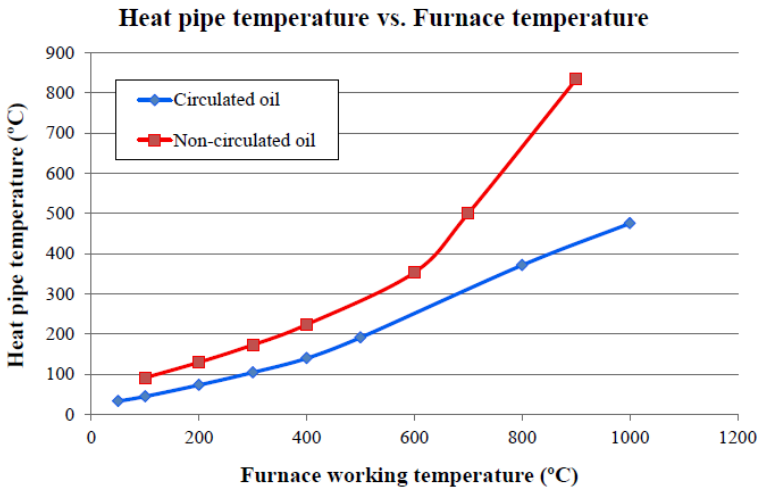

Fig 5 Relationship between heat pipe temperature and furnace temperature

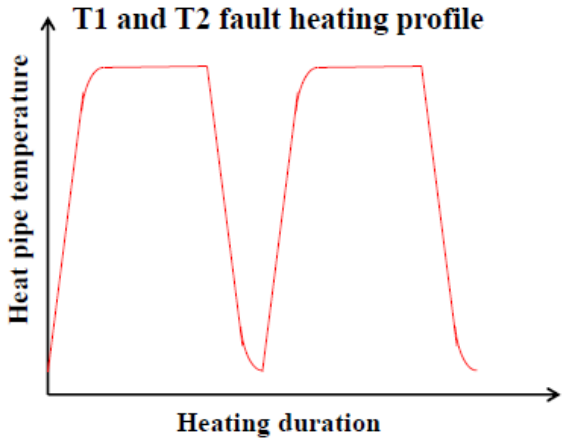

Fig 6 T1 and T2 fault heating profile

RISK ASSESSMENT

(must address all hazards identified in hazard checklist)

Title Of Experiment / Test:-		DGA of insulating oils under thermal faults simulated by tube furnace			**Date:-**	**10.Oct.2016**
Prepared By:-	**Xiongfei Wang**	**Validated By:-**		**Checked By:-**	**Review:-**	

Hazard (s) & Possible Consequences	**Persons or Equipment at Risk**	**Control measures applied to eliminate / minimise risk**	**Residual risk with control measures applied**			
			Severity	Likelihood	Risk rating	Risk Acceptable?

Oil spillage and slip hazard	Anybody close to test system	1. Oil spillage control trays used when oil is poured between vessels. 2. Spills immediately cleaned. 3. Oil absorbent pads available. 4. PPE must be worn when handling the oils.	1	2	2	Low Yes
Fire	Anyone present in laboratory	1. A thermocouple constantly monitors the hot and cold oil temperature. 2. Fire extinguisher accessible near the test cage.	4	1	4	Low Yes
Tripping hazards	Anybody entering test cage	1. Area kept tidy.	1	2	2	Low Yes
Electric shock from high voltage (240V)	Anyone present in laboratory	1. Safety earthling. 2. Operation limited to authorised, appropriately trained personnel. 3. Test carried out in the test cage. 4. WARNING notices prominently displayed.	1	1	1	Low Yes
High temperature burn	Anybody close to test system	1. Warning notices prominently displayed. 2. Heat resistant gloves and protection mask should be worn. 3. Oil is cooled to ambient temperature before handling.	4	1	4	Low Yes
High pressure	Anybody entering test cage	1. Expansion vessel to relieve volume change. 2. Pressure relief valve to prevent high pressure building up. 3. Temperature monitored continuously.	2	1	2	Low Yes
PPE		Lab coat, heat resistant gloves, mask and protection shoes to be worn.				

Risk Assessment Matrix Likelihood (1-5) x Severity (1-5) = Risk (See attached matrix for guidance)	**1 – 5**: **Low**: Tolerable – monitor and manage
	6 – 8: Medium: Review, introduce further controls to reduce to as low as reasonably possible
	9 – 25: High: Intolerable. Do not commence work, further control measures required

RECORD OF CHEMICAL USAGE WITHIN EXPERIMENT

Chemical	Reason For Use	Data Sheet /COSHH Attached?	Are Hazards Resulting From Use Described In Risk Assessment Table Above?	Method Of Disposal
Gemini X	Test object	Yes	Yes	Waste Gemini X container
Diala S4 ZX-I	Test object	Yes	Yes	Waste Diala S4 container
MIDEL 7131	Test object	Yes	Yes	Waste MIDEL 7131 container

HAZARD CHECKLIST

You should indicate the hazards present in the experiment in the table below. If a hazard is present, control measures should be stated on the risk assessment. Note that this list is not exhaustive.

Hazard Type	Present	Not Present
Electric Shock From High Voltage (1kV & Over)		√
Electric Shock From Low Voltage (Under 1kV)	√	
Tripping Hazards	√	
Slipping Hazards	√	
Fire	√	
High Temperatures	√	
Low Temperatures		√
High Pressure	√	
Low Pressure		√
Chemical Spillage	√	

Chemical Contact (Ingestion / Eye & Skin Contact)	√	
High Noise Levels		√
Working At Height		√
Head Height Hazards		√
Production Of Dust & Fumes		√
Manual Handling	√	
Production/Use Of Radiation		√
Use Of Asphyxiating Gases		√
Any Other Hazards		√

RISK ASSESSMENT SEVERITY MATRIX

SEVERITY VALUE = Potential consequence of an incident/injury given current level of controls.

5 Very High:- Death / Permanent incapacity / Widespread loss
4 High:- Major Injury (Reportable Category) / Severe Incapacity / Serious Loss
3 Moderate - Injury / Illness of 3 days or more absence (reportable category) / Moderate loss
2 Slight: - Minor injury / Illness – Immediate 1st Aid only / slight loss
1 Negligible No injury or trivial injury / illness / loss

LIKELIHOOD = what is the potential of an incident or injury occurring given the current level of controls.

5 Almost certain to occur
4 Likely to occur
3 Quite possible to occur
2 Not likely to occur
1 Almost certain not to occur

The multiple of Likelihood with Severity is the risk classification value.

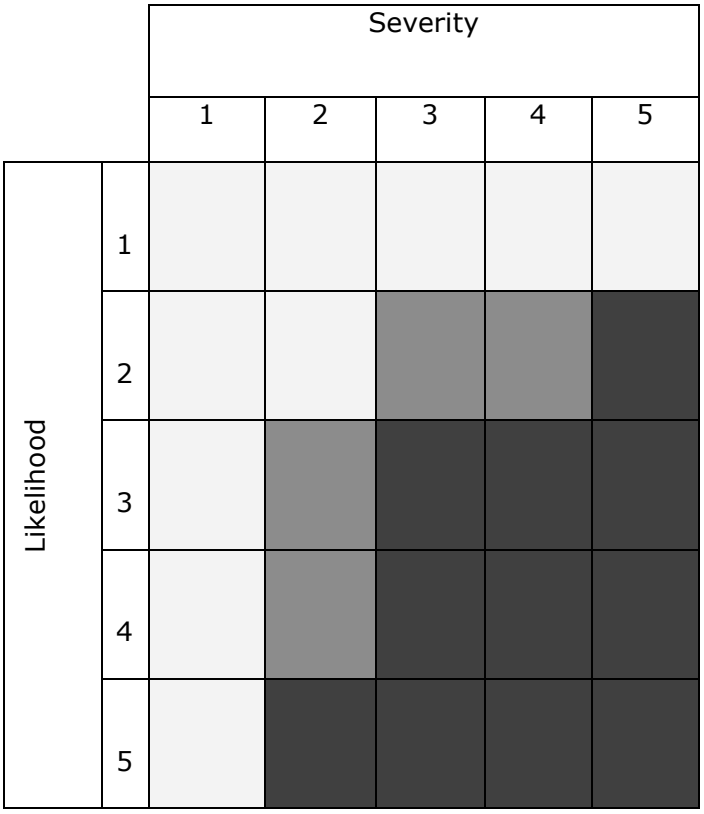

Risk Classification Value

	1–5: **Low**: Tolerable – monitor and manage

	6–8: Medium: Review, introduce further controls to reduce to as low as reasonably possible

	9–25: High: Intolerable. Do not commence work, further control measures required

COSHH Assessment Form (Basic)

Assessor **Xiongfei Wang**	**Principal Investigator/Supervisor** **Prof Zhongdong Wang**		
Assessment Date	**Dates reviewed**		
	10-October-2016		

Title of project or process:

DGA of insulating oils under thermal faults simulated by tube furnace

Technique(s)	**Frequency** Often	**Location of Work** B20 cage 3

HAZARDS IDENTIFIED

Substance	**Hazardous Properties**	**Quantity**
Synthetic Ester Oil (MIDEL 7131)	Contact with eyes may cause irritation and redness. Ingestion may cause respiratory irritation	10 litres
Mineral oil	Contact with eyes and skin may cause irritation and redness.	10 litres

Who may be exposed?
Anyone handing the oil.

What is the maximum possible exposure?
The possibility is very small when taken with care.

METHODS OF PREVENTION OR CONTROL OF EXPOSURE
Wear lab coat, lab shoes, glasses when handing the oil.
Oil pump should be used when transfer the oil.
Oil spillage trays should be used.
At least two people when remove the barrel.

1. Access control

a) restricted to competent personnel

2. Engineering controls required

None.

3. Approved PPE

b) heat resistant gloves

c) translucent lab glove

d) Protection mask

e) laboratory coat

4. Special procedures

None.

Named personnel :

Xiongfei Wang

ASSESSMENT OF EXISTING CONTROLS

The existing available control measures are sufficient to cover this work. And the possibility of hazard is very small.

TRAINING REQUIREMENTS	**STORAGE REQUIREMENTS**
None.	